AE - AEROSOLS

Third International Symposium
on
AIR QUALITY MANAGEMENT
at Urban, Regional and Global Scales
&
14 th IUAPPA Regional Conference
26-30 September 2005
Istanbul, Turkey

AEROSOLS

Proceedings of the Third International Symposium on Air Quality Management at Urban, Regional and Global Scales. 26-30 September 2005, Istanbul – Turkey

CHARACTERIZATION OF ATMOSPHERIC AEROSOL PARTICLES IN A MOUNTAINOUS REGION IN NORTHERN JAPAN

Katsumi Saitoh, Koichiro Sera[*] and Tadashi Shirai[**]

Environmental Research & Information Center of Akita Prefecture,
3-1-1 Sanno, Akita 010-8572, Japan, XLL04042@nifty.com
[*] Cyclotron Research Center, Iwate Medical University,
348 Tomegamori, Takizawa 020-0173, Japan, ksera@iwate-med.ac.jp
[**] Tokyo Dylec Co., Ltd., Naitocho Bldg. 1, Naito-machi, Shinjuku-ku,
Tokyo 160-0014, Japan, shirai@tokyo-dylec.co.jp

ABSTRACT

The purpose of this study is to clarify the chemical characterization of particulate matter (PM) in a mountainous region and examine the effect of atmospheric pollutants transported to Japan from Northeast Asian regions. Sampling of size-resolved airborne PM was carried out on the west side of Mt. Moriyoshi near the summit in northern Japan, from 1 – 16 February (winter period) and 7 – 19 July (summer period) in 2004. The concentrations of several elemental and ionic species in each size-resolved PM sample were determined by particle induced X-ray emission (PIXE) and ion chromatography analysis. From these results, in the winter period, it is suggested that soil and sea-salt particles of PM_{10} to $PM_{2.5}$ size and ammonium sulfate particles, *i.e.*, secondary-formed particles of $<PM_{1.0}$, have been transported to Japan from the continent. On the other hand, in the summer period, it is suggested that PM was formed from soil and sea-salt particles of $>PM_{10}$ to $PM_{2.5}$ size and secondary-formed particles of $<PM_{1.0}$.

Key Words: Atmospheric aerosol particles, Mountainous region, Long-range transport, PIXE, Ion chromatography

1. INTRODUCTION

The Japanese archipelago is located in the mid-latitudes off the east coast of Asia. In the winter, northwest winds (monsoons) from the Asian continent caused by an atmospheric pattern of western high and eastern low bring large amounts of snow to regions along the Sea of Japan side of Japan. These northwest winds transport various air contaminants of natural origin or man-made origin from the continent to Japan. This has been reported to affect the forest ecosystem of Japan (Nagafuchi, 2000). On the other hand, in the summer, the land and sea breeze, *i.e.*, southwestern wind and southeast wind, blows in daytime and at night, respectively. This land and sea breeze reflects local atmospheric conditions. The best way to gain insight into contaminants transported from the continent is to observe them in a mountainous region at 1200 m to 1500 m above sea level, which is in the vicinity of the top of the planetary boundary layer and is less directly affected by man-made pollution sources (Mizoguchi, 1991).

Consequently, in order to shed light on the long-range transport of atmospheric pollutants in the Northeast Asian regions, we studied a multi-probe chemical characterization and composition profile of airborne particulate matter (PM) on Mt. Moriyoshi (39° 58' N, 140° 32' E; altitude: 1454 m), located on the Sea of Japan side of northern Honshu, Japan, near Northwest China and Southwest Russia. PM samples were collected at the west side near the summit (altitude: 1167 m), from 1 – 16 February (winter period) and 7 – 19 July (summer period) in 2004, and chemical analysis of these samples was carried out. Elemental components of these samples were determined by means of particle induced X-ray emission (PIXE) analysis. Ionic species (anions: F^-, Cl^-, NO_2^-, Br^-, NO_3^-, PO_4^{3-} and SO_4^{2-}; cations: Na^+, NH_4^+, K^+, Mg^{2+} and Ca^{2+}) of these samples were analyzed by ion chromatography.

This present study focuses on the chemical characterization of PM in a mountainous region by elemental and ionic components and examines the effect of atmospheric pollutants transported to Japan from the Northeast Asian regions.

2. MATERIALS AND METHOD

PM sampling was carried out on the west side of Mt. Moriyoshi near the summit, from 1 – 16 February (winter period) and 7 – 19 July (summer period) in 2004. The PM sampling was actually performed approximately 2 m above the ground. The PM was collected using a 3-stage NLAS impactor (Tokyo Dylec Co., Ltd.; particle cut-size of stages was 10 μm, 2.5 μm and 1.0 μm for a flow rate of 3 L/min) with a two-day or three-day sampling interval on a polycarbonate filter (Nuclepore®, diameter: 25 mmΦ, pore size: 0.2 μm) and a PTFE ultra-membrane filter (HORIBA Ltd., TFH-47, diameter: 47 mmΦ). Note that HORIBA TFH-47 was used as a backup filter and that approximately 0.15% of TiO_2 is present in HORIBA TFH-47. These filter samples of size-resolved PM were stored in Millipore PetriSlide® containers and kept in portable refrigerators during transport back to the laboratory, and they were stored in a freezer (–35°C) until they were analyzed.

Elemental compositions of each size-resolved PM filter sample were determined by PIXE at Nishina Memorial Cyclotron Center, Japan Radioisotope Association. For PIXE analysis, the filter samples were mounted on a Mylar® target frame and bombarded with 2.9 MeV protons from a small-size cyclotron (Sera et al., 1992). Beam currents, the accumulated charge and the typical measuring time were 20–45 nA, 23–60 μC, and 20–22 min, respectively for the Nuclepore filter samples. For the HORIBA filter samples, these were 5–16 nA, 3–13 μC, and 9–14 min, respectively. X-ray spectra were analyzed using the SAPIX program (Sera et al., 1992). Quantitative analysis of elemental values was performed based on the Nuclepore-Br method (Sera et al., 1997). Moreover, blank filters were analyzed with all the procedures. As for the accuracy of the PIXE analysis, it was confirmed by analysis using NIST standard reference materials (Saitoh et al., 2002; Saitoh et al., 2003).

Ionic species in each size-resolved PM filter sample were determined by ion chromatography (Metrohm, Compact IC 761 for anions and Personal IC 790 for cations).

For ion chromatography analysis, half of the Nuclepore filter samples and a quarter of the HORIBA filter samples were directly treated with 10 mL of ultrapure water (made by Milli-Q Labo) for 20 min using an ultrasonic apparatus. Regarding the operating conditions during ion chromatography, the sample injection volume was 200 μL and the full-scale range of conductivity detection was 50 μS for anions. For cations, the full-scale range of conductivity detection was 1000 μS. Blank filters were analyzed with all the procedures, and the concentrations of ionic species that could be measured for the blank filters were always below the minimum determination limits. Ionic species concentrations were determined based on calibration curves generated from analysis of the continuing calibration standard solutions. Wako Pure Chemical Industries, Ltd.'s 1000 mg/L standard was used for standard solutions. The concentration of calibration standard solutions is zero (ultrapure water; made by Milli-Q Labo), 0.001, 0.005, 0.01, 0.05, 0.1, 0.5, 1 and 2 mg/L. For generation of calibration curves, determination of each concentration was repeated five times.

3. RESULTS AND DISCUSSION

In PIXE analysis of each size-resolved PM filter sample, 23 elements (Na, Mg, Al, Si, S, Cl, K, Ca, Ti, V, Cr, Mn, Fe, Ni, Cu, Zn, Ga, As, Se, Br, Rb, Sr and Pb) were determined in total. Errors for the analytical results are mainly from the spectrum fitting, the detection efficiency and the values of X-ray transmission through the absorber. For the Nuclepore filter samples, estimated relative error (100 × error/count, in %) was smaller than 10% for eight elements (Na, Al, S, K, Ca, Fe, Zn and Br), 10 – 20% for five elements (Si, Cr, Mn, Cu and Pb) and 20 – 40% for four elements (Mg, Ti, Ga and Se). For the HORIBA filter samples, estimated relative error was smaller than 10% for two elements (Cl and Ca), 10 – 20% for five elements (Na, S, Fe, Ni and Zn) and 20 – 40% for four elements (Si, K, Br and Pb).

Tables 1 and 2 show the arithmetic mean concentration and the minimum and maximum values of elemental concentrations in each size-resolved PM for the winter and summer periods. Because approximately 0.15% of TiO_2 is contained in the backup filter, Ti, V and Cr concentrations in the PM on the backup filter is difficult to determine by PIXE analysis.

The major elemental components of each size-resolved PM sample, *i.e.*, $>PM_{10}$, $PM_{10} - PM_{2.5}$, $PM_{2.5} - PM_{1.0}$ and $<PM_{1.0}$, were Na, Mg, Al, Si, S, Cl, K, Ca and Fe for both the winter and summer periods. For the major components, in the size-resolved PM samples of the winter period, concentrations of Na, Al and Cl in $PM_{10} - PM_{2.5}$ particles are several times higher than those in other particle sizes, and these are not detected in particles $<PM_{1.0}$. However, S concentration in particles $<PM_{1.0}$ is several times higher than this in other particle sizes. Mg, Si, Ca and Fe reveal a high concentration in $PM_{10} - PM_{2.5}$ particles, and $PM_{2.5} - PM_{1.0}$ particles for K. On the other hand, in the summer period, as for $PM_{10} - PM_{2.5}$ particles, concentrations of Na, Cl, Si and Fe are several times higher than those in other particle sizes, and Na, Al and Cl are detected in particles $<PM_{1.0}$. S reveals a high concentration in particles $<PM_{1.0}$ and $PM_{2.5} - PM_{1.0}$ particles. Al shows a high concentration in $PM_{10} - PM_{2.5}$ and $PM_{2.5} - PM_{1.0}$ particles, $PM_{10} - PM_{2.5}$

particles for Mn and Ca, $PM_{2.5} - PM_{1.0}$ particles for K. Comparing the arithmetic means of major elemental concentrations in the particles $>PM_{1.0}$, $PM_{10} - PM_{2.5}$, $PM_{2.5} - PM_{1.0}$ and $<PM_{1.0}$ for the winter and summer periods, elemental concentrations in the summer period samples are a little higher than the elemental concentrations in the winter period samples.

Table 1. Elemental concentrations (ng/m^3) of the size-resolved PM during winter period at Mt. Moriyoshi*

Element	$>PM_{10}$		PM_{10}-$PM_{2.5}$		$PM_{2.5}$-$PM_{1.0}$		$<PM_{1.0}$	
	Mean	Min - Max	Mean	Min - Max	Mean	Min - Max	Mean	Min - Max
Na	27.9	ND** - 72.1	190	71.3 - 285	25.9	19.8 - 31.8	–	ND
Mg	9.9	ND - 20.5	47.7	19.4 - 61.0	34.4	ND - 56.7	–	ND
Al	8.0	ND - 14.4	102	23.8 - 208	47.6	29.1 - 94.1	–	ND
Si	24.8	9.7 - 61.2	243	74.3 - 560	98.6	70.4 - 148	102	ND - 254
S	17.0	8.5 - 36.5	83.0	44.2 - 116	200	130 - 301	660	473 - 762
Cl	18.1	ND - 59.7	154	37.8 - 283	12.7	ND - 28.2	–	ND
K	3.1	ND - 6.6	21.3	8.0 - 41.8	34.9	18.2 - 57.1	10.4	ND - 51.8
Ca	8.4	1.3 - 22.0	56.3	11.0 - 94.2	17.8	8.9 - 27.2	44.5	16.3 - 122
Ti	0.2	ND - 0.6	3.5	1.2 - 7.5	2.0	1.5 - 3.3	Non-determination	
V	–	ND	0.3	ND - 0.7	0.2	ND - 0.7	Non-determination	
Cr	0.1	ND - 0.2	0.2	ND - 0.7	0.2	ND - 0.6	Non-determination	
Mn	0.1	ND - 0.2	1.6	0.5 - 3.0	3.6	1.4 - 7.8	–	ND
Fe	2.4	0.1 - 6.3	39.2	9.0 - 85.9	21.8	15.1 - 27.6	14.6	9.2 - 28.9
Ni	–	ND	0.1	ND - 0.3	0.1	ND - 0.3	0.5	ND - 1.3
Cu	–	ND	0.2	ND - 0.5	0.1	ND - 0.2	0.2	ND - 1.2
Zn	0.8	ND - 3.8	1.4	0.6 - 2.2	5.3	3.4 - 8.3	4.7	3.0 - 9.2
Ga	–	ND	–	ND	–	ND	2.0	ND - 5.5
As	–	ND	0.2	ND - 0.4	0.4	0.2 - 0.6	1.5	ND - 3.6
Se	–	ND	0.1	ND - 0.3	0.1	ND - 0.2	0.3	ND - 1.7
Br	0.4	0.2 - 0.7	1.3	0.8 - 1.9	0.9	0.5 - 1.4	3.7	ND - 10.6
Rb	–	ND	0.1	ND - 0.3	–	ND	1.3	ND - 6.5
Sr	0.1	ND - 0.4	0.3	ND - 0.5	–	ND	2.9	ND - 14.4
Pb	0.1	ND - 0.2	0.5	ND - 1.2	2.8	1.6 - 4.0	2.4	ND - 7.4

*: Mean, minimum and maximum of five samples. **: Not detectable. Not detectable cases were assumed to be zero for calculation of mean.

Table 2. Elemental concentrations (ng/m^3) of the size-resolved PM during summer period at Mt. Moriyoshi*

Element	>PM_{10}		PM_{10}-$PM_{2.5}$		$PM_{2.5}$-$PM_{1.0}$		<$PM_{1.0}$	
	Mean	Min - Max	Mean	Min - Max	Mean	Min - Max	Mean	Min - Max
Na	42.3	ND** - 145	210	155 - 340	86.7	28.1 - 133	114	ND - 434
Mg	21.4	ND - 70.5	68.6	25.3 - 138	43.8	21.3 - 78.4	14.5	ND - 72.5
Al	65.0	ND - 248	219	41.4 - 609	228	24.6 - 496	15.0	ND - 74.9
Si	34.5	22.0 - 53.2	304	101 - 629	146	29.8 - 294	71.2	27.7 - 97.0
S	31.1	9.0 - 71.1	201	77.6 - 530	1470	47.2 - 3320	1070	150 - 2650
Cl	49.5	ND - 237	136	ND - 274	5.6	ND - 27.9	69.4	ND - 347
K	2.9	2.3 - 3.5	56.7	5.7 - 109	71.0	8.0 - 195	33.4	17.8 - 48.2
Ca	10.5	1.2 - 42.4	71.3	35.3 - 165	20.2	11.0 - 35.6	49.5	17.2 - 129
Ti	0.2	ND - 0.4	5.6	1.7 - 14.2	2.4	0.7 - 6.1	Non-determination	
V	–	ND	–	ND	0.3	ND - 1.0	Non-determination	
Cr	0.9	ND - 4.6	0.2	ND - 0.8	0.2	ND - 0.7	Non-determination	
Mn	0.2	ND - 0.5	1.8	0.4 - 4.6	1.8	0.2 - 4.5	–	ND
Fe	7.6	0.7 - 31.2	64.0	6.0 - 185	29.1	2.1 - 76.9	10.3	3.4 - 25.0
Ni	0.4	ND - 1.8	0.3	ND - 0.8	0.3	ND - 0.7	0.9	ND - 4.3
Cu	0.1	ND - 0.5	1.6	0.3 - 2.6	0.7	ND - 1.5	0.2	ND - 1.0
Zn	0.5	ND - 2.1	5.4	0.5 - 18.0	12.9	0.3 - 39.7	4.8	ND - 13.4
Ga	–	ND	–	ND	0.1	ND - 0.5	0.7	ND - 1.2
As	–	ND	–	ND	0.1	ND - 0.3	–	ND
Se	–	ND	–	ND	0.1	ND - 0.4	–	ND
Br	0.6	0.4 - 0.8	2.2	1.6 - 3.0	2.0	0.8 - 3.1	2.4	ND - 5.5
Rb	–	ND	–	ND	0.1	ND - 0.6	–	ND
Sr	0.1	ND - 0.3	2.6	ND - 0.5	0.1	ND - 0.4	–	ND
Pb	0.1	ND - 0.5	2.0	0.9 - 5.2	6.2	ND - 20.2	3.7	ND - 12.9

*: Mean, minimum and maximum of five samples. **: Not detectable. Not detectable cases were assumed to be zero for calculation of mean.

As for ionic species, F^-, Cl^-, NO_2^-, NO_3^-, SO_4^{2-}, Na^+, NH_4^+, K^+, Mg^{2+} and Ca^{2+} were determined. The major ion components in the winter period samples were Cl^-, NO_3^-, SO_4^{2-}, Na^+ and NH_4^+, and these plus NO_2^- in the summer period samples. The determination limit of anions is 0.005 mg/L (0.005 – 0.012 μg/m^3), except for Cl^-, NO_2^- and SO_4^{2-}. The determination limit of Cl^-, NO_2^- and SO_4^{2-} is 0.01 mg/L (0.009 – 0.025 μg/m^3). For cations, the determination limit is 0.01 mg/L (0.009 – 0.025 μg/m^3). The detection limit is 0.001 mg/L (0.001 – 0.002 μg/m^3) for all the ionic species, and concentrations of Br^- and PO_4^{3-} were smaller than 0.002 μg/m^3 for all the samples.

Tables 3 and 4 show the arithmetic mean concentration and minimum and maximum values of ionic species concentrations in each size-resolved PM for the winter and summer periods. In the winter period, concentrations of Cl^-, NO_3^- and Na^+ in PM_{10} –

$PM_{2.5}$ particles are several times higher than those in the other particle sizes. However, SO_4^{2-} and NH_4^+ reveal a high concentration in particles $<PM_{1.0}$. On the other hand, in the summer period, Na^+ reveals a high concentration in $PM_{10} - PM_{2.5}$ particles, but NO_3^-

Table 3. Ionic species ($\mu g/m^3$) of the size-resolved PM during winter period at Mt. Moriyoshi*

Element	$>PM_{10}$		PM_{10}-$PM_{2.5}$		$PM_{2.5}$-$PM_{1.0}$		$<PM_{1.0}$	
	Mean	Min - Max	Mean	Min - Max	Mean	Min - Max	Mean	Min - Max
F^-	0.002	ND** - *0.005*	0.005	ND - 0.012	0.001	ND - *0.006*	0.005	ND - 0.024
Cl^-	0.056	0.024 - 0.087	0.089	0.035 - 0.152	0.037	0.008 - 0.082	–	ND
NO_2^-	0.004	ND - *0.012*	0.002	ND - *0.005*	0.004	ND - 0.010	0.055	ND - 0.118
Br^-	–	ND	–	ND	–	ND	–	ND
NO_3^-	0.041	ND - 0.077	0.119	0.035 - 0.231	0.096	0.041 - 0.177	0.107	0.077 - 0.141
PO_4^{3-}	–	ND	–	ND	–	ND	–	ND
SO_4^{2-}	0.075	0.046 - 0.135	0.326	0.060 - 1.200	0.395	0.251 - 0.558	1.679	1.398 - 2.179
Na^+	0.035	0.011 - 0.066	0.067	0.033 - 0.100	0.022	0.002 - 0.056	0.023	ND - 0.073
NH_4^+	0.056	0.046 - 0.074	0.063	0.051 - 0.084	0.152	0.098 - 0.213	0.519	0.294 - 0.909
K^+	0.046	0.014 - 0.080	0.054	0.008 - 0.121	0.033	ND - 0.072	0.081	0.019 - 0.109
Mg^{2+}	–	ND	–	ND	0.004	ND - 0.022	0.026	ND - 0.077
Ca^{2+}	0.013	ND - 0.025	0.015	*0.006* - 0.026	0.034	0.025 - 0.040	–	ND

Indication of italic and under bar is value of under the determination limit. *: Mean, minimum and maximum of five samples. **: Not detectable. Not detectable cases were assumed to be zero for calculation of mean.

Table 4. Ionic species ($\mu g/m^3$) of the size-resolved PM during summer period at Mt. Moriyoshi*

Element	$>PM_{10}$		PM_{10}-$PM_{2.5}$		$PM_{2.5}$-$PM_{1.0}$		$<PM_{1.0}$	
	Mean	Min - Max	Mean	Min - Max	Mean	Min - Max	Mean	Min - Max
F^-	0.007	*0.003* - 0.012	0.010	*0.005* - 0.020	0.015	0.008 - 0.028	0.049	ND - 0.129
Cl^-	0.101	*0.007* - 0.399	0.093	ND - 0.216	0.026	0.003 - 0.051	0.078	ND - 0.277
NO_2^-	0.072	0.020 - 0.122	0.117	0.033 - 0.341	0.118	0.044 - 0.161	0.117	0.084 - 0.181
Br^-	–	ND**	–	ND	–	ND	–	ND
NO_3^-	0.077	0.002 - 0.139	0.172	0.062 - 0.241	0.067	0.021 - 0.136	0.883	0.005 - 4.365
PO_4^{3-}	–	ND	–	ND	–	ND	–	ND
SO_4^{2-}	0.097	0.022 - 0.223	0.376	0.111 - 1.192	2.016	0.028 - 6.370	2.786	0.362 - 6.233
Na^+	0.063	ND - 0.188	0.103	0.030 - 0.167	0.043	0.021 - 0.062	0.002	ND - 0.012
NH_4^+	0.020	*0.009* - 0.037	0.084	*0.009* - 0.364	0.555	*0.012* - 1.897	1.027	0.162 - 2.341
K^+	0.018	ND - 0.065	0.019	ND - 0.034	0.010	ND - 0.042	–	ND
Mg^{2+}	–	ND	0.004	ND - 0.019	0.015	ND - 0.062	–	ND
Ca^{2+}	0.013	ND - 0.039	0.021	ND - 0.032	0.018	*0.011* - 0.030	–	ND

Indication of italic and under bar is value of under the determination limit. *: Mean, minimum and maximum of five samples. **: Not detectable. Not detectable cases were assumed to be zero for calculation of mean.

shows a high concentration in particles <$PM_{1.0}$. Cl^- exhibits a low concentration in $PM_{2.5}$ – $PM_{1.0}$ particles. NO_2^- concentration do not differ with particle size. SO_4^{2-} and NH_4^+ are similar in the winter period samples. Comparing the arithmetic means of ionic species concentrations in the >$PM_{1.0}$, PM_{10} – $PM_{2.5}$, $PM_{2.5}$ – $PM_{1.0}$ and <$PM_{1.0}$ particles for the winter and summer periods, like the elements, the ionic species concentrations in the summer period samples are a little higher than the ionic species concentrations in the winter period samples.

From elemental ionic species analysis results of the size-resolved PM samples, in the winter period, it is suggested that soil and sea-salt particles from PM_{10} to $PM_{2.5}$ in size and ammonium sulfate particles, *i.e.*, secondary-formed particles <$PM_{1.0}$, have been transported to Japan from the continent. On the other hand, in the summer period, it is suggested that PM was formed from soil and sea-salt particles >PM_{10} to $PM_{2.5}$ in size and secondary-formed particles <$PM_{1.0}$. The existent forms of chemical components in aerosol particles in a mountainous region will be an important factor when we consider the origin of air pollutants transported over long distances in Northeast Asian regions. Moreover, the chemical data in aerosol particles in a mountainous region will be important when judging aerosol particles in large cities or their environs.

4. ACKNOWLEDGEMENTS

This study has been financially supported by the Earth Environment Foundation in Japan and the Takizawa Institute Foundation in Japan. And we wish to thank the staff of Ani Ski Area for sampling of airborne particulate matter.

REFERENCES

Mizoguchi, T., 1991. Global environmental conservation and acid rain. Journal of Water and Waste 33, 13-19. (in Japanese)

Nagafuchi, O., 2000. Long-range transport of air pollutants and the present condition of forest decline in Yakushima Island. Japanese Journal Ecology 50, 303-309. (in Japanese)

Saitoh, K., Sera, K., Gotoh, T., Nakamura, M., 2002. Comparison of elemental quantity by PIXE and ICP-MS and/or ICP-AES for NIST standards. Nucl. Instr. and Meth. in Phys. Res. B 189, 86-93.

Saitoh, K., Sera K., Shimomura, K., 2003. PIXE analysis of NIST urban particulate matter collected on a polycarbonate membrane filter. Int. J. PIXE 13, 141–147.

Sera, K., Yanagisawa, T., Tsunoda, H., Hutatukawa, S., Saitoh, Y., Suzuki, S., Orihara, H., 1992. Bio-PIXE at the Takizawa facility (Bio-PIXE with a baby cyclotron). Int. J. PIXE 2, 325–330.

Sera, K., Futatsugawa, S., Saitoh, K., 1997. Method of quantitative analysis making use of bromine in a Nuclepore filter. Int. J. PIXE 7, 71–85.

Proceedings of the Third International Symposium on Air Quality Management at Urban, Regional and Global Scales. 26-30 September 2005, Istanbul – Turkey

DETERMINATION OF NITROGEN-CONTAINING PAH's IN AEROSOLS BY LC/MS/MS

Monica Pantiru, Jutta Lintelmann and Georg Matuschek

GSF – National Research Center for Environment and Health,
Institute of Ecological Chemistry, Network-Focus: Aerosols and Health,
PO Box 1129, D-85764 Neuherberg, Germany
pantiru@gsf.de, lintelmann@gsf.de, matuschek@gsf.de

ABSTRACT

A new method for the determination of 17 basic azaarenes and 5 amino-PAH's is presented. The analysis is performed using high performance liquid chromatography coupled with tandem mass spectrometry. As ionization technique the atmospheric pressure chemical ionization was employed. For the quantification of the analytes one precursor ion and two daughter ions per substance were selected. The procedure reaches LOQ from 2-50 pg/µl, corresponding to a concentration of 0.2-0.5 pg/m^3.

Key Words: Aerosol, Amino-PAH, APCI, Azaarene, LC/MS/MS

1. INTRODUCTION

Plenty of health hazard research questions have addressed the volatile and semi volatile nature of the ambient aerosol. However, the knowledge about more polar, less volatile substances still remains very limited. The N-PAH's belong to the chemical characteristics of the particulate air pollution responsible for health effects.
N-PAH's are commonly found in fossil fuels and their derivatives, although some may also form during combustion processes. They have been identified in tobacco smoke (Wynder and Hoffman, 1967), automobile exhaust (Grimmer, 1985), atmospheric particulates (Chen and Preston, 1998), crude oil (Grimmer et al., 1983), river and lake sediments (Wakeham, 1979), sewage (Bodzek et al., 1999) and charcoal-grilled meat (Janoszka et al., 2004).
Relative to their parent PAH's, the N-PAH's are more soluble in aqueous environments. Increased water solubility results in an increased potential for harm. For example, 1-aminopyrene demonstrates a 50-fold increase in mutagenic activity compared to the parent PAH, pyrene (Ho et al., 1981). Although N-PAH's are only present in trace amounts, care must be taken to avoid exposure due to their carcinogenic and mutagenic nature (Seixas et al., 1982, Matsuoka et al., 1982).
In order to identify and differentiate N-PAH's, many investigators have used the chromatographic techniques because of their high resolving power. These techniques have included gas (Schmitter et al., 1982, Kamata et al., 1992), thin layer (Kamata and Motohashi, 1987), supercritical fluid (Ashraf-Korassani and Taylor, 1988), and liquid chromatography (Colin et al., 1981, Schmitter et al., 1982, Borra et al., 1987, Motohashi et al., 1991, Carlsson and Östman, 1995, Wilhelm et al., 2000).

Both the low concentration level of these analytes and the complexity of the ambient aerosol matrix require the development of a selective and sensitive analytical method. Characterized by sensitivity and selectivity, the LC-MS/MS was until now not exploited for the analysis of N-PAH's.
In this study, in order to provide an analytical method which can be implemented in epidemiological studies, a high-throughput-LC/MS/MS-based method was developed for the determination of N-PAH's in aerosols.

2. EXPERIMENTAL

Materials investigated
The urban dust (SRM 1649a) is a certified reference material from the National Institute of Standards and Technology (Promochem, Wesel, Germany). This material was investigated for the presence of the analysed substances as a sample matrix. Two Chinese urban dust samples were also analyzed for the compounds.

Aerosol samples
The aerosols samples were collected on an intersection on a well-driven countryside highway near Munich. A high-volume sampler (HVS, Anderson) was used to collect filter samples of fine particulate matter ($PM_{2,5}$), operating for 24 hours at a rate of 800 L/min. Quartz-fibre filters, 203 mm x 254 mm (QF 20, Schleicher und Schuell) were used in the HVS. The filters were heated before use at 773 K for at least 12 hours in a muffle furnace (Heraeus, Hanau, Germany) to remove organic contaminants. After sampling the filters were wrapped in aluminium foil and placed in a desiccator at 4 °C until analysis.
2 aerosol samples, collected in January and February 2005, were tested for the presence of N-compounds, investigating the applicability of the LC/MS/MS for analysis of real samples.

Chemicals
1-aminonaphtalene (1ANaph), 2-aminofluorene (2AFl), 2-aminoanthracene (2AAnt), 6-aminochrysene (6AChr) and phenanthridine (Phe) were purchased from Sigma-Aldrich, Steinheim, Germany. 1-aminopyrene (1APyr) was from Fluka Chemie AG, Buchs, Switzerland. Acridine (Acr), benzo(a)acridine (BaA), benzo(c)acridine(BcA), dibenzo[a,j]acridine (DbajA), dibenzo[a,c]acridine (DbacA), dibenzo[a,h]acridine (DbahA), dibenzo[a,i]acridine (DbaiA) and 10-azabenzo(a)pyrene (10AbaP) came from Dr. Ehrenstorfer GmbH, Augsburg, Germany. 7,9-dimethylbenzo(c)acridine (7,9-DmbcA) and 7,10-dimethylbenzo(c)acridine (7,10-DmbcA) were from Sigma-Aldrich, Milwaukee, Wisconsin, USA.
Dibenzo[c,h]acridine (DbchA), 4-azapyrene (4APyr), 1-azafluoranthene (1AFlu) and 4-azafluorene (4AFl) came from the PAH research institute, Greifenberg, Germany. Benzo(f)quinoline (BfQ) and benzo(h)quinoline (BhQ) were from Ultra Scientific, North Kingstown, Rhode Island, USA.
Methanol was purchased from Merck KGA, Darmstadt, Germany, acetonitrile from Sigma-Aldrich, Steinheim, Germany, whereas the water came from a Milli-Q Ultra Plus Water System, Millipore GmbH, Schwalbach, Germany. BcA and BaA were purchased as 10 ng/µl solutions in iso-octane, 10AbaP, DbahA, DbajA, DbaiA and

DbacA as 10 ng/µl solutions in acetonitrile. Stock solutions were prepared with the other substances at a concentration of 100 ng/µl in acetonitrile. The base standards had a concentration of 10 ng/µl for amino-PAH's and 1 ng/µl for azaarenes, in acetonitrile, from which work standards were prepared by dilution.

Instrumentals

The Agilent Technologies HPLC 1100 Series tower (Palo Alto, California, USA) included a G1316A column oven, a G1329A autosampler with thermostat (G1330A), a G1311A quaternary pump and a G1322A degasser. The injected sample volume was 10 µl. Samples were chromatographed on a Gemini C18 (250 x 4.6 mm, 5µ) column from Phenomenex (Aschaffenburg, Germany) equipped with an equal-branded pre-column. Eluent A was 0.1 % formic acid in water and eluent B was methanol, with 800 µl/min flow. The gradient was increased from 70 % methanol to 90 % in 13 min, then to 100 % in 4 min and held for the next 8 min. Over the last 5 min the column was equilibrated prior to the next injection. The column oven had a temperature of 45 °C and the total analysis time was 30 min. The detection was carried out on an API 2000 Triple Quad mass spectrometer from Applied Biosystems (Toronto, Canada) equipped with an APCI ionization source. For system control and data acquisition the Analyst software version 1.4 from Applied Biosystems was used. Following source parameters were employed: TEM 475 °C, NC 2 µA, CUR 24 psi, CAD 5 psi, GS1 80 psi, GS2 50 psi. The focussing potential FP was optimized and fixed on 350 V.

Sample preparation

The urban dust sample was prepared by the procedure of Lintelmann et al. (Lintelmann et al., 2005). The Chinese urban dust samples were prepared as follows: 200 mg sample was weighed in a 75 ml centrifuge tube and 20 ml dichloromethane were added. The tube was closed and sonicated in an ultrasonic bath (Bandelin, Berlin, Germany) for two hours, shaking lightly every 15 minutes. The extracts were filtered on 597 1/2 folded paper filters (Schleicher and Schuell, Dassel, Germany), collected in 100 ml reduction flasks and reduced to a volume of ca. 1 ml on a VV 2000 Heidolph rotation evaporator (Kelheim, Germany) equipped with a Vacuubrand PC5 diaphragm pump (Wertheim, Germany). The residual solution was transferred in a 2 ml volumetric flask and completely evaporated under nitrogen stream in a Barkey (Leopoldshöhe, Germany) Vapotherm mobil S unit. 500 µl acetonitrile were added and sonicated shortly to support the dissolvation of the residue. The solution was filtered with a 0.2 µm Spartan 13/0.2 RC filter unit (Schleicher and Schuell) into an autosampler vial and subjected to LC/MS/MS analysis.

For each high-volume real sample one third of the filter was cut in small pieces, introduced in a 75 ml centrifuge bottle and sonicated with 40 ml methanol / dichloromethane 1:1 for 45 min. The samples were transferred in 100 ml reduction flasks and evaporated to a volume of 2 ml on the rotation evaporator. The residual solutions were transferred in volumetric flasks and evaporated to approx. 70 µl under a nitrogen stream. 30 µl acetonitrile were added, the samples were shortly sonicated and filtered in autosampler vials.

3. RESULTS AND DISCUSSION

Transitions and MS/MS parameters

The characteristic fragmentation pattern of each compound was used to build three transitions. The SIM (Single Ion Monitoring) as qualifier and the two most sensitive MRM (Multiple Reaction Monitoring) as quantifiers were selected for each compound. The precursor ions were found performing a Q1 total ion current scan for every substance from 50 up to 50 amu above their respective molecular weights.

A built-in syringe-pump was used for infusion of standard solutions of substances with 10 ng/µl each into the APCI interface, with collision-activated dissociation CAD gas set at 0. No adducts were formed during ionization, therefore the molecular ion $[M+H]^+$ was chosen as precursor.

The ionization parameters of the parent ions, i.e., declustering potential DP, focussing potential, entrance potential EP, and collision cell entrance potential CEP were optimized automatically and used for the product ion scan by collision-activated dissociation gas on. For the two most abundant product ions the ionization parameters, i.e., collision cell energy CE and collision cell exit potential CXP were then manually optimized.

Figure 1 shows a typical product ion scan of Benzo(a)acridine. The ions at masses m/z 202.1 and 201.1 correspond to $[M+H - CH_3N]$ and $[M+H - C_2H_4]$, respectively. The MS/MS transitions of the 22 aromatic compounds studied are summarized in Table 1.

The APCI source parameters, i.e., nebulizer gas GS1, auxiliary gas GS2, temperature TEM, curtain gas CUR and collision gas CAD in Q3 were all optimized manually by flow injection experiments.

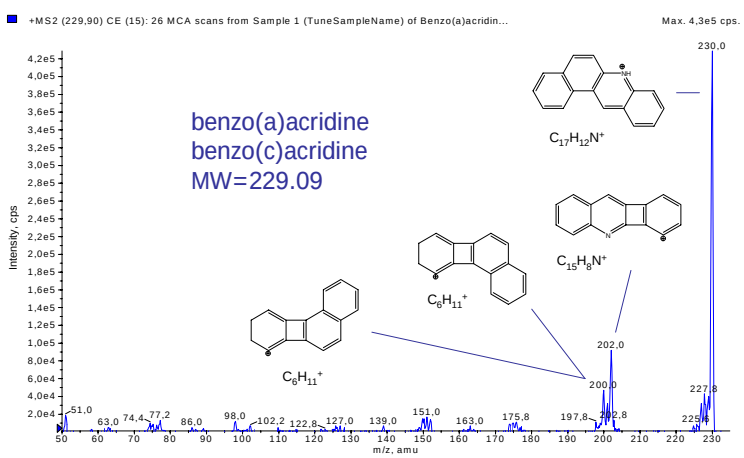

Figure 1. Typical product ion scan and fragmentation of the *m/z* 230.1

HPLC- method development

Based on the work of Bohn et al. (Bohn et al., 2004) experiments were conducted in order to reach a satisfying separation of the compounds. In principle, the baseline separation of all the compounds is not important, since the co-eluting compounds are resolved by the "two-dimensional" selectivity provided by the mass spectrometer.

Table 1. Selected transitions and parameters of the analysed compounds

Analyse	MW amu	Transition m/z	DP V	EP V	CEP V	CE V	CXP V
1ANaph	143.19	143.9 → 143.9	22	12	8	12	12
		143.9 → 126.9	25	11	8	33	11
		143.9 → 117.1	22	11	8	33	11
2AFlu	181.24	182.0 → 182.0	22	12	8	12	15
		182.0 → 165.1	20	10	8	33	14
		182.0 → 164.0	20	10	10	48	15
2AAnt	193.25	193.9 → 193.9	25	12	8	15	16
		193.9 → 177.0	28	9	7	34	15
		193.9 → 165.1	35	11	10	57	12
1APyr	217.27	218.1 → 218.1	25	10	10	14	21
		218.1 → 201.9	25	10	10	37	18
		218.1 → 188.9	22	10	11	68	15
6AChr	243.31	244.0 → 244.0	25	11	8	15	21
		244.0 → 227.1	25	9	7	38	19
		244.0 → 226.1	22	10	8	50	19
10Abap	253.31	254.0 → 254.0	20	10	8	15	21
		254.0 → 227.1	30	10	8	62	21
		254.0 → 226.1	60	10	8	65	21
4AFl	167.21	167.9 → 167.9	15	6	9	15	14
		167.9 → 138.9	20	6	9	40	10
		167.9 → 141.1	25	6	9	65	10
4APyr; 1AFlu	203.24	204.1 → 204.1	45; 20	12	7	15	17
		204.1 → 175.9	55	12	15	60	6
		204.1 → 151.1	55	12	15	60	6
BaA; BcA	229.28	230.1 → 230.1	25	10	10	20	21
		230.1 → 201.9	25; 20	10	15	55	18
		230.1 → 201.1	55; 75	10	15	65	18
DbaiA; DbajA	279.34	280.0 → 280.0	20	6	12	12; 10	12
		280.0 → 252.1	15; 20	8	8	65; 60	21
		280.0 → 251.1	47; 10	8	8	80	21
DbahA; DbacA	279.34	280.0 → 280.0	25	6	12	20	12
		280.0 → 252.1	15	8	8	65	21
		280.0 → 251.1	25	8	8	80	21
DbchA	279.34	280.0 → 280.0	25	8	8	12	21
		280.0 → 252.1	15	8	8	65	21
		280.0 → 251.1	25	8	8	75	21
7,9-DmbcA; 7,10-DmbcA	257.34	258.1 → 258.1	30	12	12	15; 12	12
		258.1 → 242.1	20	12	12	50; 55	15
		258.1 → 241.0	25; 40	12	12	55; 52	15
Acr; Phe	179.22	179.9 → 179.9	30; 25	12	10	15; 16	15
		179.9 → 151.9	20	11	6	50; 47	11
		179.9 → 126.9	25	11	6	55	11
BfQ; BhQ	179.22	179.9 → 179.9	25; 30	12	10	10; 15	15
		179.9 → 151.9	25; 20	11	6	53; 45	11
		179.9 → 126.9	15; 30	11	6	55	11

A third dimension had to be established by means of chromatography, aiming at separating the isomers of the basic azaarenes, i.e., quinolines, benzoacridines, dibenzoacridines, dimethylbenzoacridines, 1-AFlu and 4APyr, showing identical transitions respectively (see Table 1). Bohn et al. used a BDS Hypersil C18 50 x 2.1 mm 3µ (Thermo Hypersil-Keystone) column, employing three separate methods for the determination of the basic azaarenes isomers with ammonium acetate 5 mM / methanol 50/50 as eluent. Further stationary phases like BDS Hypersil C18 50 x 2.1 mm 5µ, Luna Amino 50 x 2.1 mm 5µ, pH 1.5-10, Luna Cyano 50 x 2.1 mm 5µ, pH 1.5-7 and Gemini C18 Twin Technology 250 x 4.6 mm 5µ, pH 1-12 (Phenomenex), SunFire C18 150 x 3 mm 5µ, pH 2-8 and HILIC 150 x 4.6 mm 5µ, pH 1-6 (Waters), presented as appropriated for the separation of basic substances, were tested for the basic azaarenes. Combinations of methanol or acetonitrile with solutions and additives of pH values between 2 and 8 were also tested for the gradient elution. Figure 2 shows the possible co-elution of the azaarene isomers.

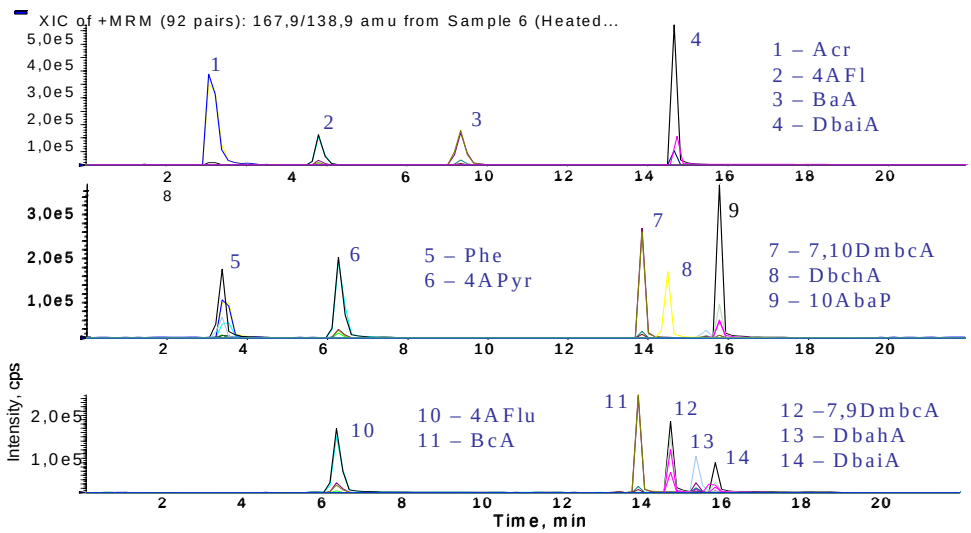

Figure 2. Elution of basic azaarenes using three separate methods on BDS 5µ column with ammonium acetate 5 mM/ methanol 50/50

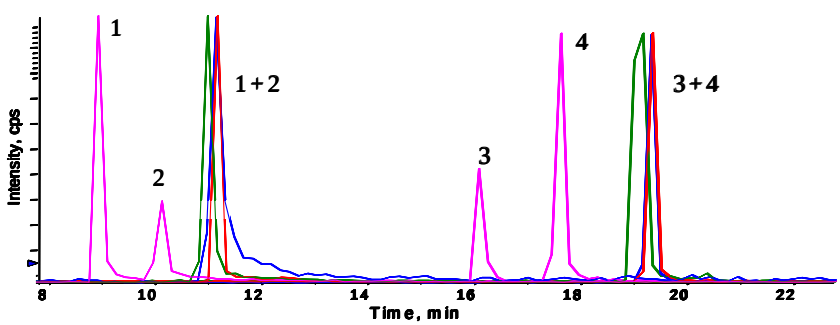

Figure 3. Separation of azaarene isomers

Only on the Gemini column the separation of these isomers succeeded. Figure 3 presents the separation of 1-azafluoranthene (1) and 4-azapyrene (2), respectively 7,9- (3) and 7,10-dimethylbenz(c)acridine (4). Beginning with 60 % acetonitrile and

using pH=8 (ammonium acetate + ammonia), pH=6.5 (10 mM ammonium acetate) or pH=3 (ammonium formiate + ammonia) the two couples of compounds could not be separated. The separation occurred finally with 0.1 % formic acid (pH=2.3), showing that both the pH value and the presence of ammonia ions influence the chromatographic separation of these substances.

The most problematic isomers are the dibenzoacridines, DbahA and DbacA, for which a partial separation could be reached using methanol instead of acetonitrile. Methanol is a protic solvent and interacts with the residual silanol groups of the stationary phase, resolving in this way the two compounds (Figure 4). A further factor, which can be employed in such delicate separation problems, is the oven temperature. In this study, setting the oven temperature on 45 °C amended their chromatographic separation further on. Their quasi co-elution is determined primarily by the steric hindrance of the nitrogen site, and the baseline separation can only be achieved by analysis times longer than 40 minutes, which however would not accomplish the goals of this work. The calculated resolution of the two peaks is 1.0, also less than 1.5 (the value normally used as the benchmark for baseline resolution), but sufficient for the correct integration of the peaks.

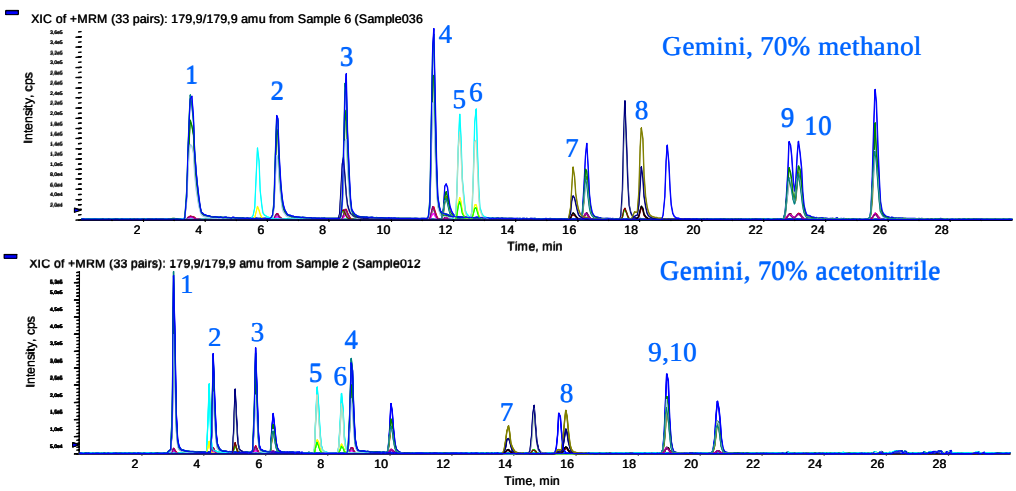

Figure 4. Comparison of organic eluents for the separation of the basic azaarenes
1 – acridine, 2 – benzo(f)quinoline, 3 – phenanthridine, 4 – benzo(h)quinoline,
5 – benzo(a)acridine, 6 – benzo(c)acridine
7 – 7,9-dimethylbenzo(c)acridine, 8 – 7,10-dimethylbenzo(c)acridine
9 – dibenzo(a,h)acridine, 10 – dibenzo(a,c)acridine

Figure 5 presents the optimized separation of the analysed compounds, with a 10 µl sample volume injected and a concentration of 250 pg/µl.
Enhancing the response is also possible by increasing the volume of sample injected. The injection of a double sample volume, 20 µl, do not affect the peak shape and produce also a signal increase of 12 to 80 %, therefore can be successfully applied for further analysis.

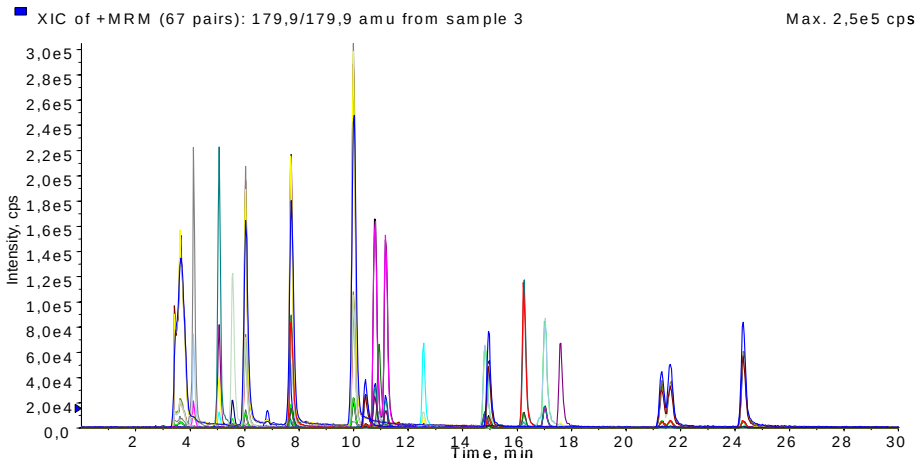

Figure 5. Optimized chromatogram of a standard mixture with 250 pg/µl

Real samples

The analysis of the SRM 1649a (urban dust) showed a considerable content of quinolines (Figure 6). The two Chinese urban dust samples were not revealing the analysed compounds, but the extraction method employed for this purpose is not optimized. The two high-volume filter samples contained 2 amino-PAH's and 10 basic azaarenes. The results are presented in Table 2. The limits of quantification were calculated using the signal/noise value delivered by the Analyst software.

Table 2. Analysis data of filter samples

	Retention time min	January pg/m^3	February pg/m^3	LOQ pg/µl
Acr	3.55	124	431	26
2AFlu	4.02	0	0	6
1ANaph	4.96	1	173	2
4AFl	5.46	1	5	5
BfQ	5.93	6	13	5
2AAnt	7.54	22	33	51
Phe	7.61	6	8	5
BaA	7.61	3	5	7
BhQ	9.92	7	12	5
DbaiA	10.3	0	0	51
4APyr	10.7	5	8	7
1APyr	10.9	0	0	4
1AFlu	11.1	6	10	10
6AChr	12.5	0	0	5
7,10-DmbcA	14.7	0	0	9
DbajA	14.9	0	0	14
BcA	16.2	4	7	11
7,9-DmbcA	17.0	1	1	7
10AbaP	17.6	0	0	8
DbahA	21.0	0	0	17
DbacA	21.8	0	0	17
DbchA	24.0	0	0	27

The stability of the retention time was checked by spiking one of the Chinese samples and comparing the observed values with the standard ones. All the retention times determined in the spiked sample were comprised in a 30 seconds retention time window, fixed during the creation of the quantification method.

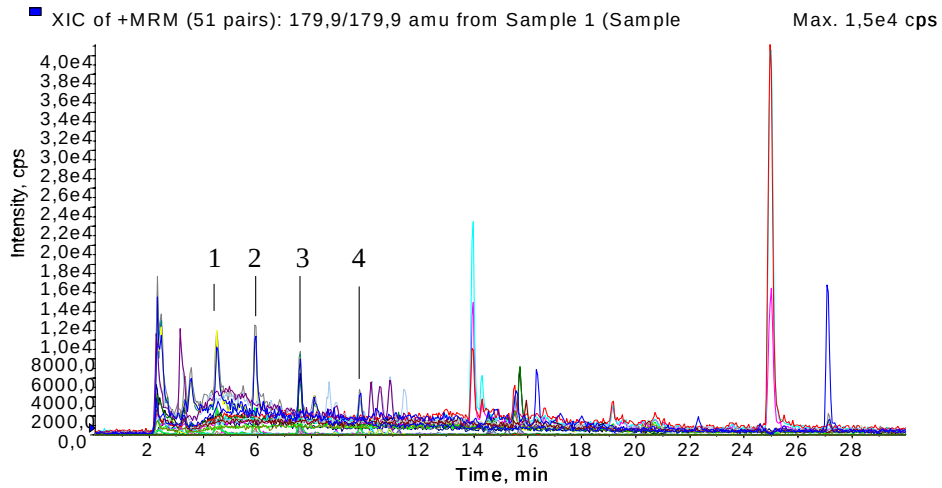

Figure 6. Chromatogramm of SRM 1649a, 1- acridine 18 ppb, 2- BfQ 16 ppb, 3-phenantridine 11 ppb and 4- BhQ 5 ppb.

Matrix effects

Considerable problems of the LC/MS/MS analysis are the so-called matrix effects. Their origins are complex, and the main problem sources are the organic and inorganic molecules present in the sample (Antignac et al., 2005).

The matrix effects underlie to the geometry of the ionization source and the kind of ionization (Souverain et al., 2004). Further influencing factors are for example the

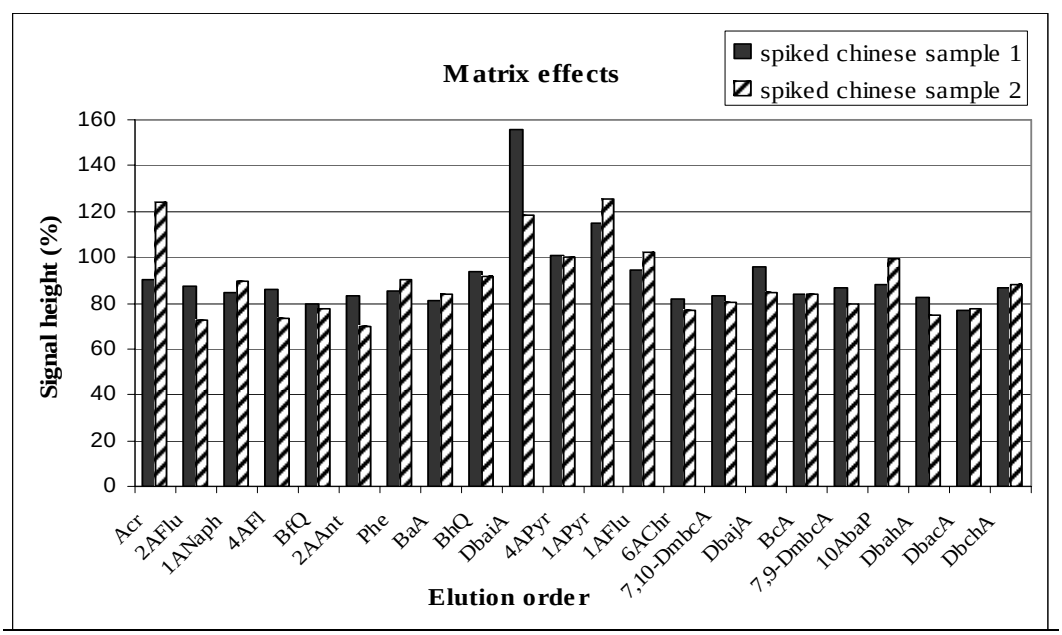

Figure 7. Ionization suppression and enhancement due to matrix compounds

physical and chemical properties of the analytes. As outputs, detection capability, repeatability, linearity and quantification are affected.
To verify the presence of matrix effects, the two Chinese sample extracts were spiked each with 250 pg/µl standard mixture, in triplicate, and analysed. Figure 7 shows the calculated recovery reported to the standard sample. Usually, the matrix effects lead to ionization suppression; however, in this study the enhancement of the ionization was also detected, but only for some compounds.

4. CONCLUSION

A new, unique method is presented for the determination of 5 amino-PAH's and 17 basic azaarenes, with good separation of isomers and limits of quantification between 2 and 50 pg/µl. The short analysis time allows the use of this method to complement the monitoring of epidemiological studies. Here, due to high sample throughput, only individually adjusted methods can be employed.
Further experiments are necessary for the development of a sample preparation procedure which allows the separation of co-extracted matrix compounds. The matrix effects have to be also studied and eliminated or at least compensated. For this purpose, the use of matrix-matched standards will be the most convenient choice.

5. AKNOWLEDGEMENTS

This work was performed within the GSF Focus Network Aerosols and Health.

REFERENCES

Antignac, J.-P., de Wasch, K., Monteau, F., De Brabander, H., Andre, F., Le Bizec, B., 2005. The ion suppression phenomenon in liquid-chromatography-mass spectrometry and its consequences in the filed of residue analysis. Anal. Chim. Acta 529, 129-136)
Ashraf-Khorassani, M. and Taylor, L.T., 1988. Chromatographic behaviour of polar compounds with liquid vs. supercritical fluid mobile phases. J. Chromatogr. Sci. 26, 331-336
Bodzek, D., Dobosz, C., Janoszka, B. and Konecki, J., 1999. Quantification of nitrogen-containing polycyclic aromatic compounds in sewage sludge by TLC-densitometry. J. Planar Chromatogr.—Mod. TLC 12, 265-268
Bohn, P., Wüst, A., Matuschek, G., 2004. Contribution of basic and neutral N-compounds to the adverse health effect of ambient aerosols. Poster at the International Workshop on Organic Speciation in Atmospheric Aerosol Research, April 5-7, Las Vegas, Nevada, USA
Borra, C., Wiesler, D. and Novotny, M., 1987. High-efficiency microcolumn liquid chromatography separation and spectral characterization of nitrogen-containing polycyclics from fossil fuels. Anal. Chem. 59, 339-343
Carlsson, H. and Östman, C., 1995. Retention mechanisms of polycylic aromatic nitrogen heterocyclics on bonded amino phases in normal-phase liquid chromatography. J. Chromatogr. A 715, 31-39

Chen, H. and Preston, M.R., 1998. Azaarenes in the Aerosol of an Urban Atmosphere. Environ. Sci. Technol. 32, 577-583
Colin, H., Schmitter, J.M. and Guiochon, G., 1981. Liquid chromatography of azaarenes. Anal. Chem. 53, 625-631
Grimmer, G., 1985. PAH- Their Contribution to the carcinogenicity of various Emissions. Toxicol. Environ. Chem. 10, 171-181
Grimmer, G., Jacob, J. and Naujack, K.W., 1983. Characterization of CH_2-homologous azaarenes in petroleum by capillary gas chromatography and mass spectrometry. Anal. Chem. 55, 2398-2404
Ho, C.H., Clark, B.R., Guerin, M.R., Barkenbus, B.D., Rao, T.K. and Epler, J.L., 1981. Analytical and biological analysis of test materials from the synthetic fuel technologies. Mutat. Res. 85, 335-345
Janoszka, B., Warzecha, L., Blaszczyk, U. and Bodzek, D., 2004. Organic compounds formed in thermally treated high-protein food, part II: azaarenes. Acta Chromatogr. 14, 129-141
Kamata, K. and Motohashi, N., 1987. Separation of methyl-substituted benz[*c*]acridines by reversed-phase high-performance thin-layer chromatography.
J. Chromatogr. 396, 437-440
Kamata, K., Motohashi, N., Meyer, R. and Yamamoto, Y., 1992. Determination of 7-methylbenz[*c*]acridines by capillary gas chromatography with electron-capture detection. J. Chromatogr. 596, 233-239
Lintelmann, J., Fischer, K., Karg, E., Schröppel, A., 2005. Determination of selected polycyclic aromatic hydrocarbons in aerosol samples by high-performance liquid chromatography and liquid chromatography-tandem mass spectrometry. Anal Bioanal Chem 381, 508-519
Matsuoka, A., Shudo, K., Saito, Y., Sofuni, T. and Ishidae, M., 1982. Clastogenic potential of heavy oil extracts and some aza-arenes in Chinese hamster cells in culture. Mutat. Res. 102, 275-283
Motohashi, N., Kamata, K. and Meyer, R., 1991. Chromatographic separation and determination of carcinogenic benz[c]acridines in creosote oils. Environ. Sci. Technol. 25, 342-346
Schmitter, J.M., Ignatiadis, I. and Guiochon, G., 1982. Capillary gas chromatography of azaarenes II. Application to petroleum nitrogen bases. J. Chromatogr. 248, 203-216
Seixas, G.M., Andon, B.M., Hollingshead, P.G.and Thilly, W.G., 1982. The aza-arenes as mutagens for Salmonella typhimurium. Mutat. Res. 102, 201-212
Souverain, S., Rudaz, S., Veuthey, J.-L., 2004. Matrix effect in LC-ESI-MS and LC-APCI-MS with off-line and on-line extraction procedures. J. Chromatogr. A 1058, 61-66
Wakeham, S.G., 1979. Azaarenes in recent lake sediments. Environ. Sci. Technol. 13, 1118-1123
Wilhelm, M., Matuschek, G. and Kettrup, K., 2000. Determination of basic nitrogen-containing polynuclear aromatic hydrocarbons formed during thermal degradation of polymers by high-performance liquid chromatography-fluorescence detection. J. Chromatogr. A 878, 171–181
Wynder, E.L. and Hoffman, D., 1967. Tobacco and Tobacco Smoke, Academic Press, New York

Proceedings of the Third International Symposium on Air Quality Management at Urban, Regional and Global Scales. 26-30 September 2005, Istanbul – Turkey

TRENDS OF LEAD IN SUSPENDED PARTICULATE MATTER IN ZAGREB AIR

Vladimira Vadjić and Janko Hršak

Institute for Medical Research and Occupational Health, Ksaverska c. 2, 10000 Zagreb, Croatia vvadjic@imi.hr , jhrsak@imi.hr

ABSTRACT

Monitoring of lead in total suspended particulate matter (TSPM) started in Zagreb, Croatia in 1971 at three measuring sites, located in the city centre and in the northern and western parts. Monitoring of lead concentrations in PM_{10} started in the northern part of the city in 1999. This paper presents the trends of annual mean values for lead concentrations in TSPM and in PM_{10} particles, as well as their comparison with the Croatian limit values and European Union (EU) limit values. The obtained data showed a decreasing trend of lead in TSPM, especially during the last ten years when the consumption of lead-free gasoline increased. Lead in PM_{10} also decreased during the period of measurement. In 1997, the annual mean lead concentration in TSPM was 0.5 $\mu g/m^3$, which is the EU limit value. Since 1999, the concentrations have fallen down and have kept below 0.25 $\mu g/m^3$.

Key Words: Aerosols, Heavy metal, Air quality monitoring, PM_{10}

1. INTRODUCTION

Levels of lead found in the air, food, water and soil vary widely throughout the world, and depend on the degree of industrial development, urbanization and lifestyle factors. Lead is inhaled as fine particles and deposited in the lungs. Since lead uptake by blood is dependent on the deposition pattern and solubility (which is influenced by chemical form and particle size), total lead content is only a surrogate for the biologically effective dose. Furthermore, airborne lead can also reach humans indirectly via deposition on soil and vegetation, and through food chains (Guidelines, 2000).

2. MATERIALS AND METHODS

The monitoring of lead concentrations in total suspended particulate matter started in Zagreb in 1971 at three measuring sites located in the city center, and in the northern and western part of the city. The monitoring of lead concentrations in PM_{10} particles started in the northern part of the city in 1999.

The location of measuring sites is shown in Figure 1.

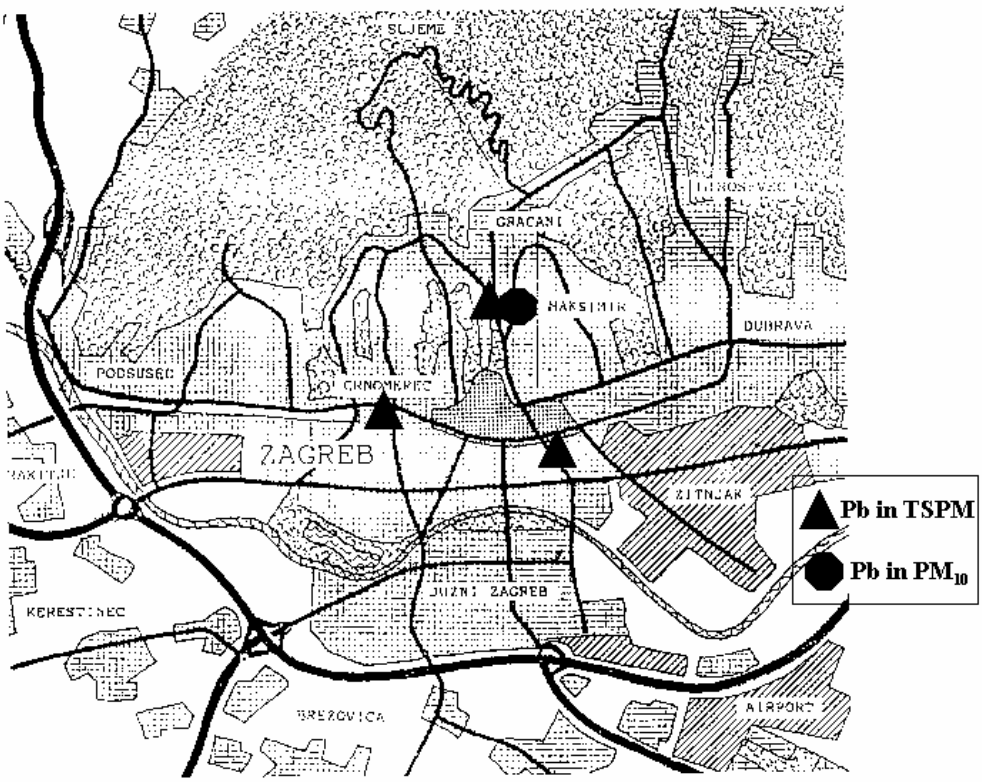

Figure 1 - Location of measuring sites

Twenty-four-hour mass concentration samples of total suspended particulate matter were collected on membrane filters of about 200 m^3 of air, while PM_{10} samples were also collected on membrane filters of about 100 m^3 of air.

Mass concentrations of TSPM and PM_{10} samples were determined gravimetrically. Detection limit values were 2.0 μg m^3 for TSPM and 1.0 μg m^3 for PM_{10} (Bešlić, 2001).

Mass concentration of lead in TSPM and in PM_{10} samples was determined by atomic absorption spectrophotometry (AAS). The detection limit for Pb was 0.0005 μg m^3.

3. CROATIAN AND EUROPEAN AIR QUALITY LIMIT VALUES

The recommended and limit values for lead in TSPM in Croatia are shown in Table 1 (Ordinance, 1996).

Table 1. Recomended (RV) and limit (LV) values for lead in TSPM ($\mu g/m^3$) in Croatia

Averaging period	Pollutant	RV	LV	Average over
Calendar year	Lead in TSPM	1	2	24 hour

Table 2 shows Air Quality Guidelines of WHO for lead for Europe (Guidelines, 2000) and Table 3 shows the limit values for lead in TSPM in European countries (Council Directive, 1999).

Table 2.Air Quality Guidelines of WHO for lead

Averaging period	Pollutant	LV ($\mu g/m^3$)
Calendar year	Lead	0.5

Table 3.Limit value for lead in the European countries

Averaging period	LV ($\mu g/m^3$)	Date by which limit value is to be met
Calendar year	0.5	From 1 January 2001

All three tables show that the Croatian limit values are more tolerant than the European, which in turn suggests that the Croatian regulations should be in agreement with the European standards.

4. RESULTS AND DISCUSSION

Figure 2 shows the trends of annual mean values for lead in TSPM in Zagreb air measured at three sites located in the city center (densely populated area), in the northern part of the city (sparselly populated housing area) and in the western part of the city (industrial area) for the period 1971-2004.

The annual mean concentrations of lead in TSPM ranged between 0.2 and 1.4 $\mu g\ m^3$ in the period 1971-1991, but since 1991, over the past fourteen years, a strong decreasing trend can be observed, resulting from an increased comsumption of unleaded gasoline in Croatia. The annual mean concentrations of lead in TSPM in 1997 were below 0.5 $\mu g\ m^3$, which is in accordance with the EU limit and WHO guideline for Europe. Since 1999, the concentrations have fallen down and they have kept below 0.25 $\mu g\ m^3$, while in 2004 they were below 0.05 $\mu g\ m^3$.

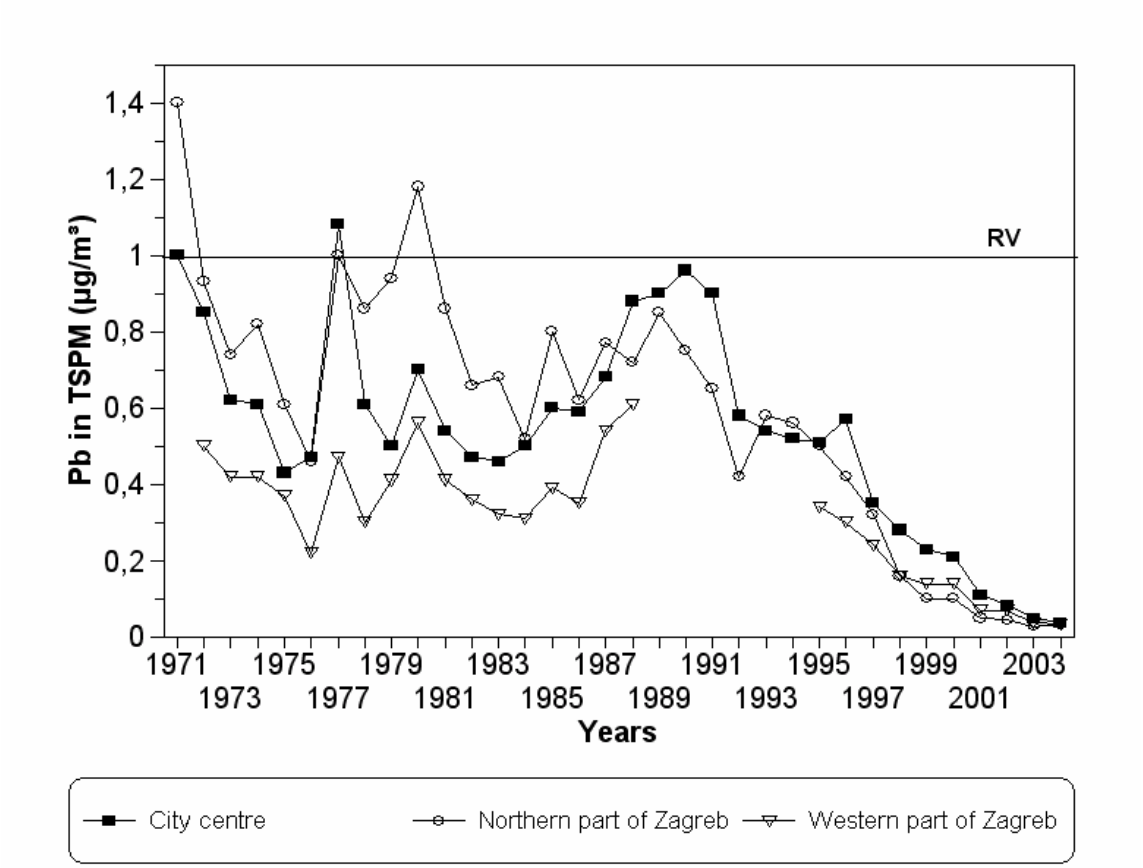

Figure 2. Trends of annual mean values for lead in TSPM in Zagreb for the period 1971-2004.

Figure 3 shows daily concentrations of lead in TSPM in 1981 and 2004, measured in the northern part of the city. These data show a significant decrease in 24-hour mass concentrations of lead in TSPM in 2004 in comparison to 1981 measurements.

Figure 4 shows the trend of annual mean values of lead in PM_{10} in the northern part of the city for the period 1999-2004.

Lead concentrations in PM_{10} particles were very low throughout the measuring period, and showed a strong decreasing trend.

Air quality in Croatia is currently assessed by comparing annual means with recommended (RV) and limit (LV) values stipulated by the Law on Air Quality Protection in Croatia and the Ordinance on Recommended and Limit Air Quality Values. The Law on Air Quality Protection in Croatia gives three categories of air quality:

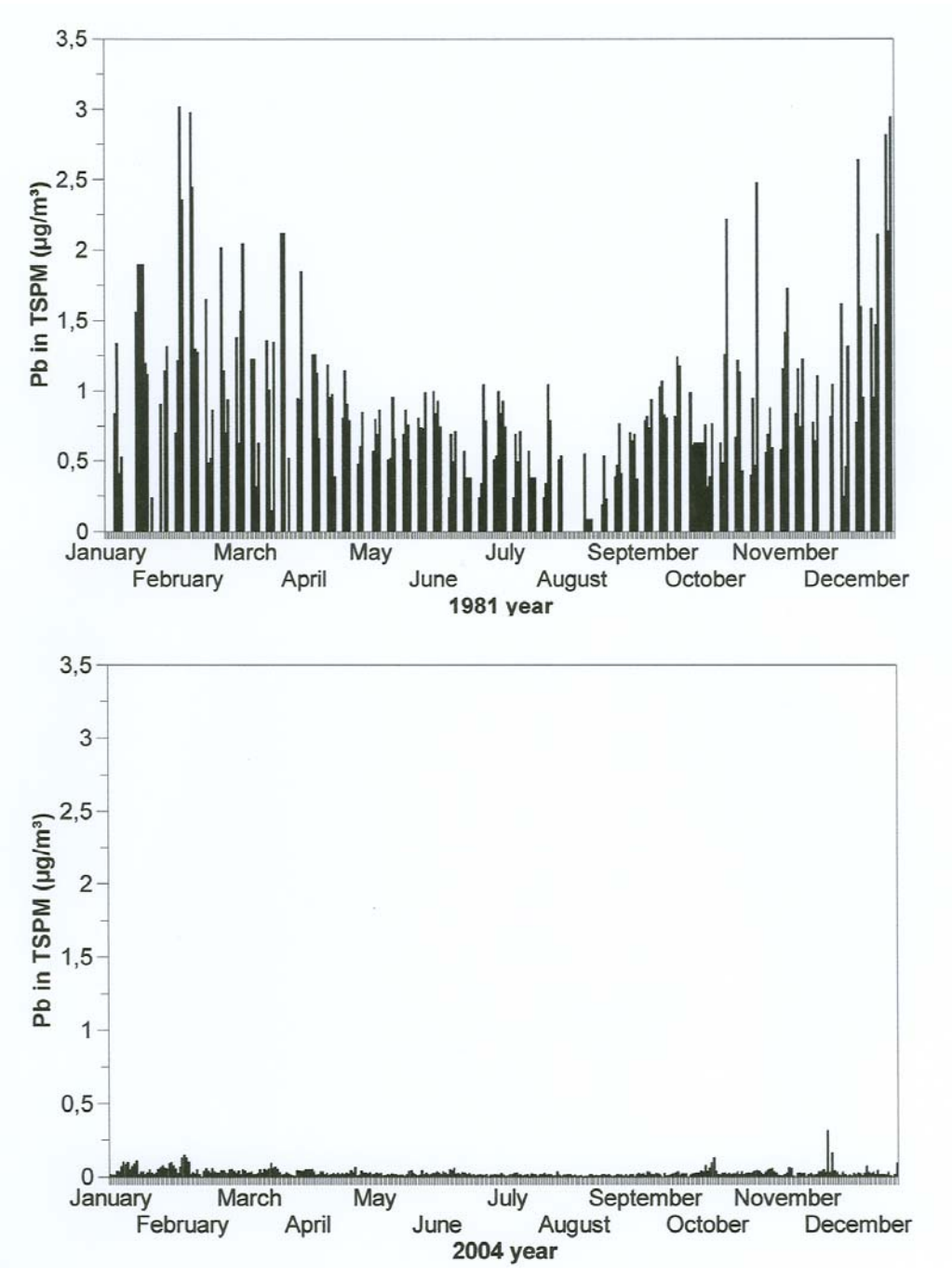

Figure 3. Daily concentrations of lead in TSPM in 1981 and 2004 measured in the northern part of the city

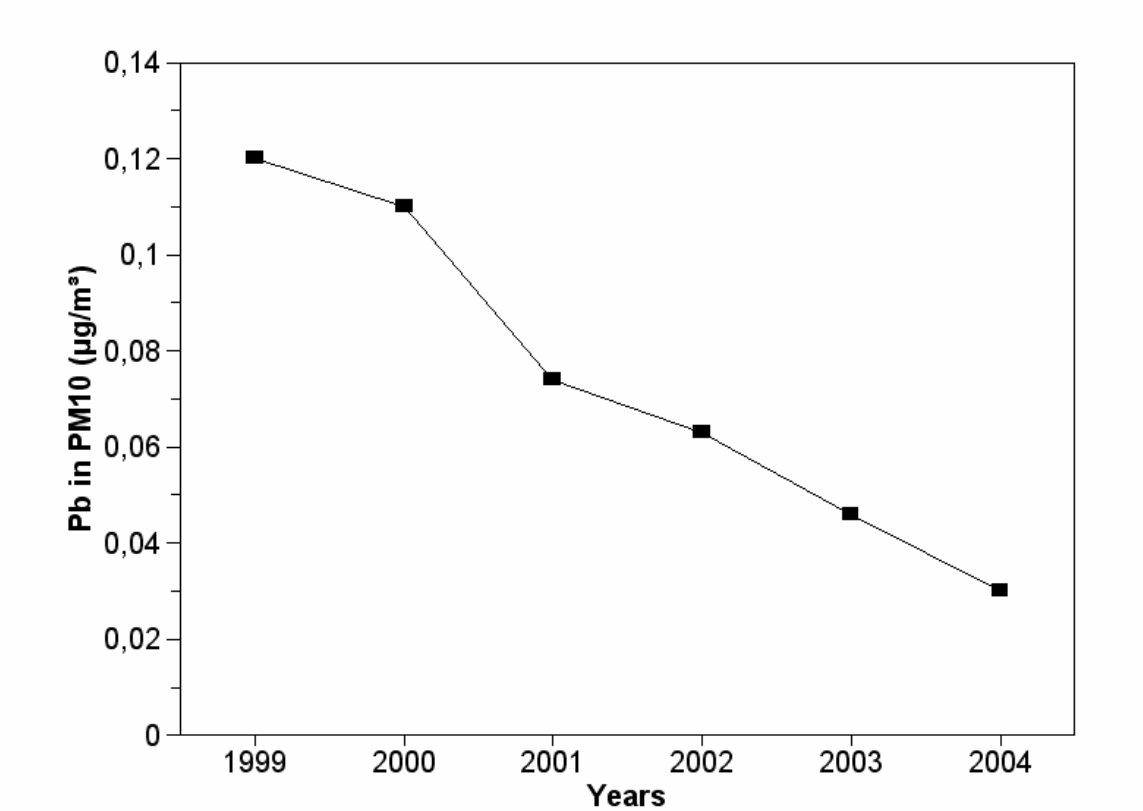

Figure 4.Trend of annual mean values of lead in PM_{10} in the northern part of the city for the period 1999-2004

1st category - clean air (the concentration levels of air pollution are below RV)
2nd category -moderately polluted air (the concentration levels of air pollution are over RV and below LV)
3rd category - polluted air (the concentration levels of air pollution are over LV).

Table 4 shows the categorisation of Zagreb air with the respect to the levels of lead in TSPM. The levels of lead in TSPM were very low and the air was of the 1st category throughout the monitoring period, except in the city centre in 1977 and in the northern part of the city in 1980.

Table 4. Categorization of Zagreb with respect to levels of Pb in TSPM

Years	1st category C<RV	2nd category RV<C<LV	3rd category C>LV
1971.	□ Λ	F	
1972.	□ F Λ		
1973.	□ F Λ		
1974.	□ F Λ		
1975.	□ F Λ		
1976.	□ F Λ		
1977.	F Λ	□	
1978.	□ F Λ		
1979.	□ F Λ		
1980.	□ Λ	F	
1981.	□ F Λ		
1982.	□ F Λ		
1983.	□ F Λ		
1984.	□ F Λ		
1985.	□ F Λ		
1986.	□ F Λ		
1987.	□ F Λ		
1988.	□ F Λ		
1989.	□ F Λ		
1990.	□ F Λ		
1991.	□ F Λ		
1992.	□ F Λ		
1993.	□ F Λ		
1994.	□ F Λ		
1995.	□ F Λ		
1996.	□ F Λ		
1997.	□ F Λ		
1998.	□ F Λ		
1999.	□ F Λ		
2000.	□ F Λ		
2001.	□ F Λ		
2002.	□ F Λ		
2003.	□ F Λ		
2004.	□ F Λ		

□ - City centre F- Northern part of Zagreb Λ- Western part of Zagreb

5. CONCLUSION

The results of monitoring lead in TSPM in Zagreb, the capital of Croatia, show that its concentrations were not high. Since 1991, a strong decreasing trend of lead in TSPM has been observed due to increased consumption of unleaded gasoline. Lead concentrations in PM_{10} particles also showed a strong decreasing trend over the entire measuring period. During the last fourteen years, concentrations were below the Croatian recommended limit value, limit values in EU, and WHO guideline for Europe.

The Croatian limit values are more tolerant than the European and need to be adjusted to the European standards.

REFERENCES

Bešlić, I., Šega, K., 2001. Gravimetrijsko određivanje koncentracija lebdećih čestica – zahtjevi točnosti mjernih parametara (in Croatian). In: Valić, F. and Šega, K. (Ed.), Proceedings of the Third Croatian scientific and professional assembly «Air Quality 01», Šibenik, Croatia, pp. 323-327.
Council Directive 1999/30/EC, 1999. Official Journal of the European Communities.
Guidelines for Air Quality, 2000. WHO, Geneva.
Ordinance on Recommended and Limit Air Quality Values, 1996. Nar. Novine broj 101, 4198-4200 (in Croatian).

Proceedings of the Third International Symposium on Air Quality Management at Urban, Regional and Global Scales. 26-30 September 2005, Istanbul – Turkey

ON THE DRY DEPOSITION OF ADMIXTURES WITH GRAVITY DEPOSITION

Kostadin Ganev, Dimiter Yordanov and Nikolai Miloshev*

Institute of Geophysics, Bulgarian Academy of Sciences, Sofia, Bulgaria,
kganev@geophys.bas.bg
* Institute of Geophysics, Bulgarian Academy of Sciences, Sofia, Bulgaria,
miloshev@geophys.bas.bg

ABSTRACT

It seems that the "big leaf" approach to the dry deposition assessment will be the one followed by the model developers in the near future. The resistance against turbulent transport of the component close to the surface - the aerodynamic resistance, is one of the major factors of dry deposition. The most popular parameterization schemes treat the aerodynamic resistance and the gravity deposition independently, most often by simply adding the gravity deposition velocity. As the gravity deposition modifies the admixture profiles and thus the turbulent fluxes in the Surface Layer (SL), this approach is obviously incorrect.

The present paper suggests a more general approach, based on the exact solution of the pollution transport (turbulent and gravity deposition) equation in the SL, which provides a correct expression for the aerodynamic resistance, accounting also for the gravity deposition effects. Some results from simple calculations, which demonstrate the importance of a joint treatment of turbulent transport and gravity deposition while calculating the aerodynamic resistance, are also shown in the paper.

Key Words: dry deposition, gravity sedimentation, aerodynamic resistance

1. INTRODUCTION

It seems that the "big leaf" approach (Erisman, van Pul and Wyers, 1994, Jakobsen, Jonson and Berge, 1996, Seland, van Pul, Sorteberg and Tuovinen, 1995, Wesley, 1989) to the dry deposition assessment will be the one followed by the model developers in the near future. These most popular parameterization schemes assume the following connection between the turbulent flux of gases or aerosol and their concentration at level z :

$$-F = k\frac{dc}{dz} = V_d(z)c(z), \qquad (1)$$

where $c(z)$ is the admixture concentration, V_d is the dry deposition velocity and $k(z)$ is the coefficient of vertical turbulent exchange.

By making analogy with the Ohms law in electrical circuits the dry deposition velocity V_d is most often presented in the form:

$$V_d = \left(r_a + r_b + r_s\right)^{-1}, \tag{2}$$

where r_a is the surface layer (SL) aerodynamic resistance, r_b is the quasi-laminar or viscous sub-layer resistance, and r_s is the surface resistance.

It seems that the most general expression for the aerodynamic resistance r_a is the following:

$$r_a(z) = \int_{z_0}^{z} \frac{dz}{k(z)}, \tag{3}$$

where z_0 is the roughness length. If it is assumed, as usual, that the SL turbulent transport of admixtures is similar to these of heat and momentum, it can be written:

$$k(z) = \frac{\kappa u_* z}{\varphi(\varsigma)}, \tag{4}$$

where κ is the von Karman constant, u_* is the friction velocity, $\varphi(\varsigma)$ is the universal function of the dimensionless height $\varsigma = z / L$, L - the Monin-Obukhov length. In such a case the expression for r_a resumes the form:

$$r_a(z) = \frac{1}{\kappa u_*}\left(f(z) - f\left(z_0\right)\right), \; f(z) = \int \frac{\varphi(\varsigma)}{z} dz \,. \tag{5}$$

From (3) it is obvious that $r_a(z_0) = 0$ and thus

$$V_{d0} = V_d(z_0) = \left(r_b + r_s\right)^{-1}, \tag{6}$$

i.e. the deposition velocity at roughness length height is subject only of the transport of the component trough the laminar layer adjacent to the surface by molecular diffusion and the various destruction or uptake processes of the component at the surface.

2. A MORE GENERAL APPROACH

The relation (1)-(2) between the turbulent flux and the component concentration in the SL is widely used, but is not the most general one. It does not account for factors, which may be important, like gravity deposition and pollution sources in the SL.

A more general approach based on the solution of the admixture transport equation in the SL is suggested by Ganev and Yordanov (1981, 2004, 2005), Venktaram and Pleim (1999). As generally accepted, the vertical transport is assumed dominant in the SL, so the concentration field is assumed to be locally horizontally homogeneous and stationary. In such a case the vertical profile $c(z)$ of the concentration of an admixture with gravity deposition $-w_g$, ($w_g > 0$) is described by the equation:

$$\frac{d}{dz} k \frac{dc}{dz} + w_g \frac{dc}{dz} = -q\delta(z - z_{source}), \tag{7}$$

where q is the capacity of a flat (locally) homogeneous admixture source, δ is the Dirac function. The boundary condition at $z = z_0$ is, according to (1), (2), (6), the following:

$$k \frac{dc}{dz} = V_{d0} c_0, \tag{8}$$

c_0 - the concentration at $z = z_0$. It is stratrforward to integrate (7), (8), which leads to the following expression forThe integration of (7), having in mind also (8) leads to:

$$kdc/dz + w_g c = (w_g + V_{d0}) c_0 - qH_{source}(z), \tag{9}$$

where $H_{source}(z)$ is the Heavyside function ($H_{source}(z) = 0$ for $z < z_{source}$; $H_{source}(z) = 1$ for $z > z_{source}$). By the transformation

$$c = x e^{-w_g r_a}, \tag{10}$$

where r_a is the aerodynamic resistance (see (3)), equation (9) can be simplified to the form (from (10) it is obvious that $x(z_0) = c_0$):

$$kdx/dz = (w_g + V_{d0}) c_0 e^{w_g r_a} - qH_{source}(z) e^{w_g r_a}, \tag{11}$$

and after some trivial manipulations an expression for $c(z)$ to be obtained:

$$c(z) = \left[1 + \frac{V_{d0}}{w_g}\left(1 - e^{-w_g r_a(z)}\right)\right] c_0 - H_{source}(z) \frac{q}{w_g}\left(1 - e^{w_g r_a(z_{source}) - w_g r_a(z)}\right). \tag{12}$$

By calculating c_0 from (12) and then inserting it in (9) the SL flux/concentration relation for the case of admixtures with gravity deposition and possible sources in the SL can be obtained:

$$k\frac{dc}{dz} = V_d(z)c(z) - H_{source}(z)\frac{V_d(z)}{V_d(z_{source})}q, \tag{13}$$

Where

$$V_d(z) = \left[\frac{1}{w_g}\left(e^{w_g r_a(z)} - 1\right) + e^{w_g r_a(z)}\frac{1}{V_{d0}}\right]^{-1}. \tag{14}$$

It is easy to calculate that in case of admixture with no gravity deposition ($w_g \to 0$) the expression (14) takes the form (2). Further, if there are no sources in the SL the flux/concentration relation transforms into the form (1).

The particular cases when $V_{d0} \to \infty$ (total absorption at $z = z_0$) and $V_{d0} \to 0$ (total reflection at $z = z_0$) can also be considered. Obviously in the first case

$$V_d(z) \to \left[\frac{1}{w_g}\left(e^{w_g r_a(z)} - 1\right)\right]^{-1}, \text{ when } V_{d0} \to \infty, \tag{15}$$

and, as it can be easily seen from (13), there will be zero concentration at $z = z_0$. In the second case $V_d \to 0$ when $V_{d0} \to 0$, but the ratio $V_d(z)/V_d(z_{source})$ remains limited, so the relation (13) obtains the form:

$$k\frac{dc}{dz} = -H_{source}(z)\frac{e^{w_g r_a(z_{source})}}{e^{w_g r_a(z)}}q, \tag{16}$$

or in the case with no gravity deposition ($w_g \to 0$):

$$k\frac{dc}{dz} = -H_{source}(z)q. \tag{17}$$

If the deposition velocity, calculated according to (1) is denoted by V_{d1}, then having in mind (6) the aerodynamic resistance r_a may be expressed in the form:

$$r_a = V_{d1}^{-1} - V_{d0}^{-1}. \tag{18}$$

Inserting (18) in (14), leads, after some simple transformations to the dimensionless relation:

$$\widetilde{V}_d = \left[\frac{1}{\widetilde{w}_g}\left(e^{\widetilde{w}_g\left(\widetilde{V}_{d1}^{-1} - 1\right)} - 1\right) + e^{\widetilde{w}_g\left(\widetilde{V}_{d1}^{-1} - 1\right)}\right]^{-1}, \tag{19}$$

where $\widetilde{V}_d = V_d / V_{d0}$, $\widetilde{V}_{d1} = V_{d1} / V_{d0}$, $\widetilde{w}_g = w_g / V_{d0}$.

The difference between $\widetilde{V}_d$ and $\widetilde{V}_{d1}$ is well demonstrated by Figure 1. It is clear that even in the cases when w_g is of the order of magnitude of V_{d0} the effect of gravity deposition on the turbulent (aerodynamic) deposition is significant. The gravity deposition modifies the admixture profiles and thus the admixture turbulent fluxes in the SL, which results in a decrease of the dry deposition velocity.

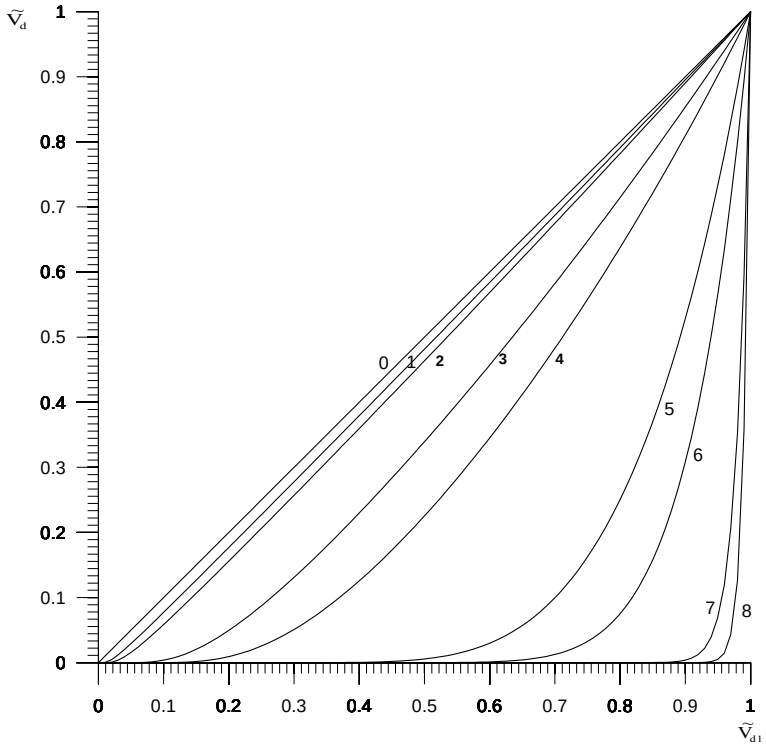

Figure 1. The difference between $\widetilde{V}_d$ and $\widetilde{V}_{d1}$ for different $\widetilde{w}_g$ values: $\widetilde{w}_g$=0 (0). 0.05 (1), 0.1 (2), 0.5 (3), 1 (4), 3 (5), 10 (6), 50 (7) and 100 (8)

If the total (turbulent + sedimentation) flux/concentration relation is concerned from (13, 14) it can be obtained:

$$-F = k\frac{dc}{dz} + w_g c = W_d(z)c(z) - H_{source}(z)\frac{W_d(z) - w_g}{W_d(z_{source}) - w_g}q\,, \tag{20}$$

$$W_d(z) = w_g\left(1 + \frac{w_g}{V_{d0}}\right)\left[1 + \frac{w_g}{V_{d0}} - e^{-w_g r_a(z)}\right]^{-1}. \tag{21}$$

Expressions (14, 21) can not be derived by using any sort of electrical analog.

Some well known relations can be derived as particular cases of (21). For example, when $w_g << V_{d0}$ (16) obtains the form (Venckatram, A. and J. Pleim, 1999):

$$W_d(z) = w_g \left[1 - e^{-w_g r_a(z)}\right]^{-1}, \tag{22}$$

and when $w_g r_a << 1$ - the form (J.H. Sienfeld and S. Pandis, 1998):

$$\begin{aligned} W_d(z) &= w_g + \left[r_a(z) + \frac{1 + w_g r_a(z)}{V_{d0}} \right]^{-1} = \\ &= w_g + \left[r_a(z) + r_s + r_b + w_g\, r_a(z)(r_s + r_b) \right]^{-1} \end{aligned} \tag{23}$$

The application of the dry deposition parameterization suggested above can be demonstrated by the following example: Let a two-layer model for k is assumed - $k = k(z)$, calculated according to (4) in the SL ($z_0 \le z \le h_{SL}$), h_{SL} - the SL height; $k = k_h = k(h_{SL})$ for $h_{SL} \le z < \infty$. Then, in the horizontally homogeneous case, the vertical profile above SL of the concentration $c(z,t)$ from an instantaneous flat source with height $h > h_{SL}$ can be obtained from the equation:

$$\frac{\partial c}{\partial t} - w_g \frac{\partial c}{\partial z} - k_h \frac{\partial^2 c}{\partial z^2} = 0\ ,\ h_{SL} \le z < \infty\ , \tag{24}$$

under the following initial and boundary conditions:

$$c(z,0) = \delta(z - h)\ ;\ k_h \frac{\partial c}{\partial z} = \beta c(h_{SL}, t)\ . \tag{25}$$

Here β is the dry deposition velocity at $z = h_{SL}$. Depending on the chosen parameterization β is equal to $V_d(z = h_{SL})$ or to $V_{d1}(z = h_{SL})$ - respectively the cases when the gravity deposition effects on the aerodynamic resistance are accounted, or not accounted for. As it can be easily shown (Galperin, Yordanov and Ganev, 2000), the solution of (20-21) is:

$$c(z,t) = e^{-\frac{w_g(z'-h')}{2k_h} - \frac{w_g^2 t}{4k_h}} \left\{ \frac{1}{2\sqrt{\pi k_h t}} \left[e^{-\frac{(z'-h')^2}{4k_h t}} + e^{-\frac{(z+h)^2}{4k_h t}} \right] - \frac{\tilde{\beta}}{k_h} e^{\frac{\tilde{\beta}(z'+h'+\tilde{\beta}t)}{k_h}} erfc\left(\frac{z'+h'+2\tilde{\beta}t}{2\sqrt{k_h t}} \right) \right\} \tag{26}$$

where $\tilde{\beta} = \beta + w_g / 2$, $z' = z - h_{SL}$ and $h' = h - h_{SL}$.

This rather simplified model is applied because it allows obtaining an analytical solution in the explicit form (26) and on the other hand is realistic enough, at any rate much more realistic if a one-layer model for k ($k = const$ for $z_0 \le z < \infty$) is assumed.

The horizontally homogeneous concentration pattern is not often observed in the real world, but in factorized pollution transport models, like the trajectory "puff" model, the multiplier that accounts for the vertical concentration distribution is also defined as a solution of (24), (25). That is why the chosen simplification can be estimated as a relevant one for demonstrating the effects of the suggested dry deposition parameterization scheme.

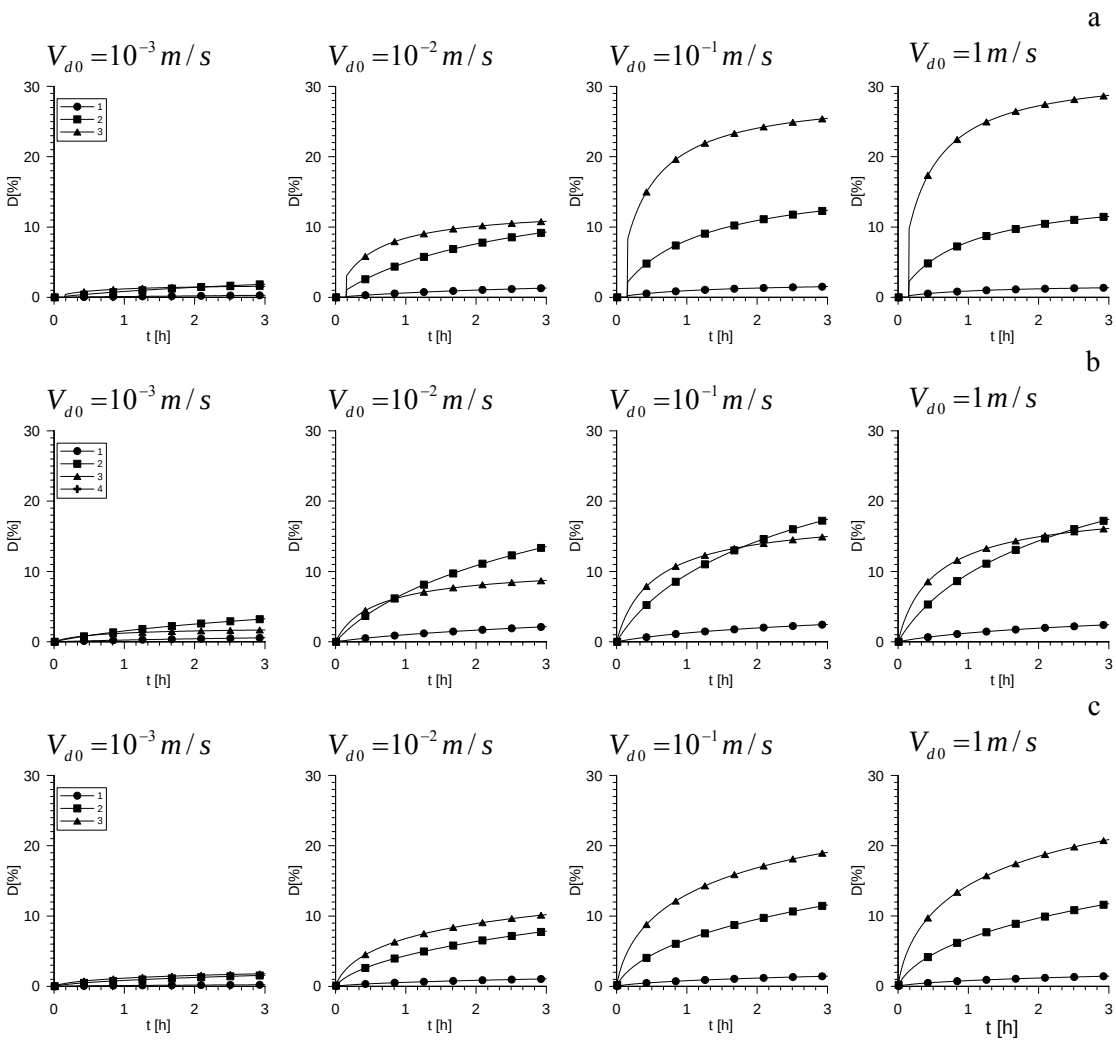

Figure 2. Time evolution of $D_h=(c'(h_{SL},t)-c''(h_{SL},t))/c'(h_{SL},t),[\%]$ for different V_{d0} values and for $w_g=10^{-3}\,m/s$ (1), $w_g=10^{-2}\,m/s$ (2) and $w_g=10^{-1}\,m/s$ (3). Cases of Stable (a), Neutral (b) and Unstable(c) stratification

Formula (26) was applied for calculating the concentrations $c'(h_{SL},t)$ and $c''(h_{SL},t)$ at SL height for the cases when gravity deposition is accounted ($\beta=V_d(z=h_{SL})$) and not accounted ($\beta=V_{d1}(z=h_{SL})$) for. The calculations were made for a wide range of V_{d0} and w_g values for the cases of stable ($u_*=0.5\,m/s$, $L=10$), neutral ($u_*=0.2\,m/s$) and unstable ($u_*=0.2\,m/s$, $L=-10$) stratification for source height

$h = 200m$. When the concentrations $c'(h_{SL},t)$ and $c''(h_{SL},t)$ at SL height are calculated, it is easy also to obtain the respective concentrations concentration c_0' and c_0'' at roughness length level ($z = z_0$). c_0' is calculated from (12) for $z = h_{SL}$ and $c = c'(h_{SL},t)$. c_0'' is calculated from the same formula for $z = h_{SL}$, $c = c''(h_{SL},t)$ and $w_g \to 0$.

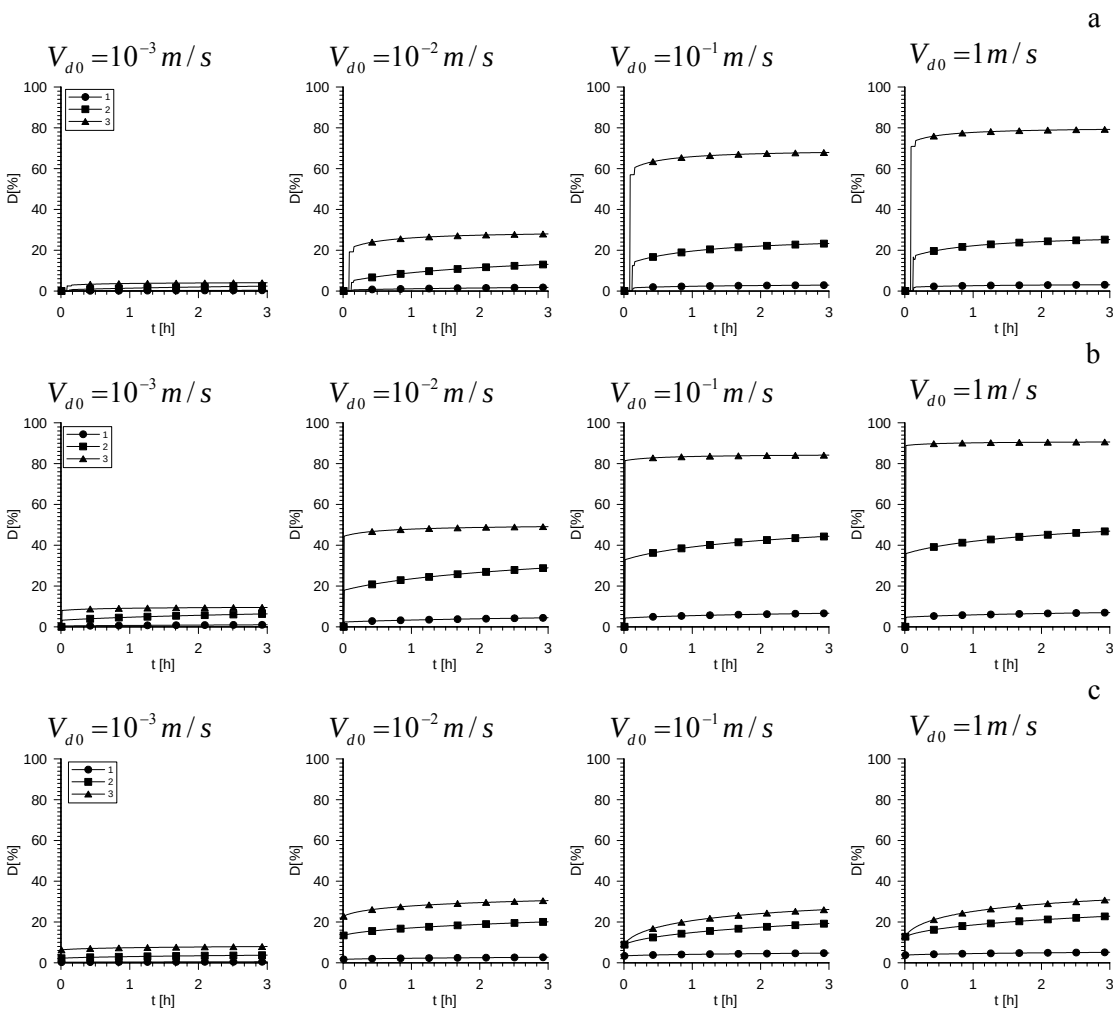

Figure 3. Time evolution of $D_0 = (c_0'(t) - c_0''(t))/c_0'(t),[\%]$ for different V_{d0} values and for $w_g = 10^{-3} m/s$ (1), $w_g = 10^{-2} m/s$ (2) and $w_g = 10^{-1} m/s$ (3). Cases of Stable (a), Neutral (b) and Unstable(c) stratification

Some of the results are demonstrated in Figures 2-3, where the time evolution of the relative differences $D_h(t) = (c'(h_{SL},t) - c''(h_{SL},t))/c'(h_{SL},t),[\%]$ and $D_0(t) = (c_0'(t) - c_0''(t))/c_0'(t),[\%]$. The following conclusions can be maid by the comparison:

- taking into account the gravity deposition may have a significant effect on the calculated concentrations – in some cases up to almost 30% for the concentration at SL height and up to 80% at $z = z_0$;

- the effect generally increase with the increase of w_g and V_{d0};
- both $D_h(t)$ and $D_0(t)$ curves are pretty similar for $V_{d0} = 10^{-1} m/s$ and $V_{d0} = 1 m/s$, regardless of the stratification and w_g values. This means that the gravity sedimentation effects on dry deposition increase significantly with the increasing of V_{d0}, until it reaches some critical value. For V_{d0} above this critical value (and certainly for $V_{d0} > 10^{-1} m/s$) the turbulence/gravity deposition interaction and thus the gravity sedimentation effects on dry deposition become much less sensitive to V_{d0} variations;
- the gravity sedimentation influence on dry deposition an on the concentration profiles strongly depends on the stratification. This dependence is not monotonic or simple, however, and is manifested in rather different for different w_g and V_{d0} values.

3. CONCLUSION

The most popular parameterization schemes treat the aerodynamic resistance and the gravity deposition independently, most often by simply adding the gravity deposition velocity. As the gravity deposition modifies the admixture profiles and thus the admixture turbulent fluxes in the SL, this approach is obviously incorrect. The present paper suggests a more general approach, based on the exact solution of the pollution transport (turbulent and gravity deposition) equation in the SL, which provides a correct expression for the aerodynamic resistance, accounting also for the gravity deposition effects. The parameterization scheme is a generalization of the formula suggested by (Venckatram, A. and J. Pleim, 1999) and (J.H. Sienfeld and S. Pandis, 1998). The demonstrated examples show the importance of a joint treatment of turbulent transport and gravity deposition in calculating the aerodynamic resistance. They also demonstrate the sensitivity of the parameterization scheme to w_g, V_{d0} and stratification variations.

4. ACKNOWLEDGEMENTS

The present work is performed due to the financial support of European Commission – 5thFP project BULAIR (Contract Nr. EVK2-CT-2002-80024) and the 6thFP Network of Excellence ACCENT (Contract Nr. GOCE-CT-2002-500337) and the Bulgarian National Science Council (Contract No. ES-1002/00). The contacts within the framework of the NATO Collaborative Linkage Grant EST.CLG 979794 were extremely simulating, as well.

REFERENCES

Erisman, J.W., A.J. van Pul, and G.P. Wyers (1994) Parameterization of surface resistance for the quantification of the atmospheric deposition of acidifying pollutants and ozone. Atmospheric Environment, **28**, No.16, 2595-2607

Galperin M., D.L. Yordanov and K.G. Ganev (2000) On the concentrations of

polydispersive aerosol in the surface air layer. Compt. rend. Acad. bulg. Sci., v.**53**, No8, 25-28

Ganev, K.G. and D.L. Yordanov (1981) Parameterization of pollution from a heavy admixture source in the surface air layer, Compt. rend. Acad. bulg. Sci., **34**, No.8, 1261-1264

Ganev, K. and D.Yordanov 2004, Parameterization of dry deposition processes in the Surface Layer for admixtures with gravity deposition, 9th Harmonisation Conference, 1-4 June 2004, Garmish Partenkirchen, 267-271

Ganev K. and D. Yordanov, 2005. Parameterization of dry deposition processes in the surface layer for admixtures with gravity deposition. (accepted for publishing in Int. J. Environment & Pollution*)*

Jakobsen, H.A., J.E. Jonson and E. Berge, 1996. Transport and deposition calculations of sulphur and nitrogen compounds in Europe for 1992 in the 50km grid by use of the multi-layer Eulerian model. EMEP/MSC-W Report 2/96

Seland, Ø., A. van Pul, A. Sorteberg and J.-P. Tuovinen (1995) Implementation of resistance dry deposition module and a variable local correction factor in the Lagrangian EMEP model. EMEP/MSC-W Report 3/95

Sienfeld J.H. and S. Pandis, 1998. Atmospheric Chemistry and Physics, Wiley, New York, 1326.

Venckatram, A. and J. Pleim (1999) The electrical analogy does not apply to modeling dry deposition of particles. Atmospheric Environment, **33**, 3075-3076

Wesley, M.L. (1989) Parameterization of surface resistance to gaseous dry deposition in regional-scale numerical models, Atmospheric Environment, **23**, No.6, 1293-1304

Proceedings of the Third International Symposium on Air Quality Management at Urban, Regional and Global Scales. 26-30 September 2005, Istanbul – Turkey

SOURCE APPORTIONMENT OF FINE PARTICULATE MATTER IN A SEMI-ARID COASTAL URBAN AREA OF SOUTH TEXAS

Kuruvilla John[1], Myoungwoo Kim[2] and Alvaro Martinez[3]

Frank H. Dotterweich College of Engineering, Texas A&M University-Kingsville, MSC 188, Kingsville, Texas 78363, Tel: 361-593-2001, Fax: 361-593-2106, k-john@tamuk.edu

2. The Institute for Sustainable Energy and Environment, Ohio University, Athens, Ohio 45701, Tel: 740-593-4751, myoungkim@ilgard.ohio.edu

3. Department of Environmental and Civil Engineering, Texas A&M University-Kingsville, MSC 213, Kingsville, Texas 78363, Tel: 361-593-3046, Fax: 361-593-2069, amartinez@even.tamuk.edu

ABSTRACT

Corpus Christi is located in a semi arid coastal region of South Texas. Continuous sampling of fine particulate matter as well as $PM_{2.5}$ speciation monitoring was conducted by the Texas Commission on Environmental Quality (TCEQ) several sites within the Corpus Christi urban airshed. Data was obtained from TCEQ for the study period of 2001-2004. The elemental species considered in this analysis included As, Br, Cr, Cu, Fe, Pb, Mn, Mo, Ni, Sn, V, Si, S, Ta, K, K^+, NH_4^+, Na, Na^+, elemental carbon, non-volatile nitrate and organic carbon. The daily averaged and the annual averaged $PM_{2.5}$ concentrations never exceeded the National Ambient Air Quality Standards of 65µg/m^3 and 15µg/m^3, respectively. However, the region was affected by long-range transport of aerosol particles associated with regional haze. Day-to-day and seasonal variations in the chemical composition reflect changes of contribution from various sources. A multivariate receptor model, UNMIX, was applied to identify potential sources of the $PM_{2.5}$. Six possible source categories were identified including sulfate from industrial sources, mobile source emissions, soil and dust, agricultural burns, sea spray and nitrates from multiple sources. Potential source contribution function (PSCF) was applied to the data to identify source contribution location and evaluate source-receptor relationship affecting the South Texas region. The middle Mississippi River valley, Ohio River valley, industrialized coastal areas of Texas, Mexico and Central America were identified as possible emission source regions contributing to the $PM_{2.5}$ mass, sulfate, nitrate, and EC/OC concentrations. Agricultural burning events were found to be distinct sources during the early spring months of April and May. This study identified atypical haze events such as the September 2002 regional haze event associated with agricultural burns in Mexico and Central America that typically affect the South Texas area.

Keywords: Fine particulate matter, $PM_{2.5}$, source apportionment, regional haze, semi-arid, coastal urban airshed

Proceedings of the Third International Symposium on Air Quality Management at Urban, Regional and Global Scales. 26-30 September 2005, Istanbul – Turkey

ATMOSPHERIC AEROSOLS BEHAVIOUR AT AN INDUSTRIAL AREA IN NORTHERN FRANCE

F. Ledoux[1], S. Bouhsina[1], L. Courcot[1], D. Courcot[2], G. Garçon[3], P. Shirali[3], A. Aboukaïs[2] and E. Puskaric[1,*]

[1]Université du Littoral Côte d'Opale, L.I.S.E., ELICO UMR 8013,
32 avenue Foch, 62930 Wimereux, France
[2]Université du Littoral Côte d'Opale, L.C.E., EA 2598,
145 avenue M. Schumann, 59140 Dunkerque, France
[3]Université du Littoral Côte d'Opale, L.R.T.E.
189A, avenue M. Schumann, 59140 Dunkerque, France
emile.puskaric@club-internet.fr

ABSTRACT

Aerosols samplings were performed taking into account wind directions simultaneously at an urban and a rural site in Northern France. Major and trace elements were studied after sampling by use of a high volume cascade impactor, to follow the behaviour of particles between the coarse particles (> 1 µm) and the fine particles (< 1 µm). The behaviour of the different elements is determined by the evolution of the mass median diameters and the mass size distribution according to the wind. The kind of compounds under which some ions are, is determined by calculation of neutralization ratios.

Key Words : Urban and Rural Aerosols, Mass Median Diameter, Mass Size Distribution, Neutralization Ratio.

1. INTRODUCTION

The Northern France, Nord – Pas de Calais, is one of the most industrialized county of France, and in 2001, it was estimated that it was responsible of 13% of the total French particulate matter emission. In this region, 60% of this kind of emissions are originated from the high industrialized Dunkerque area which has an important local as well as on a large scale, influence.
The aim of this work is the characterization of particulate aerosols in a heavy industrialized area such as the Northern France, counting a lot of heavy metals emissaries (metallurgic industries, smelters, waste incinerators...).
If a great number of studies have been lead on the coast of the North Sea, among which (Bruynseels et al., 1988 ; Injuk et al., 1992 ; Rojas et al. 1993), can be cited, few of them concern this area (Flament et al., 1987). The present study attempts to determine the composition of particles in selected size fractions according to source contribution and the behaviour of some elements in the air.

2. METHODOLOGY

2.1. Study area

The sampling sites are located at Dunkerque an important urban city with roughly 220000 inhabitants with its suburbs, and where important industrial activities are concentrated, and at a rural area, Les Moëres, a village with 860 inhabitants, situated approximately 15 km ESE of the urban site (Fig. 1).

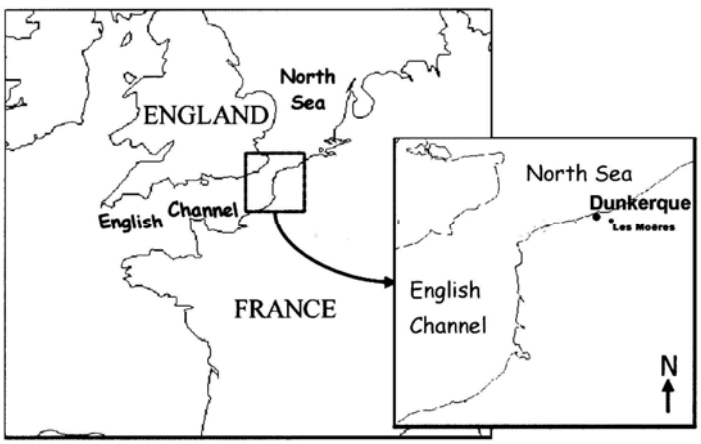

Fig. 1. Sampling location

The sampling site at Dunkerque is under the important influence of numerous aerosols sources, as urban origins, as well as particularly westside industrial sources (metallurgical plants, oil refineries, organic chemistry), and also marine sources under the northside marine influence of the North Sea. Three wind sectors are taken into account from the different wind directions with respectively the marine sector (340-60°), the continental and urban sector (60–240°) and the industrial sector (240-340°). For the rural sampling site, these three wind sectors are also used, with the difference that the 60–240° sector is only under the continental influence, and the 240–340° sector is under the complete influence of Dunkerque area.

2.2. Sampling methods

Aerosol samples were collected from January 15th 2001 to February 23rd 2001. Size-fractionated atmospheric particulate matter are sampled on Whatmann 41® cellulosic filters by use of a 5 stage plus back-up filter high volume cascade impactor (Sierra Instruments, Model 235). For each impaction stage, experimental values for the aerodynamic 50% cut-off particle diameter ($D_{p,50}$) as recommended by Willeke (1975) and used by Bayens et al. (1990) and Flament et al. (1996) in similar studies with same collection substrat and nominal flow rate (68 $m^3.h^{-1}$), are indicated in table 1.

The particles were divided in coarse particles (> 1 µm) sampled on the stages 1, 2 and 3, and fine particles (< 1 µm) collected on the stages 4, 5 and 6 (back-up).

Table 1. Calculated 50% cut-off particle diameters $D_{p,50}$ (µm) under a nominal flow rate of 68 $m^3.h^{-1}$ for the cascade impactor Sierra Model 235

Stages	1	2	3	4	5	6
$\mathbf{D_{p,50}}$	5.08	2.10	1.04	0.64	0.33	0.04

A meteorological station was set up at each sampling site to obtain local wind speed and direction, atmospheric pressure, temperature, hygrometry, rain fall.

2.3. Filters preparation

Unwashed cellulose filters present varying trace metals contents and especially for Fe, up to 5 µg per filter. So this kind of filters are treated as described by Obata et al. (1997) for Fe analysis. Filters are then dried under a laminar flow hood (Class 100, US Federal Standard 209a), and then hermetically kept in clean plastic bags and stored in a freezer (-20°C) before using. Such a treatment lowers the Fe contamination under 0.1 µg per filter, and contents of all other analysed elements are lower than limit detection.

2.4. Chemical analysis

Major elements (Cl^-, NO_3^-, SO_4^{2-}, NH_4^+, Na, Mg and Ca), and trace elements (Al, Cu, Fe, K, Mn, Pb, Sr, and Zn) were taken into account and analysed. ICP-AES (Varian Liberty II) was used to quantify Al, Ca, Fe, K, Mg, Mn, Na, Sr, and Zn, whereas Cu and Pb concentrations were determined with the GFAAS technique (Perkin Elmer, Aanalyst 600, Zeeman background correction). Water soluble ions were analysed by ion chromatography (Cl^-, NO_3^-, SO_4^{2-}) and indophenol-blue spectrophotometry (NH_4^+).

3. RESULTS AND DISCUSSION

3.1. Mass Median Diameter (MMD)

The evolution of the behaviour of the different elements was followed by their calculated (MMD) according to the wind direction (Fig. 2).

Elements with similar profiles are gathered on the same graph, but Cu, K, Pb and Zn with their particular profiles cannot be superimposed with the other elements. Na and Cl are shown separately just for considering their behaviour, since they have a great and important affinity. If at the both sampling sites, the size of the particles related to these two elements are very well correlated for the marine sector (340–60°), on the other hand these particles present different profiles especially for the 60–240° sector which is strictly continental for the rural site, and continental with urban area influence for the urban site.

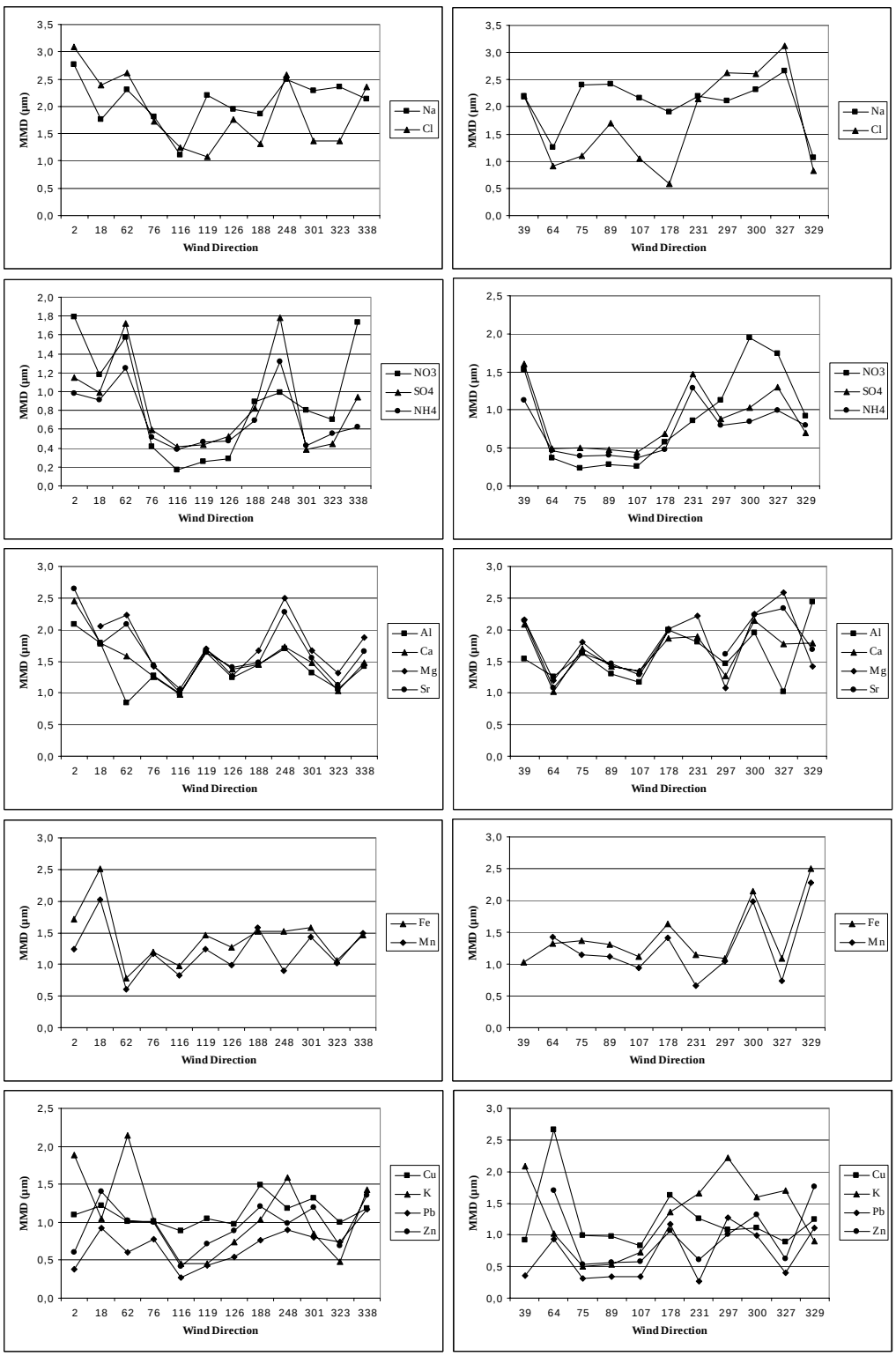

A – Urban site **B – Rural site**

Fig. 2. Evolution of MMD for elements at each sampling site *versus* wind directions

At the urban site, three groups of elements with identical profiles have been identified : (i) NO_3^-, SO_4^{2-} and NH_4^+, (ii) Al, Ca, Mg and Sr , (iii) Fe and Mn. At the rural site, these elements are gathered in exactly the same way as at the urban area, but with notably differences for the 240–340° sector, corresponding to the important influence of the industrialized area of Dunkerque, especially for NO_3^-, Al and Ca.

3.2. Mass Size Distribution (MSD)

Table 1 and Table 2 present the distribution of fine and coarse particles for the sampled elements according to the different wind sectors at the both sampling sites.

Table 1. Size distribution of particles at the urban site according to wind directions

Wind sector	Particles	Al	Ca	Cu	Fe	K	Mg	Mn	Na	Pb	Sr	Zn	Cl	NO3	SO4	NH4
340 - 60	% > 1 µm	46	50	38	51	53	73	46	83	26	67	38	82	45	31	25
marine	% < 1 µm	54	50	62	49	47	27	54	17	74	33	62	18	55	69	75
60 - 240	% > 1 µm	48	48	41	49	20	53	41	57	15	50	29	41	12	16	14
continental	% < 1 µm	52	52	59	51	80	47	59	43	85	50	71	59	88	84	86
240 - 340	% > 1 µm	41	44	40	40	24	61	44	82	27	50	35	70	33	17	17
industrial	% < 1 µm	59	56	60	60	76	39	56	18	73	50	65	30	67	83	83

Table 2 . Size distribution of particles at the rural site according to wind directions

Wind sector	Particles	Al	Ca	Cu	Fe	K	Mg	Mn	Na	Pb	Sr	Zn	Cl	NO3	SO4	NH4
340 - 60	% > 1 µm	52	56	51	54	31	72	51	80	14	63	27	70	14	19	15
marine	% < 1 µm	48	44	49	46	69	28	49	20	86	37	79	30	86	81	85
60 - 240	% > 1 µm	56	57	47	53	29	61	44	65	19	60	31	25	11	15	11
continental	% < 1 µm	44	43	53	47	71	39	56	35	81	40	69	75	89	85	89
240 - 340	% > 1 µm	58	56	34	53	49	66	50	80	34	71	43	77	49	29	32
industrial	% < 1 µm	42	44	66	47	51	34	50	20	66	29	57	23	51	71	68

The 340–60° wind sector represents correctly the marine sector for the sampling sites with Ca, Mg, Na, Sr and Cl which are in majority coarse particles (> 1 µm), with the higher percentage in this mode whatever the sector may be for Mg, Na and Sr, and also for Al at the rural site.

On the other hand, for the urban site, the other trace elements have their main percentage in the fine mode (< 1 µm) especially in the continental sector (60–240°) under the important influence of the city and in the industrial sector (240–340°), source of main anthropogenic elements. This mode is also found at the rural site for the trace elements except for Al and Fe.

The mass size distribution allows us to determine the behaviour of the different aerosols according to their size distribution, and it is well known (Safai et al., 1993) that this size distribution is generally similar and often bimodal with differences in the percentage contributions of particles present in the two modes (Horvath et al., 1996).

The MSD of the sampled elements at the both sampling sites, for a precise wind direction at each sector, are presented respectively for the major elements (Fig. 3) and for the trace metals (Fig. 4).

The major elements are characterized (Fig. 3) by a unimodal distribution for both sampling sites for the marine sector, and these ions dominate in the coarse mode (2.1-5.08 µm) except NH_4^+ with a peak in the fine mode (0.64-1.04 µm),

and SO_4^{2-} having a bimodal distribution for the urban site with a peak between 0.33 and 0.64 µm.

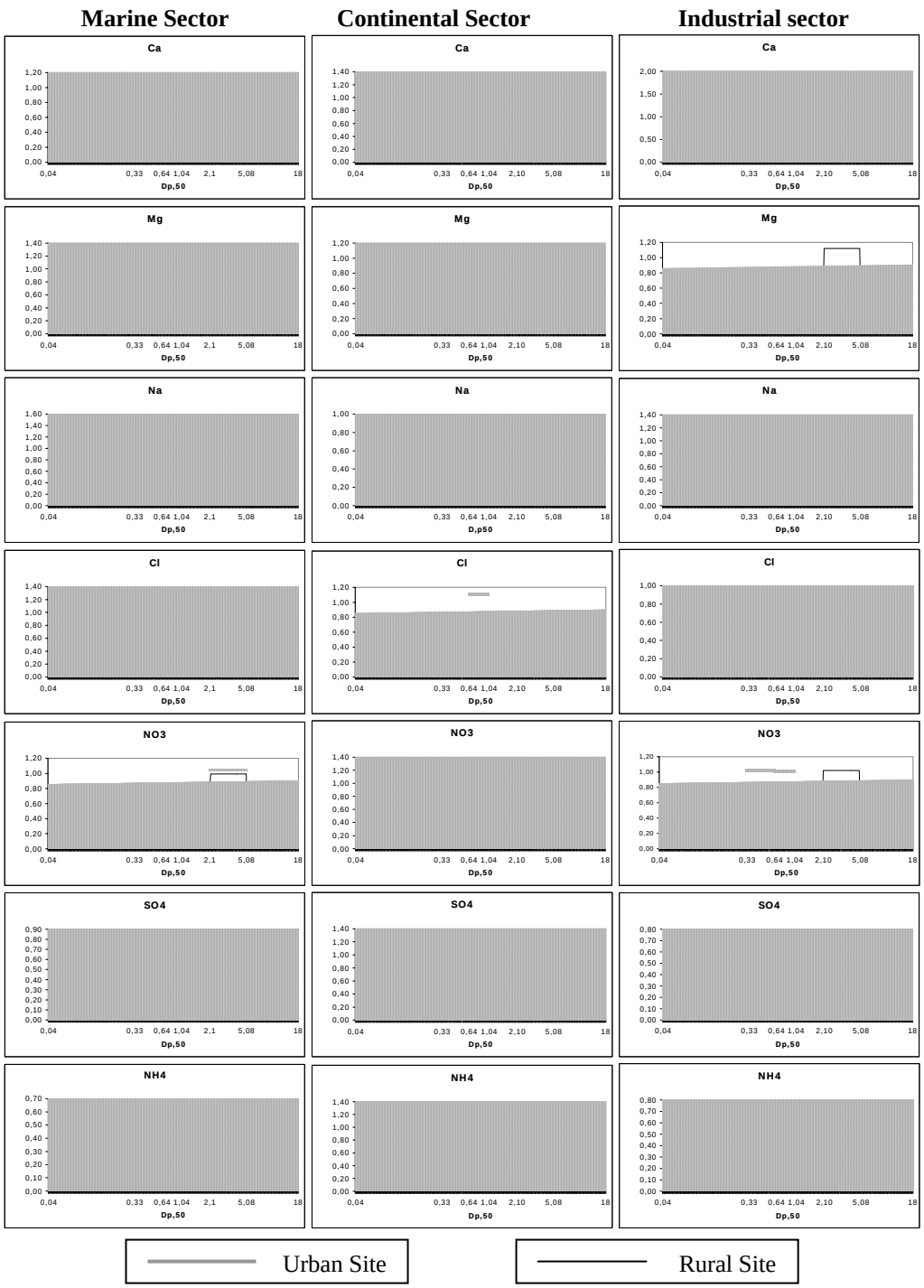

Fig. 3. MSD of major elements at the sampling sites according to wind directions

All these major aerosols have a bimodal distribution in the continental sector for the urban site, and only Ca, Cl^- and NO_3^- have the same kind of distribution for

Fig. 4 . MSD of trace elements at the sampling sites according to wind directions

the rural site. It can be noted that the elements characterized by a bimodal distribution have common peaks between 0.64-1.04 µm and 2.1-5.08 µm, but Cl^-, NO_3^-, SO_4^{2-} and NH_4^+ from the rural site, present a peak between 0.33-0.64 µm instead of 0.64-1.04 µm. This difference between the two sampling sites results probably of the importance of the influence of the urban area on the urban site. For the industrial sector, the same peaks are always present for the bimodal distribution, with the difference that for the rural site, Cl^-, NO_3^- and SO_4^{2-} have a peak at 2.1-5.08 µm and NH_4^+ with a unimodal distribution, dominates with a peak at 0.64 and 2.1 µm.

Taking into account the trace elements, (Fig. 4), we see that their distribution can be unimodal or bimodal according to wind sectors.

For the marine sector, Al, Mn, Pb, Sr and Zn at the urban site, and K and Sr at the rural site, present a unimodal distribution. Al, K and Sr dominate in the coarse mode with diameters of the particles between 2.1 and 5.8 µm. The diameters of the other particles are between 0.33 and 0.64 µm and 0.64 and 1.04 µm respectively and a wide range for Zn (0.33-1.04 µm).

For the continental and industrial sectors, all these trace elements present a bimodal distribution at the urban site. In that case, the diameters of the particles in the two modes are between 0.64 and 1.04 µm and 2.1 and 5.08 µm. The fine mode is the main result of the important influence of the industrial area, and this is particularly shown by the slipping peak from 0.64-1.04 µm to 0.33-0.64 µm for Pb and above all K and Zn. For the same sectors for the rural site, the diameters of the particles are the same in the two modes, very important between 2.10 and 5.08 µm for all elements except Zn, for the continental sector. The influence of the industrial sector appears with most particles submicrometer sized (0.64-1.04 µm).

3.3. Neutralization of Particles

From the analytical results, we have observed that most molar ratios of NH_4^+/SO_4^{2-}, NH_4^+/NO_3^- and NH_4^+/Cl^- are widely higher than theoretical values which are respectively 2, 1 and 1. This shows that a noticeable amount of NH_4^+ is combined with organic compounds as well with coarse particles as with fine particles. In coarse particles, the molar ratio NH_4^+/Cl^- is often below 1, and by this way it is possible to say that ammonium chloride is also present with coarse particles (Zuhang et al. 1999). This observation easily allows the explanation of neutralization ratios (NR) obtained during the two sampling campaigns, using the following formula :

$$NR = \frac{NH_4^+(nmol.m^{-3})}{2.nssSO_4^{2-}(nmol.m^{-3}) + NO_3^-(nmol.m^{-3})} \quad \text{(nss = non-sea-salt)}$$

The amounts of NH_4^+ are much higher in the submicronic field, and this ratio increases when the particles are in the fine mode. Fig. 5 shows that, for fine particles, this ratio is higher than 1 at the both sampling sites, and in this case, it can be supposed the presence of NH_4Cl or other forms of NH_4^+ compounds,

because lowest temperatures in winter could stabilize this compound and limit its volatilization.

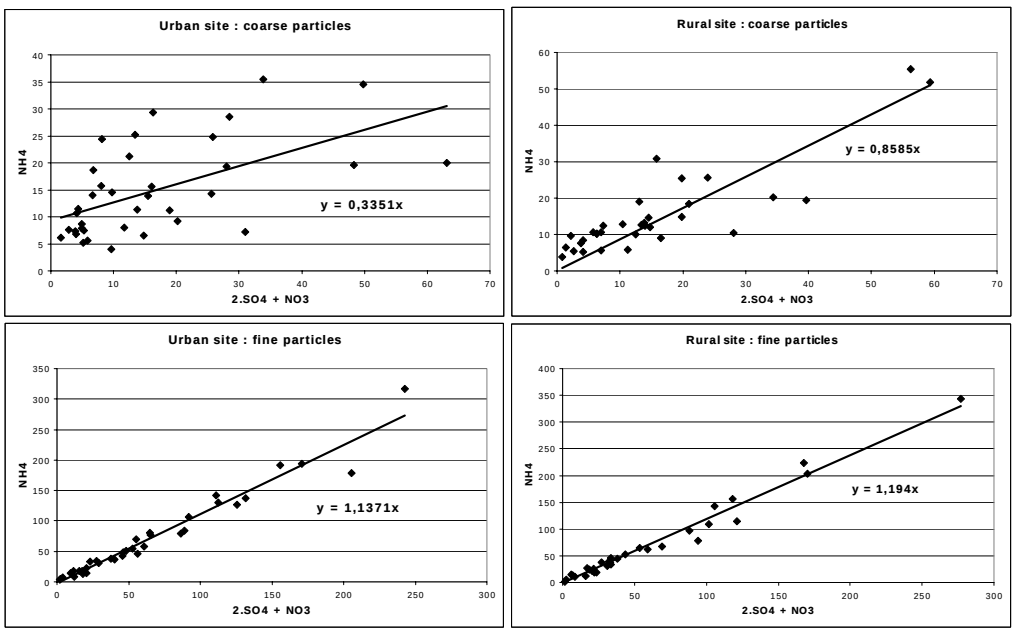

Fig. 5. Neutralization ratios (NR) at each sampling site

On the other hand, a ratio close to 1, indicates that NH_4^+ is mainly present as $(NH_4)_2SO_4$ and NH_4NO_3. For each sampling site this ratio for coarse particles is lower than 1 and indicates that SO_4^{2-} and NO_3^- are associated with other elements like Na and Ca (Harrison et al., 1994; Wakamutsu et al., 1996).

4. CONCLUSION

Mass Median Diameter reveals that the elements have different profiles according to the wind sectors, and for each sampling site, elements having industrial profiles can be classified in three groups: (1) NO_3^-, SO_4^{2-}, NH_4^+, (2) Al, Ca, Mg, Sr (3) Fe and Mn. The influence of the industrialized area on the rural site appears very well because of differences in the profiles of some trace elements. The mass size distribution study shows for most of the elements a bimodal mode, corresponding to several sources. One peak occurred between 0.33-0.64 µm or 0.64-1.04 µm, and the second between 2.10-5.08 µm. Aerosols exist in the fine and the coarse mode, but differ in percentage contribution according to the origin of the winds. Anthropogenic elements, fine particles, are identified by the industrial wind sector, and coarse particles, notably major elements, are characterized by the marine wind sector. NO_3^-, SO_4^{2-} and NH_4^+, at the urban sampling site, are mainly originated from gaz-particle conversion because they present a unimodal distribution especially in the fine mode.

According to the importance of the neutralization ratio study between NH_4^+ and $SO_4^{2-} + NO_3^-$, the behaviour of NH_4^+ in the aerosols can be explained.

5. ACKNOWLEDGEMENTS

The authors wish to acknowledge support for this work from Nord-Pas de Calais Council (n°02050163) and FEDER Grant (n°337/777)

REFERENCES

Baeyens, W., Dehairs, F., Dedeurwaerder, H., 1990. Wet and dry deposition fluxes above the North Sea. Atmos. Environ. 24A, 7, pp 1693-1703.

Bruynseels, F., Storms, H., Van Grieken, R., 1988. Characterisation of North Sea aerosols by individual particle analysis. Atmos. Environ. 22, 2593-2602.

Flament, P., Leprêtre, A., Noël, S. 1987. Aérosols côtiers dans le nord de la Manche. Oceanologica Acta 10, 49-61.

Flament, P., Bertho, M.L., Deboudt, K., Puskaric, E., 1996. Changes in the lead content of atmospheric aerosols above the Eastern Channel between 1982/83 and 1994. The science of the Total Environment, 192, 193-206.

Harrison, R.M., Msibi, M.I., Kitto, A.M.N., Yamulki, S., 1994. Atmospheric chemical transformations of nitrogen compounds measured in the North Sea experiment, September 1991. Atmos. Environ. 28, 1593-1599.

Horvath, H., Kasahara, M., Pesava, P., 1996. The size distribution and composition of the atmospheric aerosol at a rural and nearby urban location. J. Aerosol Sc. 27, 417-435.

Injuk, J., Otten, P., Laane, R., Maenhaut, W., Van Grieken, R., 1992. Atmospheric concentrations and size distribution of aircraft-sampled Cd, Cu, Pb and Zn over the southern bight of the North Sea. Atmos. Environ. 26A, 2499-2508.

Obata, H., Karatani, H., Nakayama, E., 1997. Fundamental studies for chemical speciation of iron in seawater with an improved analytical method. Marine Chemistry 56, 97-106.

Rojas, C.M., Injuk, J., Van Grieken ,R., Laane, R.W., 1993. Dry and wet deposition fluxes of Cd, Cu, Pb and Zn into the southern bight of the North Sea. Atmos. Environ. 27A, 251-259.

Safai, P.D., Khemani, L.T., Momin, G.A., Rao, P.S.P., Pillai, A.G., 1993. Mass size distribution and chemical composition of aerosols in the Silent Valley, India. Indian Journal of Radio and Space Physics 22, 56-61.

Wakamatsu, S., Utsunomiya, A., Suk Han, J., Mori, A., Uno, I., 1996. Seasonal variation in atmospheric aerosols concentration covering Northern Kyushu, Japan and Seoul, Korea. Atmos. Environ. 30, 2343-2354.

Willeke, K.,1975. Performance of the slotted impactor. Am. Ind. Hyg. Assoc. J. 36, 683-691.

Zuhang, H., Chan, C.K., Fang, M., Wexler, A.S., 1999. Size distribution of particulate sulfate, nitrate and ammonium at a coastal site in Hong Kong. Atmos. Environ. 33, 843-853.

Proceedings of the Third International Symposium on Air Quality Management at Urban, Regional and Global Scales. 26-30 September 2005, Istanbul – Turkey

COMPARISON OF SOURCE APPORTIONMENT OF PARTICLUATE POLLUTANTS AT DIFFERENT PARTS OF TURKEY

Güray Doğan, Ebru (Yörük) Tuna and Gürdal Tuncel

Middle East Technical University, Department of Environmental Engineering, 06531 Ankara, Turkey, gdogan@metu.edu.tr

ABSTRACT

In this study, a receptor oriented method, positive matrix factorization (PMF) is used for the apportionment and quantification of the sources in the Mediterranean, Black Sea and Central Anatolia regions. The results of the PMF analyses showed that aerosol at the Black Sea, Central Anatolia and Mediterranean atmosphere consists of 8, 6 and 7 components, respectively. Two of these components, namely a crustal component and a long range transport component are common in all three stations. Three factors, namely a fertilizer factor, which is highly enriched in NH_4^+ ion, a sea salt component and an arsenic factor are common in the Mediterranean and the Black Sea aerosols. The rest of the factors analyzed in each station are considered as site specific. A second crustal component and a metal factor are distinct sources identified in the Antalya region. The specific sources of Amasra region are three metal factors. The other sources identified at the Çubuk station are identified as motor vehicle source, mixed urban factor, NO_3^- factor and Cd factor.

Key Words: Positive Matrix Factorization, Mediterranean, Black Sea, Central Anatolia, Aerosol

1. INTRODUCTION

Turkey is located in the center of Asia, Africa and Europe and is affected from different emission variations of these three continents. Europe, Eastern Asia (Russia and Ex-Russia) countries and Middle East region are taken into consideration with their high industrial emissions. The emissions from Africa are mainly the transport of Saharan dust to the neighbor countries to the Mediterranean Sea. Therefore, it is essential to determine the source profiles of each sub-region of Turkey to understand the differences and similarities in the source types affecting each region.

In order to determine the source profiles, a receptor oriented method, called Positive Matrix Factorization (PMF) is used. Recently, PMF is most commonly used source apportionment tool instead of Conventional Factor Analysis (CFA) and Principle Component Analysis (PCA). The main advantages of PMF over the other receptor oriented methods are: (1) It utilizes information more efficiently by using error estimates of the measured parameters. (2) It separates sources with better resolution than CFA. (3) Its positive loadings and scores are much more useful for chemical

mass balance models (Huang, 1999). (4) Quantitatively, the factor mass profiles produced by the PMF model can apportion them among the factors in a more reasonable manner. (5) PMF can feed subjective information into factor analysis by using enforced rotation techniques (Qin et al., 2002) and (6) handling of missing and below detection limit values are much better than handling of these values in FA.

PMF uses a weighted least-squares fit with the known error estimates of the elements of the data matrix used to derive the weights. It produces quantitative non-negative solutions which can be written as:

$$X = GF + E \tag{1}$$

or by using the element-wise notation, bilinear factor analytic model is written as:

$$x_{ij} = \sum_{h=1}^{p} g_{ih} f_{hj} + e_{ij} \tag{2}$$

where X is known i x j matrix of the j measured chemical species with species in i samples. G is an i x h matrix of source contributions of the samples (time variations). The F is an h x j matrix of the source compositions (source profiles). E is the residuals matrix, i.e., the difference between the measurement X and the model as a function of the factors G and F.

Based on the standard deviation values of each data point PMF computes individual error estimates for each observed data point. This feature of PMF makes the missing and below detection limit data to be handled by adjusting the corresponding error estimates.

In this article, source profiles of stations located at the Mediterranean coast, Black Sea coast and Central Anatolia are compared.

2. EXPERIMENTAL

The locations of sampling stations are given in Figure 1. The Mediterranean station is located on the Mediterranean coast of Turkey, approximately 20 km to the east of the city of Antalya (31.0ºE, 36.8ºN). The station is located on a rock structure at a height of 20 meters above sea level. In this study, results of 1992 and 1993 aerosol samples will be discussed. During this period, approximately 600 daily aerosol samples were collected.

The Black sea station is located at Bartın, Amasra (32.3^{o}E, 41.5^{o}N), 3 km away from the Black Sea coast of Turkey, between April 1995 and July 1997. Data, which consists of concentrations of approximately 40 elements and ions in 354 daily aerosol samples collected on the Black Sea coast of Turkey, were used.

The Central Anatolia station is located at Çubuk, which is approximately 50 km away from the city of Ankara (33.10^{o}E, 40.10^{o}N). Çubuk station is the only operational EMEP station in Turkey. The station is operated by the Ministry of Health and collected data is delivered to the EMEP secretariat, where it is entered to the EMEP data base. The station became operational in 1992 and air and

precipitation samples are being collected since 1993. In this study, aerosol samples collected between February 1993 and December 2000 were used.

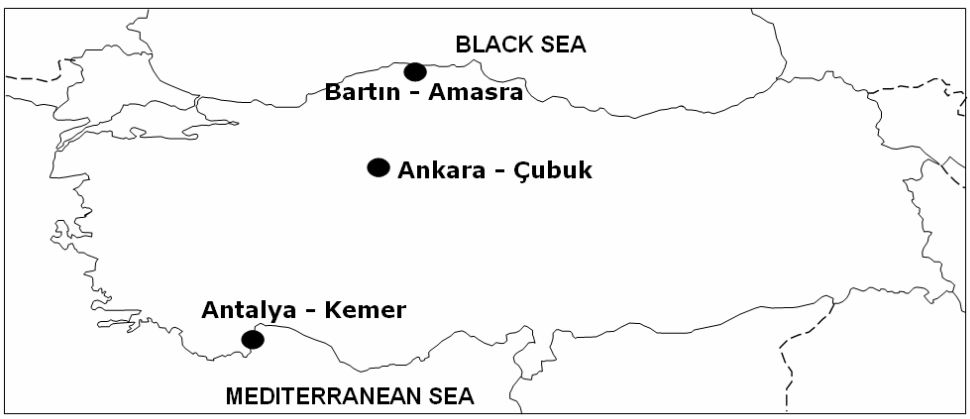

Figure 1. Locations of the sampling stations

During this time period 1806 daily aerosol samples were collected. Aerosol samples were analyzed in the laboratories of Ministry of Health, Refik Saydam Hygiene Center.

A detailed discussion of sampling and analytical methodology is discussed elsewhere (Güllü et al., 1998). Sampling at Antalya and Amasra stations were done using a Sierra Anderson Model SAUV-10H PM-10 High Volume Air Sampler, where atmospheric particles are collected on Whatman-41 cellulose filters. In these two stations, the analysis of the samples were done using atomic absorption spectrophotometer (AAS), ion chromatography (IC), VIS-spectrophotometer and instrumental neutron activation (INAA) methods. Except INAA analysis, the other analyses of these two stations are carried in our laboratories. The INAA analyses were performed in Massachusetts Institute of Technology. For Amasra and Antalya stations, since the elemental concentrations of aerosols are low, a quality control program is applied. This program includes preparation of samples, analyses of blank samples, SRM analyses, parallel analyses and re-analyses of certain samples.

In the Central Anatolia station, the samples were collected with Hi-Vol samplers on cellulose filters. The gas phase pollutants, SO_2, HNO_3 and NH_3, sampling are done using specific chemical impingements. All of the samples collected in this station are analyzed by the Ministry of Health, Refik Saydam Hygiene Center Laboratory. The analysis of the samples was done using AAS, IC and VIS-spectrophotometer. For Çubuk station, an EMEP Quality Assurance manager at the Chemical Coordinating Center and a National Quality Assurance manger of Turkey are responsible for implementing harmonized quality assurance system, including documentation of standards and reference materials.

The global minimum of the PMF solutions were tested by using different seeds for the pseudo-random initial values (Kim et al., 2004). In this study robust mode was

used to reduce the influence of possible outliers on the PMF solution. That is, a data point is processed as an outlier if the residual exceeds α times the standard deviation (Song et al., 2001). The α value of 2.0 was used for Antalya and Amasra data sets where as of 4.0 was used for the Çubuk station. To control the rotations a parameter called FPEAK is used in the PMF algorithm. PMF is run several times with different FPEAK values to find out a range within which the objective function Q value does not change much. The final acceptable rotations were determined by trial and error and based on the evaluation of the resulting source profiles (Song et al., 2001).

The success of PMF strongly depends on the estimated uncertainties for each data values. The uncertainty estimation provides a useful tool to decrease the weight of missing and below detection limit data in the solution as well as to account for the variability in the source profiles. The concentrations values were used for the measured data and the error estimate, S_{ij} for the measured concentration, X_{ij}, of chemical component j in sample i was calculated using the formula (Qin et al., 2002):

$$S_{ij} = T_j + U_j \sqrt{\max\left(\left|X_{ij}\right|, \left|Y_{ij}\right|\right)} + V_j \max\left(\left|X_{ij}\right|, \left|Y_{ij}\right|\right) \qquad (3)$$

where Y_{ij} is the fitted value for X_{ij} using a PMF and T, U and V are matrices of same size as the observed matrix X. Different approaches are available to estimate uncertainties in measured values. In some researches sum of analytical uncertainty with the one third of the detection limit were also used for the measured value error estimate. Values below detection limit were replaced by half of the detection limit values and their overall uncertainties were set at 5/6 of the detection limit values. Missing values were replaced by the geometric mean of the measured values and their accompanying uncertainties were set at four times this geometric mean values.

To be able to figure out the most reasonable solution, 3 to 10 factor run solutions are interpreted and for Antalya and Amasra stations, crustal enrichment factors are calculated for each of the solution by using F-Loading values of each factor. For the crustal enrichment factor calculations, in most of the cases, Al is used for the reference element. Explained variance of each element in each factor was also used to identify sources represented by factors. The software also produce so called "G-factor matrix", which consist of factor score values for each factor.

3. RESULTS AND DISCUSSION

For the Antalya station, seven sources were resolved and explained variations of factors are represented in Table 1. To check the correct solution, crustal enrichment factor of the crustal factor is calculated using F-Loading value of Factor 3 and is represented in Figure 2. The EFc calculation is performed by using Mason's reference soil composition (Mason, 1966). Aluminum is used as the reference element for EFc determination. For the soil factor, it is expected to observe EFc values between 1 and 10. As depicted from the figure, the EFc values of elements are generally around unity indicating that this factor is a real crustal factor.

Table 1. Explained Variations of Antalya Factor Results

	PMF 1	PMF 2	PMF 3	PMF 4	PMF 5	PMF 6	PMF 7
NO_3^-				0.52			
SO_4^{2-}				0.75			
NH_4^+	0.97						
Na		0.63					
Mg		0.32					
Al			0.74				
Cl		0.83					
K			0.35				0.26
Ca						0.64	
Sc			0.55			0.28	
Ti			0.65				
V			0.23	0.46			
Cr			0.21		0.52		
Mn			0.51				
Fe			0.6				
Co			0.51				
Ni			0.24		0.28		
Zn				0.49			
As							0.96
Se				0.45			
Br		0.28			0.35		
Sb					0.68		0.16
Cs			0.31		0.2		
La			0.44			0.31	
Ce			0.41			0.36	
Sm			0.41			0.36	
Eu			0.51			0.29	
Gd						0.83	
Tb			0.33			0.34	
Dy			0.59				
Yb			0.46			0.31	
Lu			0.49			0.33	
Hf			0.44			0.37	
Pb					0.23		
Th			0.48			0.30	
%Variance	5.07	7.30	28.00	11.40	9.90	16.40	5.20
Probable Source	Fertilizer	Marine	1st Crustal	1st Anthr.	2nd Anthr.	2nd Crustal	Local Anthr.

Factors 3 and 6 of PMF are two crustal factors with high loadings of crustal elements. However, there are some significant differences in compositions of these two soil factors. Factor 3 has high loadings of elements Al, Sc, Ti, Mn, Fe, Co, and

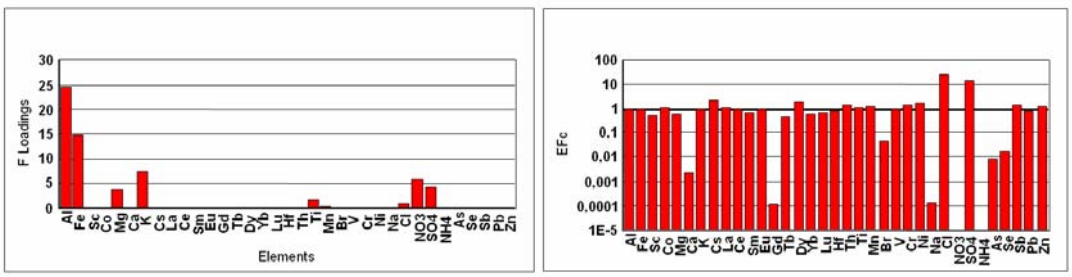

(a) (b)

Figure 2. The F-Loading and EFc profiles of Antalya crustal factor

rare earths. Factor 6 is another crustal factor. However, this factor has high Ca loading and moderate loadings of Sc and rare earth elements. Loadings of major crustal elements such as Al and Fe are less than 0.2 in this PMF factor, indicating that this is a soil factor enriched with Ca, Sc and rare earth elements. Transport of dust form Saharan to Mediterranean region is well documented (Moulin et al., 1997). Calcium is known to be a good marker element for Saharan Dust (Chiapello et al., 1997).Güllü et al. (2004) have shown that rare earth elements are enriched in transported Saharan Dust particles compared to local dust in the Eastern Mediterranean atmosphere. Based on these previous observations, Factor 6 probably represent atmospheric aerosol transported from North Africa. Factor 3 and Factor 6 explains 28 % and 16.4% of the system variances, respectively. Factor 2 is loaded with Na, Mg, Cl and Br and is a marine factor, representing sea salt component in Eastern Mediterranean aerosol. This factor explains 7.30% of the system variance.

Factor 1 is consisted only of NH_4^+ ion. Previous studies in the same location have clearly demonstrated that NH_4^+ in this region is strongly associated with fertilizer use (Güllü et al., 1998). Consequently Factor 1 in PMF is identified as fertilizer factor. Factor 4 has high loadings of NO_3^-, SO_4^{2-}, V, Zn and Se. This factor is identified as mixed anthropogenic factor, owing coexistence of coal combustion related species, such as SO_4^{2-}, Se, oil combustion related element V and Zn which is an element generally associated with industrial activities. Factor 5 has high loadings of Cr, Ni, Sb, Br and Pb. This factor is a second mixed anthropogenic factor as it includes well known marker of particles emitted from motor vehicles, such as Pb, Br and elements associated with particles emitted from smelters, such as Cr, Ni, and Sb. The Cr smelter in the city of Antalya, is the most likely candidate for this factor, because, the smelter is located within the city and ant mechanism that brings its emissions to our station is also expected to bring urban emissions. Lead and Br which are indicators of urban plume is also observed in this particular factor. Factor 7 with high loadings of As and Sb is the second anthropogenic factor. This factor is attributed to local anthropogenic emissions. This factor explains 5.20 % of the system variance.

The explained variation profiles of PMF results of Amasra station is depicted in Table 2. The PMF results showed that Black Sea aerosols have eight components. The first factor of Amasra station explains the most of the variance of litophilic elements indicating that this factor is due to re-suspension of soil. The crustal factor explains 24.12% of the system variance. The third factor is highly loaded with Na

and Cl and is identified as marine factor. As well as smaller fraction of variances of NO_3^- ion and crustal elements variances are also explained in this factor.

There are three metal factors identified for Amasra region with different seasonal trends and different elemental composition. The monthly contributions to the metal factors are represented in Figure 3. Elements with mixed sources such as Mn, V, Cr, and Ni are slightly enriched in Factor 3. As observed from the Figure 3a, there is no net seasonal variation for this factor. Factor 5 is the second metal factor with high explained variation of Co. As seen from Figure 4a, Co, Br, Cl, As, Se, Sb and Zn are highly enriched in this factor. Figure 3b indicates that the factor scores are higher during summer period. Factor loading values of Factor 5 is given in Figure 5. In this factor NH_4^+ has the highest concentration; besides NO_3^- and some crustal elements are also in high concentrations. The third metal factor is Factor 8, explaining almost all variance in Zn. As in the case of Factor 2, factor scores of Factor 8 do not show any seasonal variation. All three metal factors explain 19.20% of the system variance.

Factor 4 explains most of the variance in As concentrations. The factor also explains variances of some crustal and anthropogenic elements. Factor scores of this factor are presented in Figure 2d and are higher during winter month, suggesting a local contribution. Factor 6 is a clear SO_4^{2-} factor. The significant part of the variances of SO_4^{2-} and NH_4^+ are explained by this factor. This factor also explains the variances of Sb, Pb and some crustal elements. The EFc values are calculated for this factor and represented in Figure 4b. Chloride, SO_4^{2-}, As, Se, Sb and Zn are enriched in this factor. An important point to note in this factor is that species SO_4^{2-}, As and Se are well documented thermal power plant marker species. Since all power plant marker species are enriched in Factor 6, this factor represents a component derived from power plant emissions. Factor 7 explains variance of Se concentrations. Besides, smaller fractions of variances of other anthropogenic and crustal elements are also explained. This factor is considered as combustion factor.

In Central Anatolia region aerosols are composed of 6 components. The explained variances of factor results are represented in Table 3. Since the number of tracers measured at Çubuk station is less, it is very difficult to interpret the results. Factor 4 is identified as the crustal factor since this factor explains variances of some major litophilic elements like Ca, Mg and K. However, this factor also explains almost all variances of NH_3. Observing NH_3 in a factor can be due to fertilizer volatilization over the region. Consequently, Factor 4 is probably a soil-fertilizer application within Turkey.

Factor 1 explains high variance of NO_2 and low variances of Mg, Ca and HNO_3. This factor can be related to motor vehicle emissions. The main source of Mg and Ca in the atmosphere is the resuspension of soil dust. These parameters are frequently observed to be associated with motor vehicle factors in source apportionment studies, because transport of traffic related pollutants to the receptor also brings road dust to the sampler (Liu et al., 2003). Factor 2 has high concentration of SO_2. The source of

Table 2. Explained Variations of Amasra Factor Results

	PMF 1	PMF 2	PMF 3	PMF 4	PMF 5	PMF 6	PMF 7	PMF 8
NO_3^-	0.08	0.08	0.28	0.16		0.16		
SO_4^{2-}		0.09		0.11		0.51	0.23	
NH_4^+		0.14	0.06		0.08	0.56		0.06
Na			0.64	0.11				
Mg	0.38	0.06	0.23			0.06		
Al	0.67	0.09				0.07	0.05	
Cl			0.75					
K	0.18		0.08	0.31	0.13			
Ca	0.36		0.07			0.11		0.07
Sc	0.68	0.11						
Ti	0.43		0.08	0.07			0.08	
V	0.12	0.12		0.17		0.20		0.10
Cr	0.15	0.16	0.10	0.10				0.13
Mn	0.25	0.31				0.10	0.10	0.08
Fe	0.45	0.25	0.06	0.12				
Co					0.73	0.08		
Ni	0.15	0.13		0.27		0.05		0.08
Zn							0.07	0.90
As				0.83	0.06		0.05	
Se							0.95	
Br	0.09		0.29	0.16		0.13		
Sb		0.06		0.35		0.20		0.07
Cs		0.71			0.14			
La	0.66	0.10						
Ce	0.66							
Sm	0.69	0.12						
Eu	0.19		0.18	0.24				
Tb			0.38				0.29	
Dy	0.26	0.07	0.26					
Yb	0.52						0.10	
Lu	0.63							
Hf						0.44		
Pb		0.12	0.07	0.07		0.26		0.15
Th	0.50				0.25			
%Variance	24.12	8.24	10.96	9.32	5.27	9.09	6.68	5.50
Probable Source	Crustal	1st Metal	Marine	Local Anthr.	2nd Metal	Anthr.	Combust.	3rd Metal

this component is local. Factor 3 includes high variances of SO_4^{2-}, NH_4^+ and Ca. This factor is due to long range transport of pollutants.

Factor 5 and Factor 6 are not very clear. Factor 5 includes primarily NO_3^- and Factor 6 is composed of NH_4^+, HNO_3 and Cd. The variance in the factor is explained mostly by Cd.

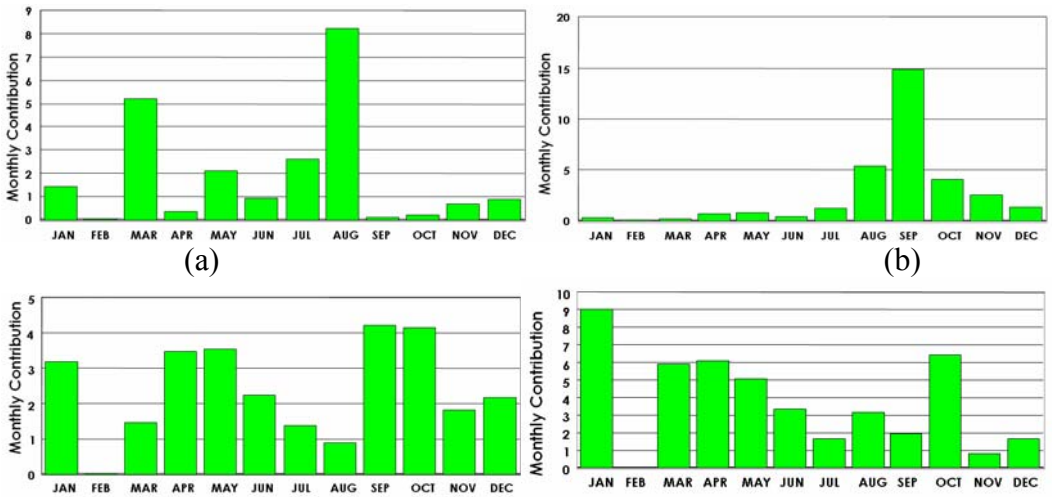

Figure 3. Monthly contributions of (a) Factor 2, (b) Factor 5, (c) Factor 8 and (d) Factor 4 of Amasra Station

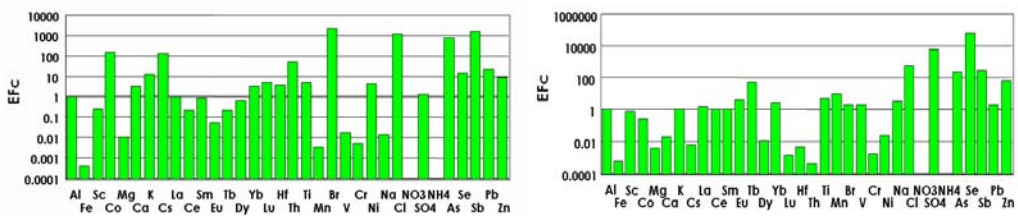

Figure 4. Crustal enrichment factor results of (a) Factor 5 and (b) Factor 6 of Amasra Station

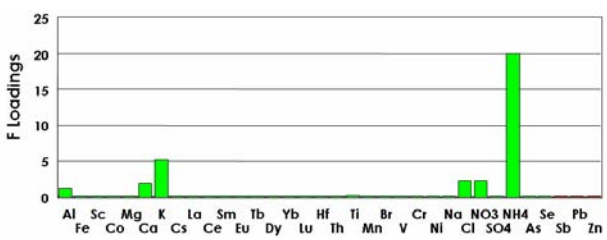

Figure 5. Factor Loading value of Factor 5 of Amasra Station

4. CONCLUSION

The evaluations up to now showed that the measurements that were held in three stations have two similar factors. First one is crustal component which is composed of litophilic elements and the second one is the anthropogenic component, which is mainly composed of SO_4^{2-} and transported to each station site by means of long range transport. The PMF analyses in the Mediterranean and Black Sea regions showed that aside from these three factors, sea salt, arsenic and particles due to use of fertilizer are other common components. However, since the marker elements for the characterization of factors did not measured in Çubuk station, it is impossible to judge on the existence of similar aerosol components in the Central Anatolia region.

The other factors identified in each of the regions are realized to be distinct to each station site.

Table 3. Explained Variations of Çubuk Factor Results

	PMF 1	PMF 2	PMF 3	PMF 4	PMF 5	PMF 6
NO_3^-					1	
SO_4^{2-}			0.93			
NH_4^+			0.50		0.05	0.18
Mg	0.08			0.57		
K				0.42	0.20	
Ca	0.10		0.33	0.29		
Cd						0.95
NH_3				0.89		
SO_2		0.98				
NO_2	0.93					
HNO_3	0.18		0.05	0.15		0.41
% Variance	11.73	8.91	16.45	21.09	11.36	14.00
Probable Source	Motor Vehicle	Mixed Urban Factor	Long range factor	Crustal	NO_3^- Factor	Cd Factor

REFERENCES

Chiapello, I., Bergametti, G., Chatenet, B., Bousquet, P., Dulac, F., Soares, E.S., 1997. Origins of African dust transported over the northeastern tropical Atlantic. Journal of Geophysical Research-Atmospheres 102, 13701-13709.

Güllü, G., Ölmez, İ., Aygun, S., Tuncel G., 1998. Atmospheric trace element concentrations over the Eastern Mediterranean Sea: Factors effecting temporal variability. Journal of Geopys. Res. 103, 21943-21954.

Güllü, G., Ölmez, İ., Tuncel, G., 2004. Source apportionment of trace elements in the Eastern Mediterranean atmosphere. Journal of Radioanalytical and Nuclear Chemistry, Vol 259, No.1, 163-171.

Kim, E., Hopke, P.K., Edgerton, E.S., 2004. Improving source identification of Atlanta aerosol using temperature resolved carbon fractions in positive matrix factorization. Atmospheric Environment 38, 3349-3362.

Liu, W., Hopke, P.K., Han, Y.J., Yi, S.M., Holsen, T.M., Cybart S., Kozlowski, K., Milligan M., 2003. Application of Receptor Modeling to Atmospheric Constituents at Potsdam and Stockton, NY. Atmospheric Environment 37, 4997-5007.

Mason, B., 1966. Principles of Geochemistry. 3rd Ed. John Wiley, New York.

Moulin, C., Lambert, C.E., Dulac, F., Dayan, U., 1997. Control of atmospheric export of dust from North Africa by the North Atlantic oscillation. Nature 387, 691-694.

Qin, Y., Oduyemi, K., Chan, L.Y., 2002. Comparative testing of PMF and CFA models. Chemometrics and Intelligent Laboratory Systems 61, 75-87.

Song, X.H., Polissar, A.V., Hopke, P.K., 2001. Source of fine particle composition in the northeastern US. Atmospheric Environment 35, 5277-5286.

CHANGE OF ATMOSPHERIC AEROSOL COMPOSITION IN BEIJING DUE TO AIR POLLUTION CONTROL

R.J. Zhang [1*] Z.F. Wang[1] M.G. Zhang[1] S. Yabuki[2], Y. Kanai[3], and A. Ohta[3]

[1] REC-TEA,NZIRC, LAPC, Institute of Atmospheric Physics, Chinese Academy of Sciences, Beijing, 100029, China
[2]The Institute of Physical and Chemical Research, Wako, Saitama, 351-0198 Japan
[3]Geological Survey of Japan, National Institute of Advanced Industrial Science and Technology,* zrj@mail.iap.ac.cn

ABSTRACT

Atmospheric aerosols samples were collected with a cascade sampler in a northern neighborhood of Beijing in November and December 1999. The elemental concentration and size distribution of aerosols were analyzed by using PIXE technique. The observed data are studied and compared with previous data at the same sampling site from February and March 1999. Based on the observations, the elemental concentrations and distributions and their changes are studied. Results show that S concentrations of atmospheric particles in the winter of 1999 decreased by 53% compared to the previous year. On the other hand, the concentrations of Cu in the winter of 1999 increased by 72% over precious winter and were mainly enriched in fine particles other in coarse particles. This is because clean fuels (such as diesel oil and natural gas) were used in heating period heating instead of coal in the winter of 1999. Concentration of Pb in atmospheric particles in the winter of 1999 decreased by 72% compared to the previous year due to introduction of non-leaded gasoline. These results demonstrate that the chemical composition and source of atmospheric particles have changed greatly in recent years. The pollution due to atmospheric particles in Beijing has been obviously lessened because of air pollution controls introduced by the Beijing municipal government.

Key Words: PIXE, Atmospheric aerosols, Elemental concentration, Heating period.

1.INTRODUCTION

Atmospheric aerosols play an important role in the radiative budget of the earth and atmosphere system, by directly scattering solar radiation and absorbing solar and terrestrial radiation, and by indirectly influencing the physical and optical properties and lifetime of cloud(Zhang et al., 2005). These two effects depend not only on aerosol mass loading and global mean values, but also on their physical, chemical, and radiative properties and their space distributions. Atmospheric aerosols are also one of the major pollutants, especially in cities, impairing visibility and causing harmful effects on human health (Zhang et al., 2000). Atmospheric particles are also the major pollutant in Chinese cities, especially in North China (An et al., 2000). In Beijing, the concentration of total suspended particles often exceeds the air pollution standards, and furthermore, Beijing is regarded as one of the most seriously polluted cities in the world (Elsom,1996).

In the past, the aerosol pollution in Beijing resulted from to the type of coal combustion used in 1980s (Zhao and Wang, 1991;Zhang et al., 2002). As the number of automobiles has increased sharply with the development of economy, air pollution in Beijing has become more and more

serious. The fine particles which always form the “black pot” covering over Beijing in recent years, especially in winter, are a mixture of products of SO_2 from burning coal and NO_x from automobile emission created through complex physical and chemical transformations. The fine particles, which disperse in the air from the surface to 800 meters, not only have a strong scattering effect on solar radiation but can also act as carriers of bacteria and viruses harmful to human beings. In order to provide scientific reference for economical and effective control strategies and to evaluate the effects of these strategies, we need better knowledge of the concentration and composition of atmospheric aerosols.

In Beijing, winter is the season with the worst pollution. The composition of atmospheric aerosols in Beijing in winter has been studied since the beginning of the 1980s (Wang et al., 1981; Ren et al., 1982,Wang and Zhu, 1990; Zhang et al., 2002; Zhang et al., 2004), and very limited works were done in the 1990s. From 1999, the local government undertook many measures to control the air pollution in Beijing. Since 1999, the local government has controlled the emission of local dust from building sites, house reconstruction, road construction and so on. Since 1999, the automobiles in Beijing have used non-leaded gasoline instead of ethyl gasoline. Before 1999, coal was used as the main fuel for heating in winter. After 1999, diesel oil and natural gas have been used as fuel for all mid-sized and big boilers in main urban regions. What is the change in chemical composition of atmospheric particles in Beijing under these control actions? In this paper, through observations in November and December of 1999, the elemental concentrations of aerosols in Beijing and their changes in recent years are investigated and discussed. We will analyze these changes according to total and elemental concentrations, elemental size distribution, and enrichment factors.

2. OBSERVATIONS

2.1 Sampling

The observation site is located on the top of a two-storey building, 50m south of the 325 m Meteorological Tower (116°22′E, 39°58′N), which is north of the North Third Ring Road in Beijing.

The aerosol samples were collected using eight-stage cascade impactors (PIXE International Corporation), with 8 fraction levels of <0.25,0.25-0.5,0.5-1,1-2,2-4,4-8,8-16, and >16μm. Samples were taken at the height of 6 m high during 3-6 November and 21-24 December 1999. The sampling time was from 8:30 to 17:30 during the daytime and 17:30 to 8: 30 during the night, Beijing standard time. The flow rates at the beginning and the end of each sample time were recorded, and the average of the two flow rates was used as the sample flow rate. In this study, 12 groups of 96 samples for 6 days were obtained in November and December 1999.

2.2 Analysis of the samples

The samples were analyzed by PIXE in Beijing Normal University. The PIXE analyses were carried out by using 2.5MeV proton bombardments with a beam of 30 40nA. Elemental concentrations and particle size distributions for 20 elements were determined (Mg, Al, Si, P, S, Cl, K, Ca, Ti, V, Cr, Mn, Fe, Ni, Cu, Zn, As, Se, Br, and Pb). The details about the experimental PIXE setup and the procedures have been given by Zhu and Wang (2000). In the past two decade, PIXE method has been widely used to study chemical composition of aerosols in China (Zhu and Wang, 1998; Zhang et al., 2002).

3. RESULTS AND DISCUSSION

3.1 Total elemental concentrations and their changes

The soil mass concentration is estimated in by summing the elements predominantly associated with soil, plus oxygen for the normal oxides using concentration of Al, Si, Ca, Fe, and Ti according to Malm et al.(1994). Figure 1 shows the soil mass concentration of aerosols at different sampling times at the same site in 1999. The total concentration of atmospheric particles in early 1999 is close to that in 1981. But in winter 1999, the total concentration decreased greatly, about 50% less than in early 1999. The major contributors of total concentration are crustal elements such as Al, Si, Fe, Ca, and Ti. The origin of crustal aerosols is mainly from local dust. They have a coarse mode (>2μm) and account for about 80% of the total elemental concentration. No dust storm activity appeared during four measurement periods based on Beijing meteorological observation and surrounding meteorology stations, which means that the crustal aerosols were produced by local sources. Since soil concentrations in December is lower than in February, and March, it is reasonable to think the measures initiated by the government have successfully taken effect in controlling potential sources for local dust.

Table 1 shows the ratios of elemental concentrations of particles in November (before the heating period) and December (during the heating period) in 1999. Concentrations of Pb and Br decreased during the heating period. The amount of decline for concentrations of S, K, V, Zn, As, Se, and Cr is between 20% and 40%. The elements with high increases in concentrations are Al 40% , Si 80% , Ti 146% , Cu 100% and Fe 20% . The change in concentrations of other elements is within ±20%.

Major factors influencing S concentration are source strength and meteorological conditions. Figure 2 shows the S concentrations and relative humidity on 9-12 March 1999. The S concentration of particles in each of three days is 2.8, 4.6, and 8.3 $\mu g/m^3$, respectively, with corresponding relative humidity of 38%, 61%, and 75%. This demonstrates that S concentration increases considerably with increasing relative humidity

The weather during the observations in February, November, and December 1999 was clear while the weather during the March observation was cloudy with high relative humidity. As a result, the S concentration in March is higher than in February. Table 2 shows the weather conditions and concentrations of S, K, V, Ni, Cu, and Pb in 1999. February was at the heating period and March was in the end of the heating period in Beijing. But the S concentration in March was 62% higher than in February due to higher relative humidity in March. The relative humidity in December was close to that in February in 1999, but the S concentration in December had decreased by 53% compared to February. Coal was used in Beijing as the boiler fuel in the winter of 1998. But in the winter of 1999, all big and mid-sized boilers in main urban regions in Beijing were reformed, and clean fuel(such as diesel oil and natural gas) was used instead of coal. The observation of particles in February 1999 was used to represent conditions in the winter of 1998. Results indicate that the pollution control policy implemented by the local government probably made S concentrations decrease greatly in the winter of 1999.

The K, V, and Ni concentration in March, November and December however, are much lower than those in February. The concentrations of K, V, and Ni in winter of 1999 decreased by 59%, 68%, and 44% compared to the previous winter, respectively. Not that March is the end of the heating period. It is reasonable that the concentrations of K, V, and Ni in November and December were lower than in February. This indicates that burning coal generates more K, V and Ni than burning oil does.

The concentration of Cu in December 1999 increased by 72% compared to February 1999. Previous research by Wang et al.(1986) showed that most Cu in the atmosphere in Beijing was

from petrochemical industry. In December 1999, diesel oil was used as boiler fuel in urban regions, which resulted in increased atmospheric Cu and decreased atmospheric S.

The main source of lead in the urban atmosphere is the combustion of leaded gasoline in which lead has been added as an antiknock agent and as a lubricant for valve seats. After combustion, the lead is released through exhaust emission into the air in the form of fine inorganic particles, which can be inhaled. Lead is harmful to persons, especially to children. Beijing is a fast-developing metropolis, and in recent years, the number of automobiles in Beijing has increased dramatically. But non-leaded gasoline was not used until 1998. According to our observations, in February 1999, atmospheric Pb concentration was above 240ng/m^3 (Zhang, et al., 2002), which was much higher than that of 133ng/m^3 in winter of 1983 in Beijing at the same site (Wang et al., 1986). The concentration of atmospheric Pb concentration in winter of 1987 at another urban site nearby was 500ng/m^3 (Wang and Zhu,1990). In November 1999, the concentration of atmospheric Pb was 137 ng/m^3. In December 1999, it was 50ng/m^3, which was much less than that in 1983 and is close to the concentration in rural area of North China observed by Wang (1986). Investigation by Wu et al. (2002) shows that the concentration of Pb in gasoline was 0.027g/l before 1998 and 0.005g/l after 1998. It is obvious that Pb concentration has decreased in Beijing because of the use of non-leaded gasoline.

3.2 Distribution of elemental concentration

The size distribution of elemental concentrations can reflect to some extent the sources of aerosols. Figure 3 gives the concentration distribution of Fe, K, Pb, S, and Cu in November and December 1999. Fig.3a shows the size distribution of a single peak of Fe. The concentration of Fe reaches a maximum at stage 5(4-8μm) in November before the heating period and reaches a maximum at stage 8(>16μm) during the heating period. Results also show that bigger particles exist in winter. The size distributions of Si, Ca, Ti, Fe, and Al are similar to that of Fe. This demonstrates that they come from the same source, which is local dust. In November, elemental distribution of K has a single peak which appears to be at 0.5-1μm. This fine mode distribution of K is probably caused by combustion of leaves at the end of autumn in Beijing. Pb is similar to K (Fig.3b, 3c), however, the present sources of Pb is not very clear and need to be studied further. Figure3d shows the distribution of S. The concentration of S in particles during the heating period is smaller than before the heating period which shows that combustion of diesel oil and natural gas in winter has no obvious contribution for S in atmospheric particles. The elemental distribution of Cu showed a double-peak mode in 1983 (Wang, et al., 1986). Here it is a double-peak mode before the heating period, and a single-peak, fine mode in winter, which may be due to the combustion of diesel oil(Fig.3e).

3.3 Enrichment Factors analysis

Various formation mechanisms and sources of aerosols have different enrichment extents. The enrichment factor of an element in aerosol is often used to represent enrichment extent, and are defined as

$$EF=(C_x/C_r)_a/(C_x/C_r)_r \quad (1)$$

where C_x is the concentration of element x, C_r is that of a reference element, the subscript a refers to the aerosol, while r refers to the reference material. Usually, Al, Si, and Fe are chosen as reference materials. Here Si is selected as a reference element to calculate the enrichment factors of elements in aerosols in Beijing relative to crustal elements (Winchester et al., 1981). Results are given in Table 3.

Figure 4 shows the enrichment factors of Cu in Beijing in 1999. It shows that enrichment

factors of Cu in fine particle were much higher than in coarse particles and has an increase trend especially in the heating period in 1999. It indicated these no only Cu concentration in fine particles increased greater than in coarse particles but also were mainly enriched in fine particles other in coarse particles.
The enrichment factors of Cu, Zn, Cr, Ni, and V increase greatly in the heating period, especially for small particles. The enrichment factor of Cu in the heating period is 4 times greater than before the heating period. The enrichment factors of S, Mn, Br, and Pb decrease obviously in the heating period. Also in the heating period, the enrichment factors of S and Pb decrease by more than 60%. The enrichment factors of other elements change little.

4. CONCLUSIONS

Through the observation of chemical composition of particles in Beijing in 1999, the following results are obtained.
1 The total concentrations of 20 elements of particles at the end of 1999 decreased by almost 50% compared the beginning of 1999, and coarse mode particles account for about 80% of the total concentration in winter. Probable reasons are the measures taken by the Beijing municipal government to control dust emission.
2) The concentration of S in atmospheric particles in December of 1999 was only 47% of that in February 1999. The concentrations of K, V, and Ni in the winter of 1999 decreased by 59%, 68%, and 44% compared to the previous winter, respectively. The reason for the decrease of S, K, V, and Ni is that diesel oil and natural gas were used as fuel instead of coal during the heating period in the winter of 1999, and coal burning decreased.
3) The concentrations and enrichment factors of atmospheric Cu increase greatly in winter in Beijing due to the use of diesel oil as boiler fuel in Beijing. Cu were mainly enriched in fine particles other in coarse particles.
4) The present atmospheric Pb concentration is much less than it was in the 1980s. This demonstrates that the effectiveness of using non-leaded gasoline in recent years.
Based on our measurements, the effects of measures such as controlling soil emission, boiler reconstruction, and using clean gasoline are apparent. However, we can not eliminate other possibilities that influence our measurements, for example, seasonality of aerosol concentration. More measurements, especially long-term continuous measurements of particles, are needed to draw quantitative conclusions.

5. ACKNOWLEDGMENTS

This work is supported by National Basic Research Program of China (2006CB400501), the Hundred Talents Program (Global Environmental Change) by Chinese Academy of Sciences and Natural Science Foundation of China (No.40205017)

REFERENCES

An J. L, Zhang R. J. and Han Z.W., 2000, Seasonal change of total suspended particles in the air of 15 big cities in northern parts of China, Climate and Environmental Research, 5(1), 25-29. (In Chinese)
Elsom Derek, 1996. Smog Alert: Managing Urban Quality, Earthscan Publications Ltd. London, 225p.

Malm W C, Sisler J F, Huffman D. et al.,. Spatial and seasonal trends in particle concentration and optical extinction in the United States. 1994, J.Geophys.Res.,1994, D1, 99 1347-1370.
Ren L.X., Lu W.X. and Wang M.X., 1982. A study of elemental concentrations in atmospheric aerosol from Beijing in late winter, Scientia Atmospheric Sinaca, 6(1), 11-17(in Chinese).
Wang X.F. and Zhu G.H., 1990. Elemental concentration and size distribution of atmospheric particles in the north urban area in winter/summer, Scientia Atmospheric Sinaca,14(2), 199-206 (in Chinese).
Wang A. P., Yang S.L. and Sha, Y., 1996. Chemical characterization of individual fly ash particles from coal-fired power plant, Chinese Journal of Environmental Chemistry, 15 (6), 496-504(in Chinese).
Wang M.X., Ren L.X., and Lu W.X., 1986. Elemental concentration and their size distribution of Beijing aerosol in January, Advances in Atmospheric Sciences,3(2), 199-207.
Zhang M.G., Han Z.W., and Lei X.E., 2000, Numerical simulation of TSP concentration distribution in Tianjing, Climate and Environmental Research,5(1),30-35(in Chinese).
Winchester, J.W., Lu W.X., Ren L.X., Wang M.X., and W. Maenhaut, 1981. Fine and coarse aerosol composition from a rural area in northern China, Atmospheric Environment, **15**,933-937.
Wu Y., Hao J.M., Li W. and Fu L.X., 2002, Calculating emissions of exhaust particulate matter from motor vehicles with PART5 model, Chinese Journal of Environmental Science,23(1), 6-10(in Chinese)
Zhang M., 2004, Modeling of organic carbon aerosol distributions over East Asia in the springtime, China Particuology, 2(5), 192-195.
Zhang R.J., Wang M.X. and Xia X.A., 2002, Chemical composition of aerosols in winter/spring in Beijing, Journal of Environmental Sciences, 14(1), 7-11.
Zhang Y.H., Zhu X.L, Zeng L.M., Wang W., 2004, Source apportionment of fine-particle pollution in Beijing, Urbanization, Energy, and Air Pollution in China, The National Academies Press, p139-153.
Zhao D.S. and Wang M.X., 1991, Urban pollution atmospheric aerosol of coal combustion, China Environmental Science Press, 404p(in Chinese).
Zhu G.H. and Wang G.F., 2000, Cross-check of PIXE analysis between three laboratories, Climate and Environmental Research, 5(1), 80-84, 2000 (in Chinese).
Zhu G.H. and Wang G.F, Investigation of the particulate derived from indigenous zinc smelting using PIXE analytical technique, Nuclear Instruments and Methods on Physics Research B,1998, 136: 966-969.

Table 1. Ratios of elemental concentrations of particles in November to December in 1999.

Element	Mg	Al	Si	P	S	Cl	K	Ca	Ti	V
Ratio (Nov./Dec.)	0.91	1.41	1.81	1.03	0.75	0.57	0.73	0.90	2.47	0.60
Element	Cr	Mn	Fe	Ni	Cu	Zn	As	Se	Br	Pb
Ratio (Nov./Dec.)	0.71	0.87	1.26	1.02	2.01	0.63	0.74	0.55	0.38	0.38

Table 2. Weather condition and concentrations of S,K,V, Ni, Cu and Pb in 1999

Observation time	Feb 23-26	Mar 9-10	Nov 2-6	Dec 21-24
S($\mu g/m^3$)	3.29	5.34	2.07	1.55
K(ng/m^3)	2197.4	1620.0	1214.1	890.2
V(ng/m^3)	9.5	5.7	5.0	3.0
Ni(ng/m^3)	105.0	65.6	57.0	59.0
Cu(ng/m^3)	98.1	89.2	84.0	169.0
Pb(ng/m^3)	240.0	205.5	137.0	53.0
Rh	31%	57%	39%	27%
Weather condition	Clear	Cloudy	Clear	Clear

Table 3. Enrichment Factors of atmospheric particles in Beijing in 1999.

Time	March		November		December	
Elements	Fine-mode	Coarse-mode	Fine-mode	Coarse-mode	Fine-mode	Coarse-mode
Al	4.61	2.20	3.47	2.13	2.72	1.77
S	1533.70	151.84	1205.37	129.13	649.11	76.91
Cl	904.48	119.45	1596.52	145.27	790.28	50.52
K	2.70	0.86	6.06	1.05	1.95	0.72
Ca	1.93	4.16	3.28	6.10	2.06	2.83
Ti	1.19	1.76	0.80	1.09	0.88	1.47
V	0.58	0.84	1.54	1.78	1.44	0.44
Cr	10.32	2.77	12.45	19.18	13.59	5.92
Mn	9.06	2.48	12.02	3.72	7.16	1.99
Fe	1.28	1.50	1.91	1.99	1.48	1.36
Ni	20.56	15.63	19.37	39.97	31.07	18.54
Cu	72.00	22.06	128.30	54.50	395.48	30.66
Zn	262.11	40.72	566.31	71.94	319.06	24.93
As	1485.19	366.59	4035.64	1398.88	2697.35	509.48
Se	12423.86	4081.63	29056.60	15587.53	15536.72	4141.57
Br	1007.22	99.77	747.17	95.92	233.05	23.67
Pb	1220.20	109.02	1644.41	156.80	522.87	40.96

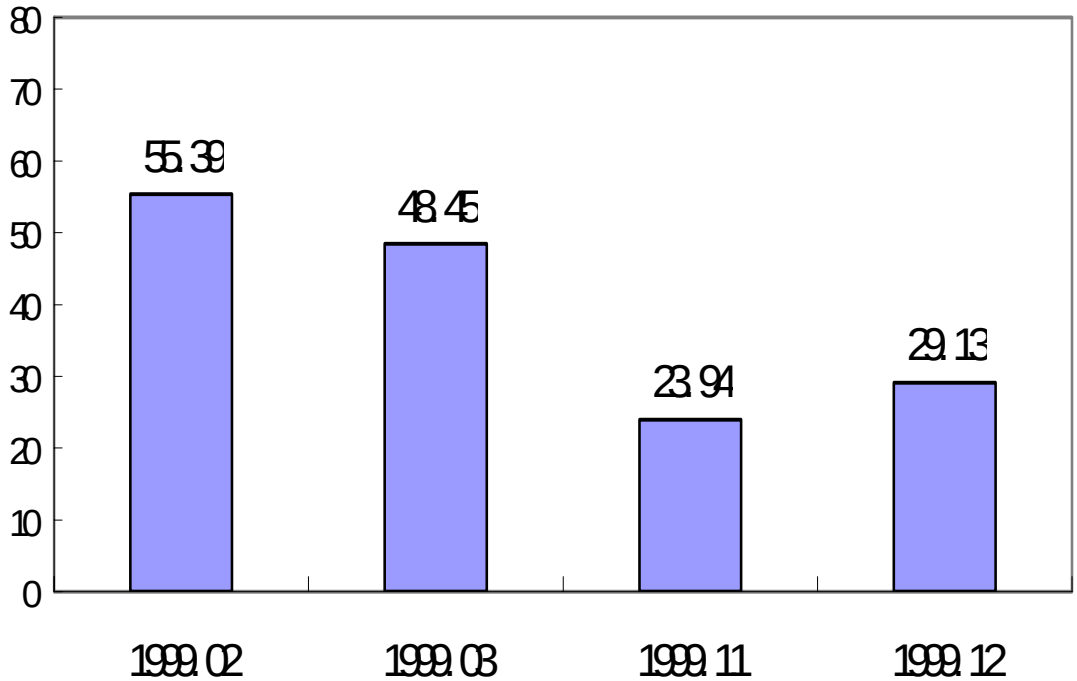

Figure1. Soil concentration of aerosol in 1999 in Beijing

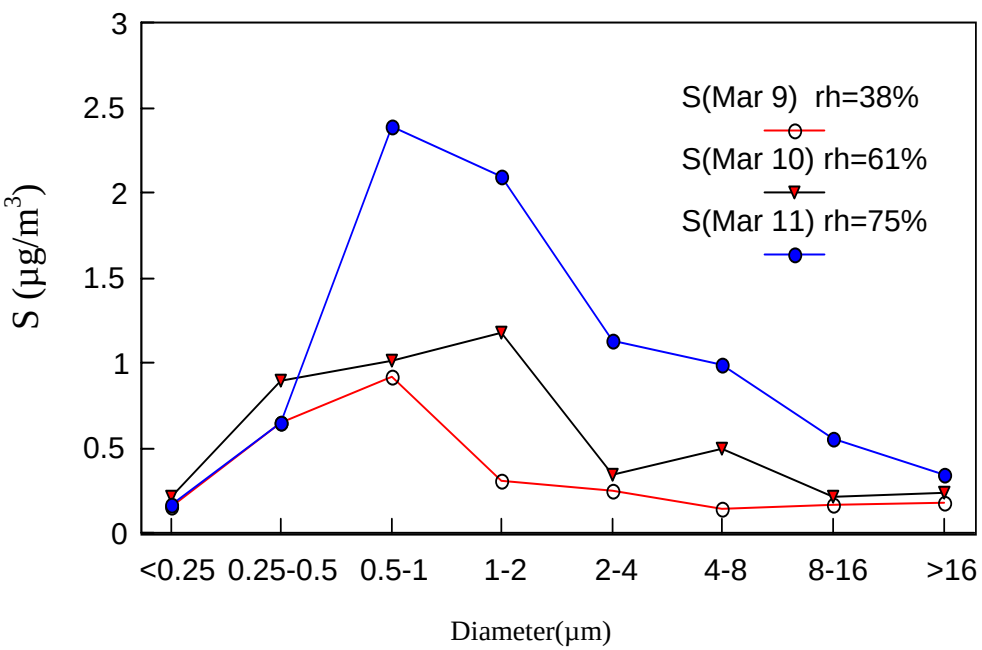

Figure 2. Elemental concentration of S and relative humidity in March 1999.

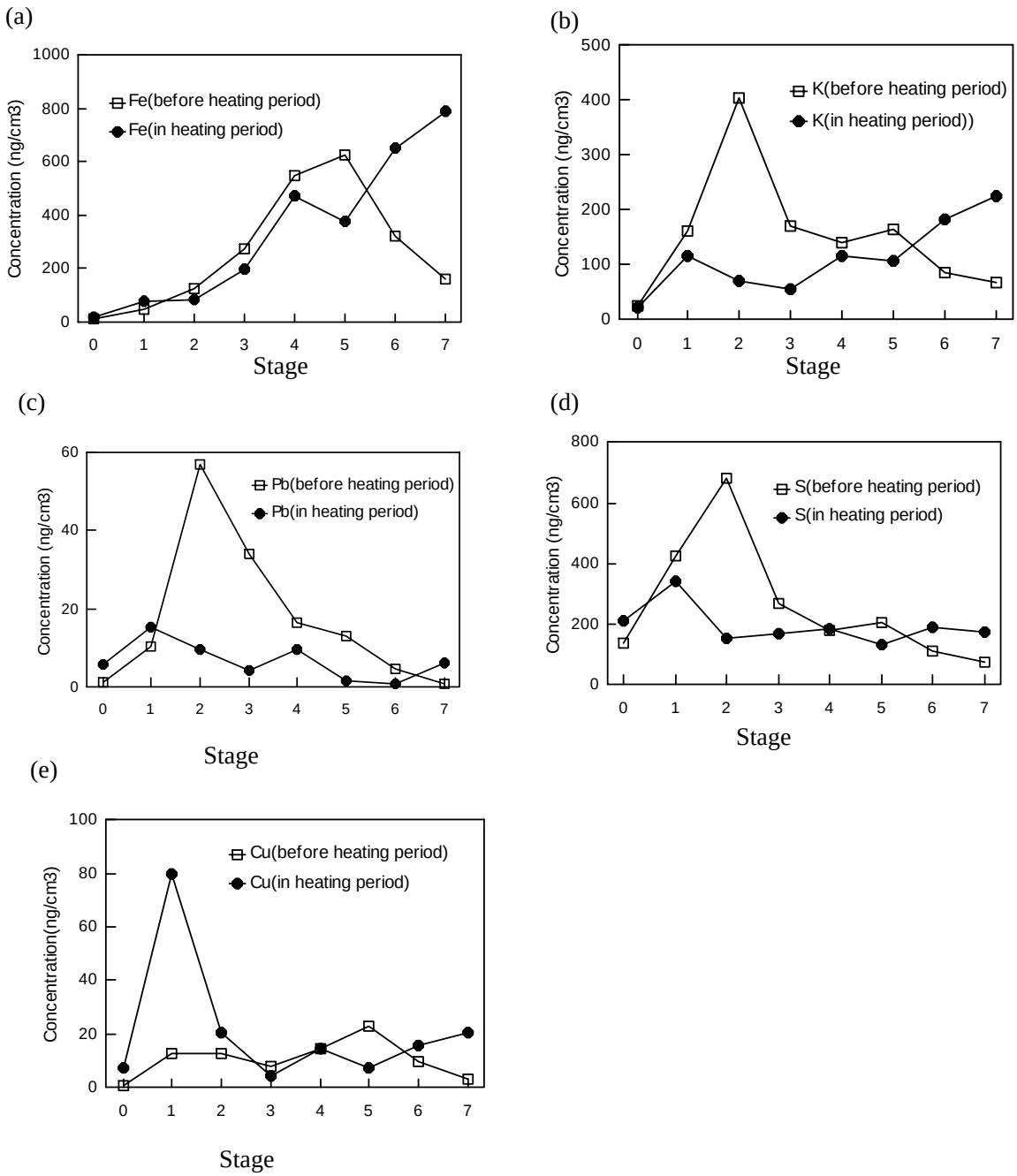

Fig.3 Size distribution concentration of (a)Fe, (b)K, (c) Pb, (d) S, and (e)Cu in November and December 1999

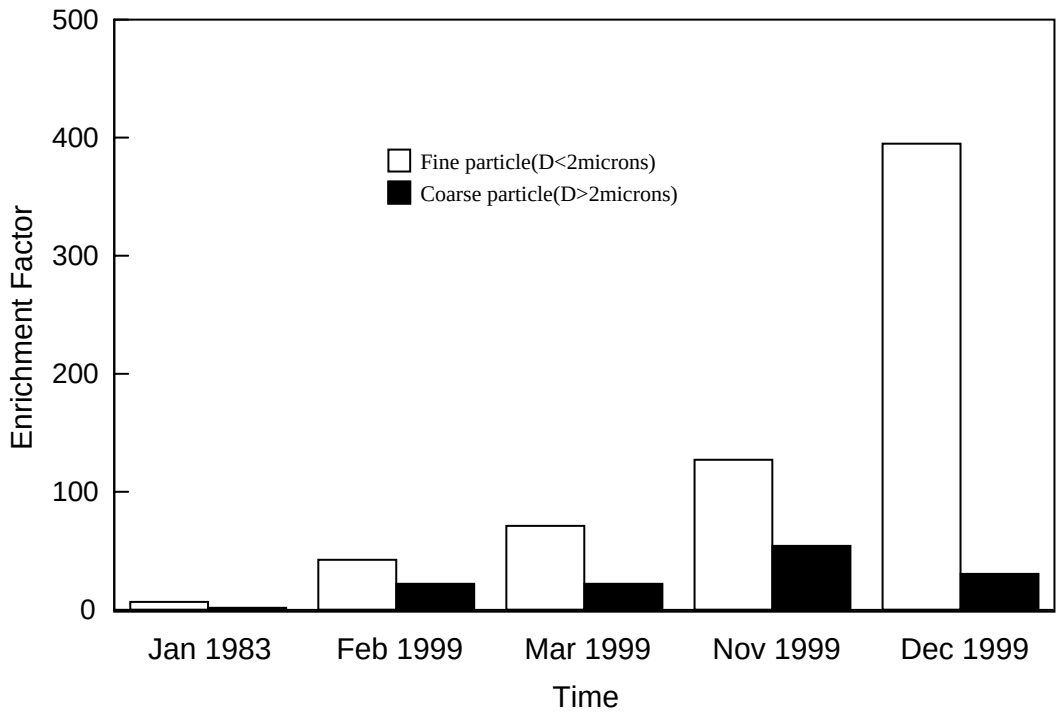

Figure 4. Enrichment factors of Cu in Beijing

Proceedings of the Third International Symposium on Air Quality Management at Urban, Regional and Global Scales. 26-30 September 2005, Istanbul – Turkey

VARIATION OF AEROSOL COMPOSITIONS DURING DRY AND WET SEASONS IN NORTHERN THAILAND

Arpa Wangkiat[1], Supat Wangwongwatana[2] and Shin'ichi Okamoto[3]

[1] Rangsit University, Department of Environmental Engineering, Phaholyothin Rd., Lakhok, Phathum-Thani 12000, Thailand, arpa@rangsit.rsu.ac.th
[2] Pollution Control Department, Ministry of Natural Resources and Environment, Phahonyothin Road, Sam Sen Nai, Phayathai, Bangkok 10400, Thailand, supat.w@pcd.go.th
[3] Tokyo University of Information Sciences, 1200-2 Yatoh-cho, Wakaba-ku, Chiba, 2650072 Japan, okamoto@rsch.tuis.ac.jp

ABSTRACT

Investigations of particulate matter of an aerodynamic diameter less than 10 μm (PM_{10}) were monitored at four sampling stations around big anthropogenic emission sources in northern Thailand: lignite mining and coal-fired power plants area in Mae Moh valley during February-July 2004. One hundred and twenty PM_{10} samples were collected by Mini-Volume air samplers. Aerosol compositions were analyzed for 30 elements, 4 ionic species, and elemental and organic carbons (EC, OC). The average mass concentrations of PM_{10} in dry and wet season were 79.25-105.99 and 19.57-28.09 $\mu g/m^3$, respectively. The most abundant chemical compositions of PM_{10} in dry season were EC, OC, K^+, Cd, Ga, Si, Al, S and K. All of the chemical compositions in wet season are 40-80 % lower than dry season except Ga and Se which are the marker species of coal fired power plant and often found in PM less than 1 micron in diameter are only decrease by 2-20% and in some stations are even higher during wet season. An additional of US.EPA Chemical Mass Balance Model version 8(CMB_8) receptor modeling for PM_{10} during dry season was calculated. The results reveal that biomass burning and vehicle emission are the major sources of PM_{10} with ranging from 25.42-54.09 % and 32.44-55.62 %, respectively.

Key Words: PM_{10}, Chemical characterization, receptor modeling

1.INTRODUCTION

High levels of Particulate matter have existed in the area of Mae Moh in Northern Thailand. Especially during dry season in January-April, people in this area have seasonally experienced problematic high levels of (PM_{10}). Given by the 1999 through 2003 data of Mae Moh air monitoring stations of Electrical Generating Authority of Thailand (EGAT) and Pollution Control Department (PCD) shows that the average value of PM_{10} exceeded Thailand's 24 hours air quality standard at 120 $\mu g/m^3$. To define environmental impact and Implication of population health from PM_{10} in the area, knowledge and behaviour of chemical composition of aerosol is important. This knowledge also can be used as a reference for worldwide comparison and future studies. The outcome of this study will yield the essential information for aerosol compositions during dry and wet seasons and will help to estimate the impact of various sources on the atmosphere in northern Thailand.

2. EXPERIMENTAL METHODS

The study was performed at the Mae Moh rural area, which is located approximately 25 km east of Lampang province in northern Thailand (about 630 km north of Bangkok). The Electricity Generating Authority of Thailand (EGAT) has its biggest, and also national biggest, coal-fires power plant, and mine operation in this area. PM_{10} samples were collected at 4 air monitoring stations located in different part of the area (see Figure 1). The first sampling station (site A) is in the western part of the power plant and mining area at Provincial Waterworks Authority in Mae Moh government center. The second sampling station is in a rural community in the eastern part (Mae Chang village, site B). The major occupation in this village is chopstick production and people normally open burn the waste wood to heat the wood chopstick. Site C and D are in the northern part of the area. The station in site C (Tasi village) is close to a four lanes heavy traffic road. Pra tu pa Camp (site D) is situated in the forest area where forest fires often occur during dry season.

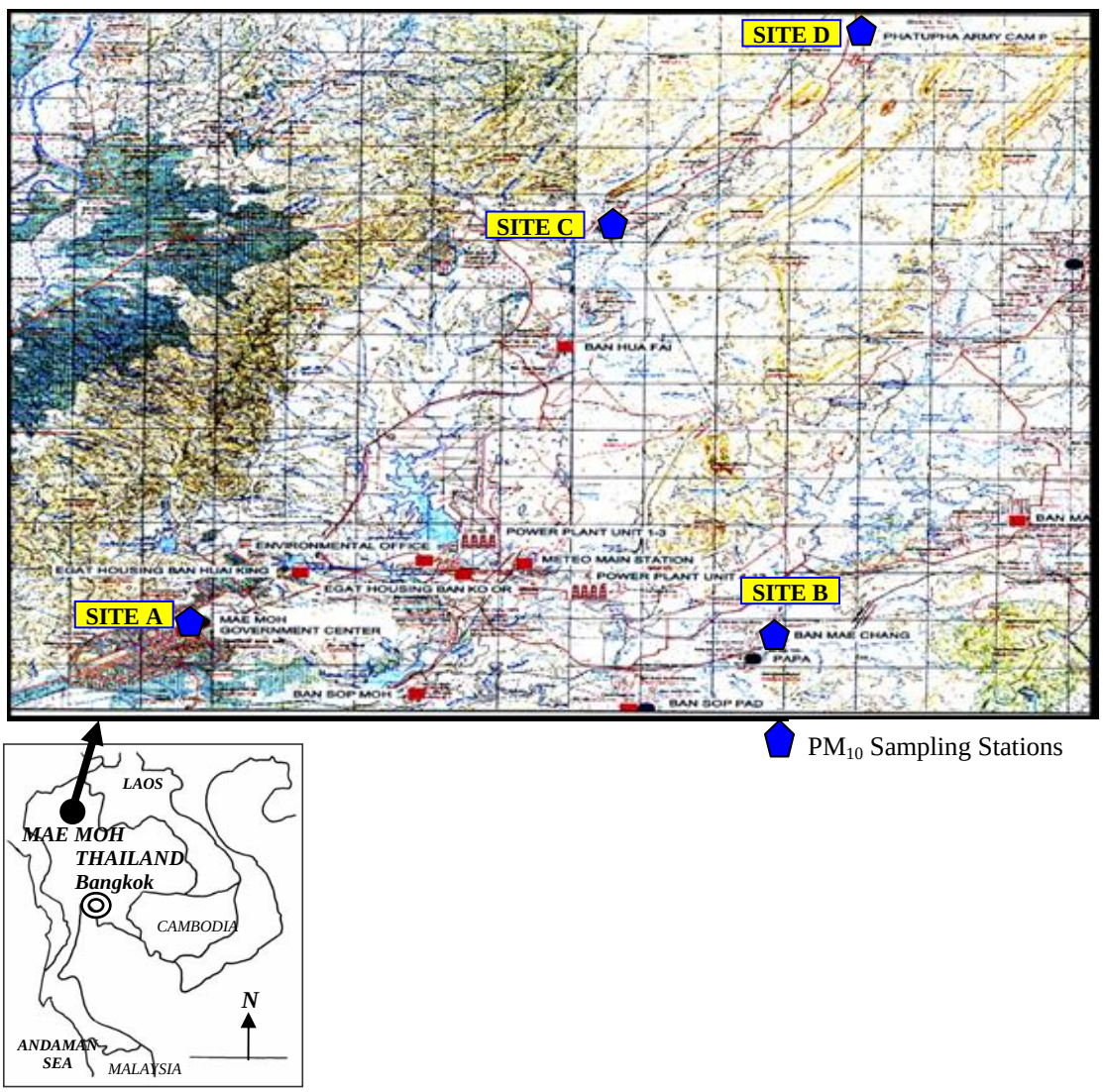

Figure 1. Mae Moh area (sampling sites are highlighted)

Two sets of PM_{10} Mini-Volume portable air samplers (Airmetrics) were used concurrently for 24 hours ambient collecting at a flow rate of 5 L/min. One set was equipped with a Membrane PTFE filter; the other set was equipped with a Quartz - fibre filter. The sampling period was during February – July, 2004 managing into 39 days sampling for 4 stations. However, after the samples were screened out as the missing of mass, electricity and so on. Thirty samples from each site altogether 120 samples which yielded 240 filters (120 Membrane PTFE and 120 Quartz-fibre filters) were analyzed.

Mass concentrations of particles on the filters were determined gravimetrically. The filters after stabilized in the controlled conditions of an electronic desiccators chamber at 40-50 % RH and 20±2 ^{o}C for 24 hours were pre and post weighted in a microbalance with 10 μg sensitivity (Meitler, AE 240). Laboratory blank filters were routinely weighted to control the weighting condition. The filters after weighing were stored in a 5 ^{o}C refrigerator until being use or analyze chemically. The Quartz-fibre filters before sampling were additionally heat treated to 550 ^{o}C for more than 5 hours to minimise the organic interference of organic carbon analysis.

The collected Membrane filters were used for elemental analysis, while particulate samples collected by quartz-fibre filters were used for ionic species and carbonaceous analysis. The elemental analysis for Al, As, Ba, Br, Ca, Cd, Cl, Cr, Cs, Cu, Fe, Ga, K, La, Mg, Mn, Ni, P, Pb, S, Sb, Sc, Se, Si, Sm, Sr, Te, Ti, V and Zn was carried out using Analysis Energy Dispersive X-Ray Fluorescence (Oxford ED 2000) at Radiation and Isotopes Department of Kasetsart University. The K^{+}, NH_4^{+}, NO_3^{-} and SO_4^{2-} ionic species were analyzed by Shimazu Ion Chromatography at Faculty of Resources and Environment, Kasetsart University. Total carbon (TC) and Organic carbon (OC) were analyzed by CHNS/O analyzer (Perkin Elmer 2400 series II) at the Scientific and Technological Research Equipment Centre, Chulalongkorn University. In this study elemental Carbon (EC) was calculated by subtracted TC with OC.

Additional of CMB_8 (US. EPA Chemical Mass Balance Model version 8) receptor modeling for PM_{10} during dry season was calculated to evaluate the source contribution

3. RESULTS

PM_{10} mass concentrations observed during the sampling period are displayed in Table 1. The maximum PM_{10} value in every site during dry season is exceeded Thailand's 24 hours PM_{10} standard (120 μg/m^3). The highest of 185.84 μg/m^3 PM_{10} concentrations was found at site C, which 24-hr PM_{10} standard was exceeded on 4 sampling days. The average concentration of PM_{10} during dry season is over 100 μg/m^3 at site A and C. Consistency with abundance of mobile sources at site A and C, when the PM_{10} standard was exceeded OC, EC, and Al were high. While average concentrations at site D and B are 88.52 and 79.25 μg/m^3, respectively. PM_{10} concentrations in wet season are decreased 56.75-81.38 % of dry season and concentrations of all sites are below 50 μg/m^3. The variation of daily PM_{10} concentrations from all four sites is shown in Figure 2.

Table 1. Comparison of PM_{10} concentrations in dry and wet seasons.

Site	Dry season (Feb-April)				Wet season (May-July)			
	No. of samples	PM_{10} conc. ($\mu g/m^3$) avg.	min	max	No. of samples	PM_{10} conc. ($\mu g/m^3$) avg.	min	max
A	14	105.99	72.40	142.60	16	22.09	14.72	33.02
B	13	79.25	33.61	161.89	17	28.09	11.07	47.87
C	13	103.03	57.31	185.84	17	19.57	14.65	28.24
D	13	88.52	41.69	154.13	17	21.10	13.36	31.59

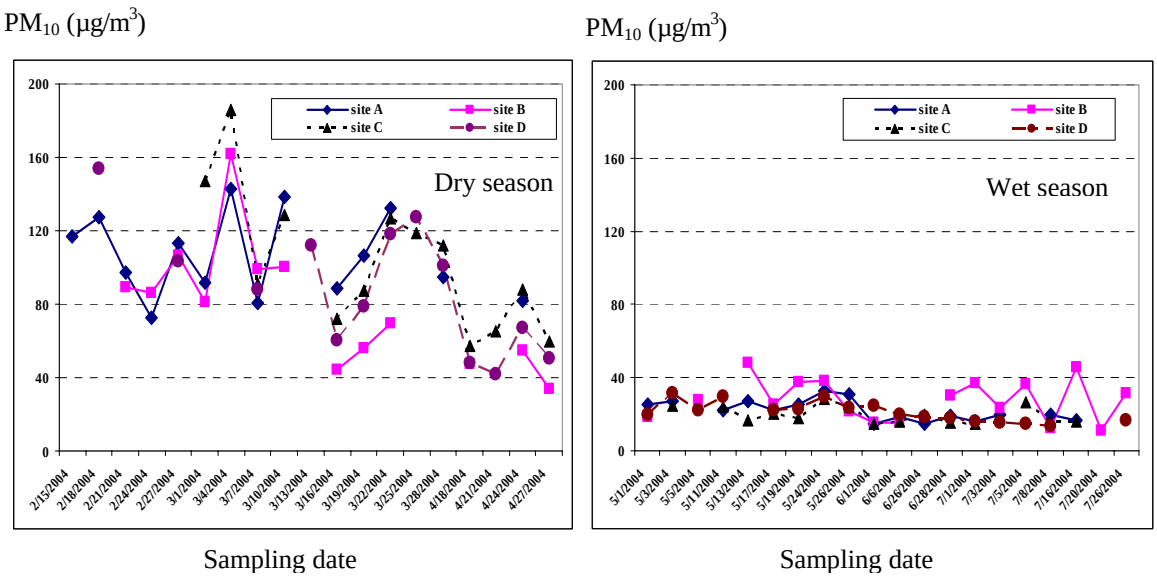

Figure 2. Variation of PM_{10} mass concentrations in wet and dry seasons.

The average concentration of each chemical composition is presented in Table 2 and comparison between dry and wet seasons is displayed in Figure 3. Most of the elemental compositions are higher in site C. The concentrations of OC and EC are relatively high at all of sampling sites. The majority of elemental chemicals found are Al, Ca, Fe, K, S, Si of which there is 40-80 % decrease in wet season, except Ga and Se which are the marker species of coal fired power plant and often found in PM less than 1 micron in diameter (Pavagsu *et al*., 2002) are only decrease by 2-20% and in some stations are even higher during wet season (see Figure 3).

The data inputs for CMB_8 model in this study were only dry season samples collected from February-April 2004 since the wet season samples had the very low PM_{10} mass concentrations of which most chemical compositions were under their detection limits. In this study, soil, road dust and biomass burning profiles for CMB_8 calculation are specific local to Mae Moh area developed by Wangkiat *et al.* (2004) while vehicle emission profile was investigated by Chow *et al.* (1997) from Santa Barbara County, California. Based on the results from the initial test, CMB_8 was run with individual source profile of soil, road dust, biomass burning and vehicle emission but yielded no meaning output, thus soil and road dust were put together to be one input source in the model by their average compositions.

Table 2. Average concentrations of aerosol compositions and PM_{10} in μg/m^3.

	Site A	Site B	Site C	Site D
Al	0.19 (0.045-0.504)	0.176(0.039-0.452)	0.257(0.035-0.712)	0.188(0.029-0.523)
Ca	0.081 (0.022-0.181)	0.071(0.024-0.154)	0.098(0.025-0.218)	0.074(0.023-0.179)
Cd	0.326(0.135-0.568)	0.531(0.157-0.996)	0.592(0.167-4.037)	0.455(0.124-0.987)
Fe	0.054(0.015-0.098)	0.095(0.029-0.642)	0.069(0.025-0.128)	0.059(0.023-0.111)
Ga	0.316(0.215-0.407)	0.516(0.197-0.684)	0.602(0.317-2.280)	0.489(0.172-0.712)
K	0.132(0.038-0.211)	0.134(0.041-0.407)	0.139(0.044-0.352)	0.135(0.045-0.3180
Mg	0.078(0.051-0.107)	0.103(0.034-0.209)	0.167(0.000-0.523)	0.130(0.031-0.314)
Mn	0.024(0.023-0.024)	0.026(0.022-0.032)	0.033(0.020-0.072)	0.024(0.014-0.035)
S	0.129(0.017-0.340)	0.141(0.034-0.421)	0.166(0.030-0.420)	0.167(0.034-0.511)
Sb	0.087(0.054-0.146)	0.095(0.050-0.180)	0.110(0.049-0.182)	0.111(0.067-0.163)
Sc	nd	0.005(0.002-0.015)	nd	0.005(0.001-0.010)
Se	0.086(0.058-0.137)	0.088(0.045-0.266)	0.110(0.011-0.301)	0.098(0.011-0.225)
Si	0.277(0.051-0.736)	0.298(0.039-0.851)	0.459(0.034-1.123)	0.295(0.033-0.840)
Sm	0.044(0.034-0.053)	0.041(0.004-0.106)	0.058(0.044-0.080)	0.049(0.033-0.079)
Sr	0.216(0.153-0.318)	0.248(0.092-0.411)	0.187(.065-0.304)	0.211(0.127-0.330)
Zn	nd	0.063(0.047-0.078)	nd	nd
OC	8.133(0.280-24.050)	8.527(0.450-25.790)	10.389(0.890-33.060)	8.169(1.010-22.760)
EC	12.716(0.490-36.120)	12.843(0.100-42.350)	17.275(1.170-81.310)	13.009(1.660-47.520)
SO_4^{2-}	1.037(0.182-2.445)	1.381(0.767-2.243)	0.979(0.696-1.346)	1.273(0.908-1.972)
NO_3^-	0.435(0.035-1.648)	0.194(0.054-0.489)	0.288(0.024-1.197)	0.236(0.042-0.427)
NH_4^+	0.317(0.029-0.852)	0.253(0.025-0.630)	0.274(0.026-0.607)	0.269(0.027-0.573)
K^+	0.471(0.142-0.965)	0.405(0.065-0.855)	0.443(0.101-0.822)	0.376(0.080-0.633)
PM_{10}	61.25(14.72-142.60)	50.26(41.87-161.89)	56.99(28.24-185.84)	50.32(31.59-154.13)

Note: 1. Compositions that more than half of the samples below method detection limit were screened out
2 The average is calculated considering only the days when the compositions are above the method detection limit.
3 The values in parenthesis are minimum-maximum concentrations

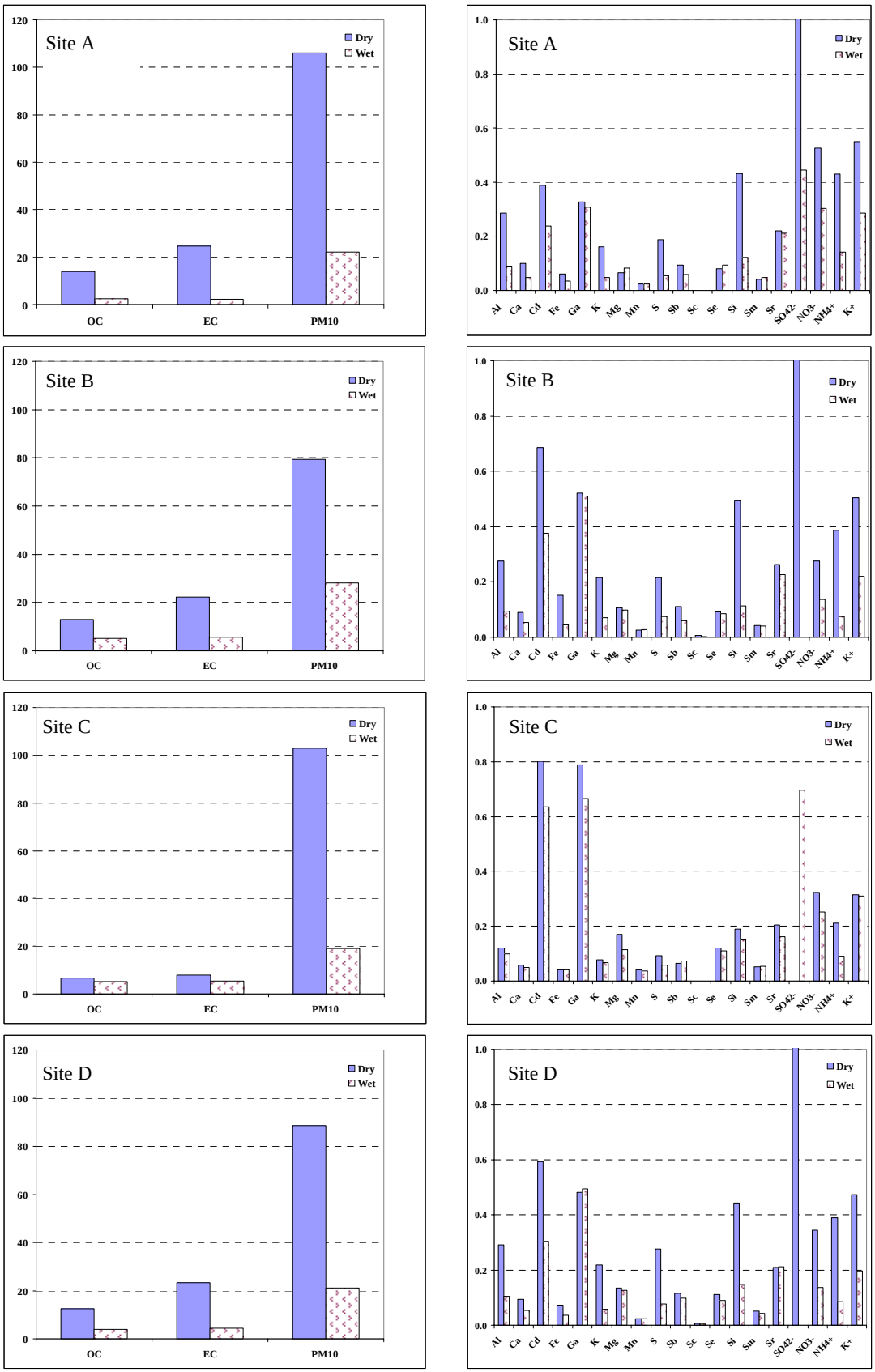

Figure 3. Comparison of PM_{10} chemical compositions for wet and dry seasons.

The estimations of the source contributions for PM_{10} from all station data are presented in Table 3. The results reveal that biomass burning and vehicle emission are the major sources of PM_{10} in Mae Moh area with ranging from 25.42-54.09 % and 32.44-55.62 %, respectively. As expected, the contribution of biomass burning is the highest at site B and D. The reason may be that in site B, people normally open burns the waste wood while at site D forest fire often occur during dry season. Vehicle exhaust emission is the greatest contributor at site A, which is located in the government center area where the number of vehicles and traffic in this area are rather higher than the other stations.

It can be noted that the contributions of soil and road dust in this study have the least proportion of 0.28-1.83 %, while unidentified source contributions are ranged from 10.2 -19.38 %.

When comparing the results of this study to the former study of source apportionment at Ban Hua Fai, Ban Dong sub district and Mae Moh district in which Thirty-one of PM_{10} samples were collected by Dichotomous air samplers during January-April 2001 (Wangkiat *et al*., 2003). It is suggested that soil and road dust in this study could be underestimate, while vehicle emission may be overestimate due to some similarity of the profiles of vehicle emission, and soil and road dust.

Table 3. Comparison of PM_{10} mass contribution in this study with another literature.

Air monitoring station	PM_{10} contribution (%)			
	Biomass burning	Vehicle emission	Soil and Road dust	Unidentified sources
Site A	25.42	55.62	0.28	18.68
Site B	54.09	34.87	0.84	10.20
Site C	44.01	34.87	1.83	19.29
Site D	50.89	32.44	1.14	15.53
Ban Hua Fai *	50.42	19.24	35.13	-

Note: * Wangkiat *et al.* (2003)

4. CONCLUSION

The results of the study indicate that chemical compositions of soil, road dust related such as Al, Ca, Fe, K, S, Si were significant decreased of wet season. CMB_8 identified biomass burning and vehicle emission as major sources contribution in all sampling sites. The concentration of Ga and Se which are abundant in fine size rage of power plant emission are not different during dry and wet season. In order to investigate the influence of power plant contribution in the area, size separation of particulate ambient and source sampling should be studied.

5. ACKNOWLEDGEMENT

The authors thank Pollution Control Department of Thailand for the financial support to carry out this study.

REFERENCES

Chow, J.C., Fairley, D., Watson, J.G., Demendal, R., Fujita, E.M., Lowenthai, D.H., Lu, Z., Frazier, C.A., Long, G., Cordova, J., 1997. Sources and chemistry of PM10 aerosol in Santa Barbara county, C.A. Atmospheric Environment 30, 1489-1499.

Pavageau, M., Pecheyan, C., Krupp, E.M., Morin, A., and Donard, O.F.A., 2002. Volatile metal species in coal combustion flue gas. Environmental Science and Technology 36, 1561-1573.

Wangkiat, A., Harvey, N.W., Okamoto, S., Wangwongwatana, S., Rachdawong, P., 2003. Source apportionment of PM_{10} in Mae Moh area, Thailand. In Sokhi, R.S., Brechler, J. (Ed.), Proceedings of the 4^{th} international conference on urban air quality measurement, modeling and management, Czech republic, 115-118.

Wangkiat, A., Harvey, N.W., Okamoto, S., Wangwongwatana, S., Rachdawong, P., 2004. Characterization for some emission sources in CMB calculation for Mae Moh area, Thailand. International Journal of Environment and Pollution 21, 223-239.

Proceedings of the Third International Symposium on Air Quality Management at Urban, Regional and Global Scales. 26-30 September 2005, Istanbul – Turkey

IDENTIFICATION OF POTENTIAL SOURCES AND SOURCE REGIONS OF AMBIENT AEROSOL IN NORTHEAST ASIA USING ADVANCED HYBRID RECEPTOR MODEL JOINTED WITH POSITIVE MATRIX FACTORIZATION

J. S. Han[a], K. J. Moon [a] and Y. J. Kim[b]

[a]Department of Air Quality Research, National Institute of Environmental Research, Environmental Research Complex, Kyeongseo-dong, Seo-gu, Incheon, 404-170, Republic of Korea, first-author: iamiyan@me.go.kr

[b]ADvanced Environmental Monitoring Research Center at Gwangju Institute of Science and Technology, Oryong-dong, Buk-gu, Gwangju, 500-712, Republic of Korea

ABSTRACT

The size- and time-resolved measurement of particulate trace elements was made using an eight-stage DRUM sampler and S-XRF system from 29 March to 29 May in 2002 at Gosan, Korea, which is one of the representative background sites in East Asia. As a result, continuous 3-hr average concentrations were obtained for 19 elements including S, Si, Al, Fe, Ca, Cl, Cu, Zn, Ti, K, Mn, Pb, Ni, V, Se, As, Rb, Cr, Br. The size-segregated data sets were applied to newly developed hybrid receptor model, advanced concentration weighted trajectory (ACWT) jointed with positive matrix factorization (PMF), in order to identify the possible sources areas and estimate their contributions to particulate matter mass in separate size ranges.

Key Words : Source apportionment, Drum sampler, Receptor model, Positive matrix factorization, Advanced concentration weighted trajectory

1. INTRODUCTION

To develop effective control strategies for anthropogenic pollutants in ambient air, it is necessary to identify the pollution sources and exactly estimate their influence on ambient concentration. For that reason, various receptor models, such as potential source contribution function (PSCF) (Hopke et al., 1993), concentration weighted trajectory (CWT) (Seibert et al., 1994), and residence time weighted concentration (RTWC) (Stohl, 1996), have been developed by using the backward trajectories of air parcels in combination with air quality measurements. However, the commonly used hybrid receptor models have several drawbacks. These statistic receptor models often showed unrealistic source areas for the flux of anthropogenic pollutants influenced by a trailing effect of trajectories in previous works (Han et al., 2004; Lupu and Maenhaut, 2002; Lin et al., 2001).

In this study, advanced concentration weighted trajectory (ACWT) was newly developed in order to complement the weak points in the previous hybrid receptor modeling. This model combines the estimated motion of air backward in time not only with the measured chemical composition of pollutants, but also with the source inventories in the domain. Moreover, the pathways of trajectories that have low intensity of pollutants on arrival are removed from the potential source regions with a

point filter. This feature makes the estimation of hot spot possible and the confidence level of the result increase.

In this study, the result of ACWT hybrid receptor model was especially combined with positive matrix factorization (PMF) analysis while the most previous studies directly applied the composition of collected material to the input data of a receptor model. As a result, it is possible to identify the regional distribution of various aerosol sources impacting the chemical composition of ambient aerosol in Northeast Asia. At this time, PMF analysis has been performed on the Gosan aerosol data collected by a DRUM sampler which has merit to collect the fine particles in six stages below 2.5 . The size-segregated composition data with high time resolution are expected to improve the efficiency of PMF analysis and the accuracy of anthropogenic source apportionment.

2. SAMPLING AND ANALYSIS

Ambient aerosol collection using an eight-stage Davis Rotating Unit for Monitoring (DRUM) sampling system was made at the western tip of Gosan, Jeju Island, Korea (33^o 17' N, 126^o 10' E, 70m asl), which is a representative background site in East Asia, from 29 March to 29 May 2001. During the measurement period, two Asian dust (AD) outbreaks were observed on 8-10 April and 17 April. In this study, aerosol data pertaining to those AD periods were not subject to PMF and ACWT models in order to focus on the estimation of anthropogenic aerosol sources.

The DRUM sampler collects size-resolved aerosol samples on Apiezon^{TM} coated Mylar^{TM} strips in eight stages, having the equivalent aerodynamic cut-off diameters 0.07, 0.26, 0.34, 0.56, 0.75, 1.15, 2.5, 5.0, and 12 (Cahill et al. 1985). The DRUM sampler was operated continuously during the 61-day sampling period. The collected aerosol samples were then analyzed for inorganics (19 elements between aluminum and lead) using synchrotron X-ray fluorescence (S-XRF) at the Lawrence Berkeley National Laboratory Advanced Light Source (Perry et al., 2004). A detailed description of the sampling and analysis methods is provided by Cahill et al. (1993).

3. DESCRIPTION OF MODEL SIMULATION

3.1. Data Analysis By PMF

Two-way Positive Matrix Factorization (PMF2) method was developed by Paatero (Paatero, 1997) to provide flexible modeling approach that effectively uses the information in the data. A robust mode of PMF2 has been selected for handling outlier data, in order to degrade the disproportional affect of excessively large data points (Paatero, 1996). In this study, the value α=4 was chosen for the outlier threshold distance in the present study as done by Lee et al. (1999) and Hien et al. (2004). In addition, The other important parameter of PMF2, F_{peak} was used to control the rotational freedom until an appropriate distribution of the edges is achieved.

3.2. Trajectory Calculation And Model Details

3-day backward trajectories were computed by a three-dimensional trajectory model, HYSPLIT4 (Version 4.7) (Draxler, 1998). In this study, 3-day back-trajectories are used in order to focus on the estimation of the primary aerosol source areas in Northeast Asia. The arrival elevation of 750m is within the average mixed height

during the measurement period (1571m), which means that there could be effective coupling between transport and surface measurement. NCEP/NCAR reanalysis data with 6hr resolution on a $2.5^{o}\times2.5^{o}$ global grid have been used as meteorological data input to the trajectory model. Backward trajectories were computed by isobaric method eight times a day at 01, 04, 07, 10, 13, 16, 19, 22 hr UTC, corresponding to the measured data.

The position errors for 3-day back-trajectories are of the order of 100km (Stohl, 1998), but the use of the analyzed wind field can make the trajectory uncertainty reduce significantly (Lin et al., 2001). Moreover, the grid size $1^{o}\times1^{o}$, which is comparable to the uncertainty at the end of a 3-day trajectory, was used in this study, in order to remove the effect of trajectory uncertainty from the results of receptor model. Therefore, the effect of trajectory uncertainty can be efficiently eliminated from the results of receptor model. Figure 1 shows the grid system and the method deriving initial and boundary conditions. The model domains include the most of China, Korea peninsular, Japan, and Taiwan. At this time, China is divided into four regions, including Central China (C China), South China (S China), North West China (NW China), and North East China (NE China), based on the boundary lines of provinces. Most of the simulation results are based on this regional-scale domain.

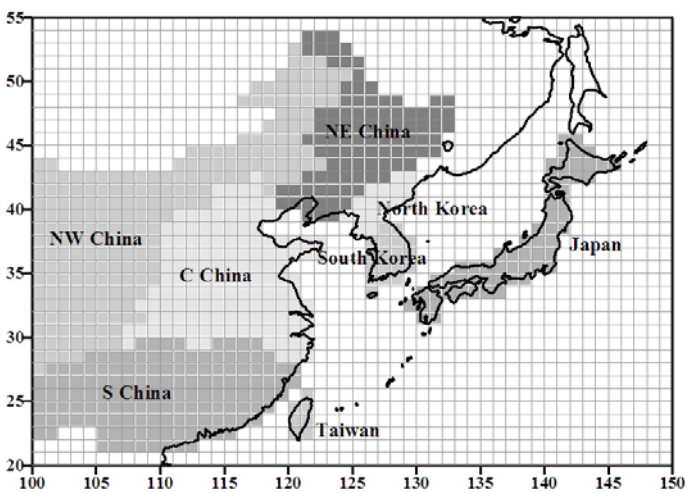

Figure 1. Model domain and grid structure.

3.3. Advanced Concentration Weighted Trajectory (ACWT)

In the present work, a method of weighting trajectories with associated concentrations (CWT) (Seibert et al., 1994) was improved using source inventory and point filter. It is assumed that the pollutants emitted within grid cell is swept into the air parcel and transported to the receptor site without loss through diffusion, chemical transformation, or atmospheric scavenging (Cheng et al., 1993). This method starts with the first guess concentration field based on Eq. (1). The redistributing concentrations along trajectory *l*, C_{kl} is computed with the equation

$$C_{kl} = C_l \frac{S_{kl} \times N_l}{\sum_{k=1}^{N_l} S_{kl}} = C_l \frac{S_{kl}}{\overline{S_l}} \qquad (1)$$

, where l is the index of the trajectory, C_l is the concentration observed on arrival of trajectory l, S_{kl} is the amount of source emission in segment k of trajectory l, and $\overline{S_l}$ is total source emission produced on the pathway of trajectory l. After the redistribution is finished for all trajectories, the mean weighted concentration calculated for each grid cell (i, j) with the equation

$$C_{ij} = \frac{1}{\sum_{l=1}^{M}\sum_{k=1}^{N_l}\tau_{ijkl}} \sum_{l=1}^{M}\sum_{k=1}^{N_l} C_{kl} \times \tau_{ijkl} \qquad (2)$$

, where M is the total number of trajectories, N_l is total number of segments of trajectory l, τ_{ijkl} is the residence time of segment k of trajectory l in grid cell (i, j). Eq. (2) is similar to the equation of the average weighted concentration in CWT, but the redistributed concentrations C_{kl} are used instead of the measured concentration C_l. In addition, this method is different from other models such as RWTC in some respects. Especially, it does not use the logarithmic concentrations and the information of source emission was applied to the redistribution of concentration along trajectory l. This feature eliminates the errors by a trailing effect observed in other receptor models and makes the solution physically realistic.

ACWT modeling procedure contains a point filter, which eliminates areas passed by trajectories with low concentration of pollutants. The point elimination was applied to the grid cells that have trajectory endpoints associated with low measured concentration on arrival and lower height level than a constant vertical limit. In the present study, the height of 500m lower than the start points of trajectories was applied to the filtering function

$$F(i,j) = \begin{cases} 1.0 & C_l \geq 0.05 \\ 0.5 & C_l < 0.05 \quad h_{ijkl} \geq 500 \\ 0.0 & C_l < 0.05 \quad h_{ijkl} < 500 \end{cases} \qquad (3)$$

,where h_{ijkl} is the height of segment k of trajectory l in grid cell (i, j). This restriction is also expected to reduce the trailing effect observed in other receptor models.

In previous works, hybrid receptor models directly applied the measured concentration of each pollutant to calculating the weighted concentration in each segment of trajectories (Han et al., 2004; Lupu and Maenhaut, 2002; Hsu et al., 2003). As a result, the estimated source regions revealed mixed spatial distribution because each pollutant could be emitted by various sources. In this study, ACWT model was associated with PMF results in order to identify the source locations classified by emission sources. The weighting scheme in ACWT method was conducted using not the measured sample concentration, but the source intensity resolved from PMF analysis; C_l in Eq. (1) is replaced to the source intensity observed on arrival of trajectory l, and C_{kl} in Eq. (1) and (2) means source intensity of segment k observed on arrival of trajectory l. The transformed logical algorithm of ACWT model is summarized in Figure 2.

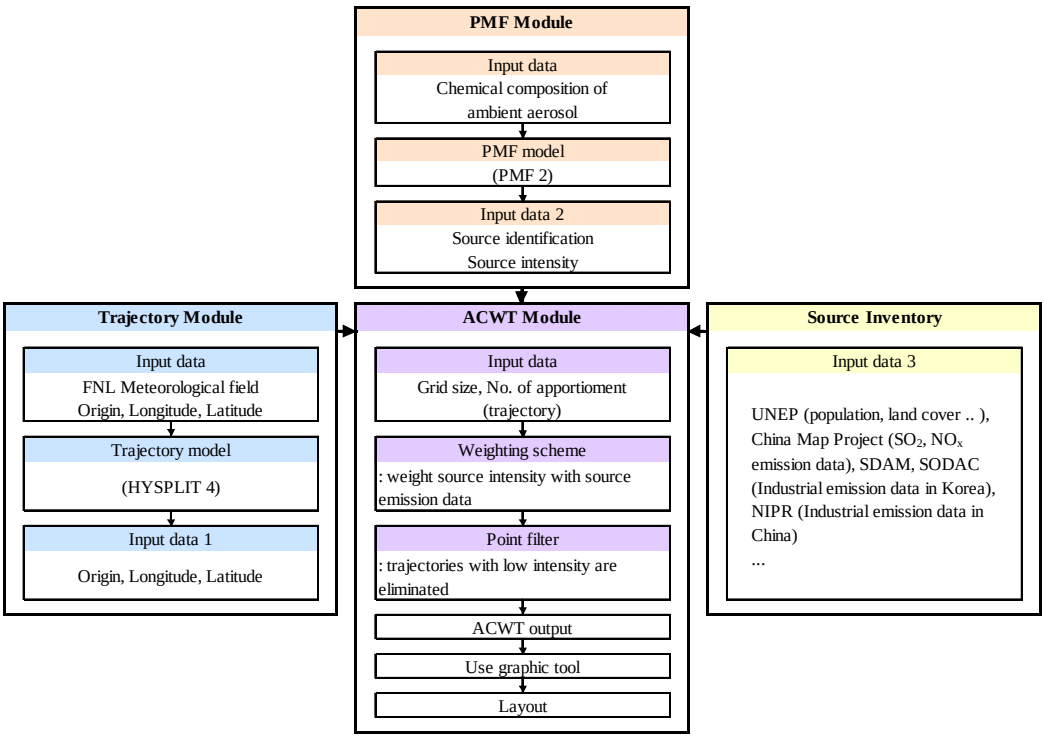

Figure 2. Logical algorithm of ACWT model applied to this study.

4. EMISSION INVENTORY USED IN THE MODEL

In the present work, several emission databases were used to estimate the aerosol source regions. The emission database for NOx and SO_2 are derived from the China Map project, and the emissions from natural sources such as soil dust and Chinese loess are obtained from Earth Science Data Interface of Global Land Cover Facility (GLCF). In addition, industrial SO_2 and dust emission data are derived from the database on the emission source inventory in Korea and China's environment yearbooks. Obtained emission data were then assigned to the model domain with grid size $1^o \times 1^o$ shown in Figure 1 to redistribute the source intensity along trajectory.
Generally, ambient particulate materials can be produced by a wide range of emission sources including natural and anthropogenic sources. In order to identify the origin and transport pattern for each aerosol source, different source inventories should be used for the individual sources. In the case of the emission sources related to the land cover, such as Chinese aerosol and biomass burning, global land cover data sets (GLCF, 2001) was used to redistribute the source intensities, and the strength of volcano emission was weighted by the SO_2 emission inventory by volcano (Carmichael, 2000a). NOx and SO_2 emission data in East Asia (Carmichael, 2000b) were used for motor vehicle and coal combustion sources, respectively. Residual oil fired boiler and municipal incineration sources used population distribution to redistribute the source intensity. Finally, the intensities of industrial sources, such as ferrous metal source, copper smelter, oil heating furnace, and nonferrous metal source were rearranged by using province-level pollution data for China (NIPR, 2005; Dasgupta, 1997) and Korea (NIER, 2005).

5. MODEL SIMULATION RESULTS

5.1. Potential Source Intensities Estimated By PMF

In previous work (Han et al., 2005), used parameters and verified result of PMF were described in detail for all size ranges. Overall, twelve distinct primary sources were resolved in fine size ranges (0.07~1.15) for the ambient aerosols collected at the Gosan site in spring of 2001 excluding AD periods. The resolved sources include not only natural sources such as Chinese aerosol, and volcano emission, but also anthropogenic sources including biomass burning, municipal incineration, coal combustion, oil heating furnace, residual oil fired boiler, gasoline vehicle, diesel vehicle, nonferrous metal source, ferrous metal sources, and copper smelter.

Figure 3 represents the corresponding temporal variations of these potential sources in fine size range (0.07~1.15). The mass concentration of each source was calculated from the sum of scaled intensity values in the resolved size ranges. Overall, apparent differences in temporal variations of these anthropogenic sources confirm the independence of the estimated source contributions.

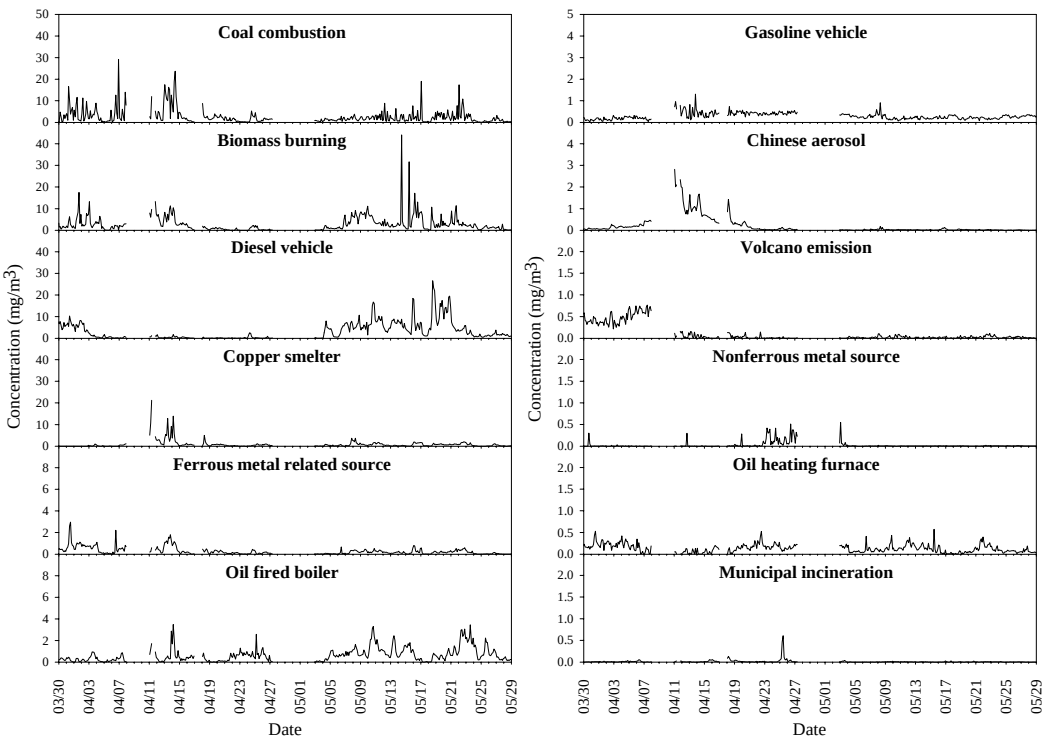

Figure 4. Temporal variations of fine PM mass (0.07~1.15) by each of the resolved sources during the non-AD periods.

The average source contributions in fine size range (0.07~1.15) are shown in Figure 4. The contribution of natural sources including Chinese aerosol and volcano emission, was much lower than that of anthropogenic sources. Especially, the contributions of diesel vehicle, biomass burning, and coal combustion were larger than other anthropogenic sources, accounting for 29.5%, 25.3%, and 23.3%, respectively. Vehicle emission sources including gasoline and diesel vehicle

occupied about 32%, the largest portion of the fine aerosol mass. In addition, the sources related to fossil fuel combustion contributed to more than 30%.

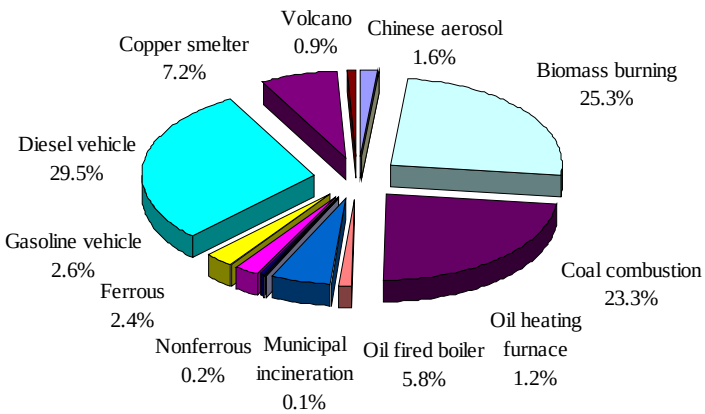

Figure 5. Average source contributions to the mass concentration of fine particle (0.07~1.15).

5.2. ACWT Results

ACWT model was applied to the twelve aerosol sources resolved from PMF in fine size range (0.07~1.15). Overall, apparent differences in spatial distributions of these potential sources confirm the independence of the estimated source contributions. Moreover, the strong spatial gradients of flux value effectively separate the large source areas in the field.

The potential areas of natural sources were more obviously distinguished from other anthropogenic sources as shown in Figure 4. The ACWT results for Chinese aerosol showed that the sources areas were mainly located in the bare ground and sand desert in Northeast China. This region partially includes Gobi sand desert and loess plateau in Central China. Because the AD periods were eliminated from the PMF analysis, this result indicates that the long-range transport of small mineral particles from China could be occurred during NAD periods in dry spring season.

Although the source intensity was smaller than other sources, the influence of volcano emission produced in Japan apparently observed. The concentration gradients of volcano emission show that the area below the island of Kyushu was a hot spot source. In the region, there are several active volcanoes, which intermittently produce a large amount of ash and gas plume.

Fuel combustion sources contributing more than 1% to the fine PM mass such as diesel vehicle, coal combustion, and biomass burning were also distinguished by the flux distribution. The emission flux of diesel vehicle was concentrated around the populated and industrial centers, which includes Taiwan, major industrial areas in China including Shanghai, Shenyang, Anshan, and Dalian, and central metropolitan region in Korea. The marine areas located between Taiwan and Japan were also suggested to be moderate source areas of diesel vehicle influenced by the movements of shipping. Compared with the results for diesel vehicle, the possible source areas for coal combustion were more widely distributed to the inland provinces. The flux of coal combustion source was not only concentrated around the coastal provinces

from Guangdong north to Liaoning, but also centered on a west-to-east belt across the inland of China, from Hubei Province to Hebei Province.

In the case of biomass burning, the spatial distribution pattern was different with other industrial anthropogenic sources that closely tied to industrial centers. ACWT model resolved the cultivated regions in South and Central China as the main biomass burning sources impacting the ambient aerosol at Gosan, Korea. The region contains the rich Yangzi River Basin producing about 40% of total grain in China. Therefore, it is inferred that field combustion of agricultural residues considerably emitted fine particles in this area. In addition, the source regions were widely spread over the grassland and forest located in Northeast China implying the impact of biofuel combustion.

The potential source areas of gasoline vehicle and oil fired boiler were also different. The source areas of gasoline vehicle were mainly distributed in Central and South China centering around Taiwan, Guangzou, and Shanghai while the flux of oil fired boiler source was concentrated around Northeast China including Liaoning and Jilin provinces.

Major industrial areas such as Anshan, Beijing, Zheongzhou, Hangzhou, and Guangzhou were resolved as the potential source areas of ferrous metal source. the major source locations of the oil-heating furnace were also similar to those for ferrous metal source implying these industrial sources can be mutually related. The source locations of copper smelter were a little different with these two sources. They were only observed in Shanghai and Beijing industrial areas, and central Korea.

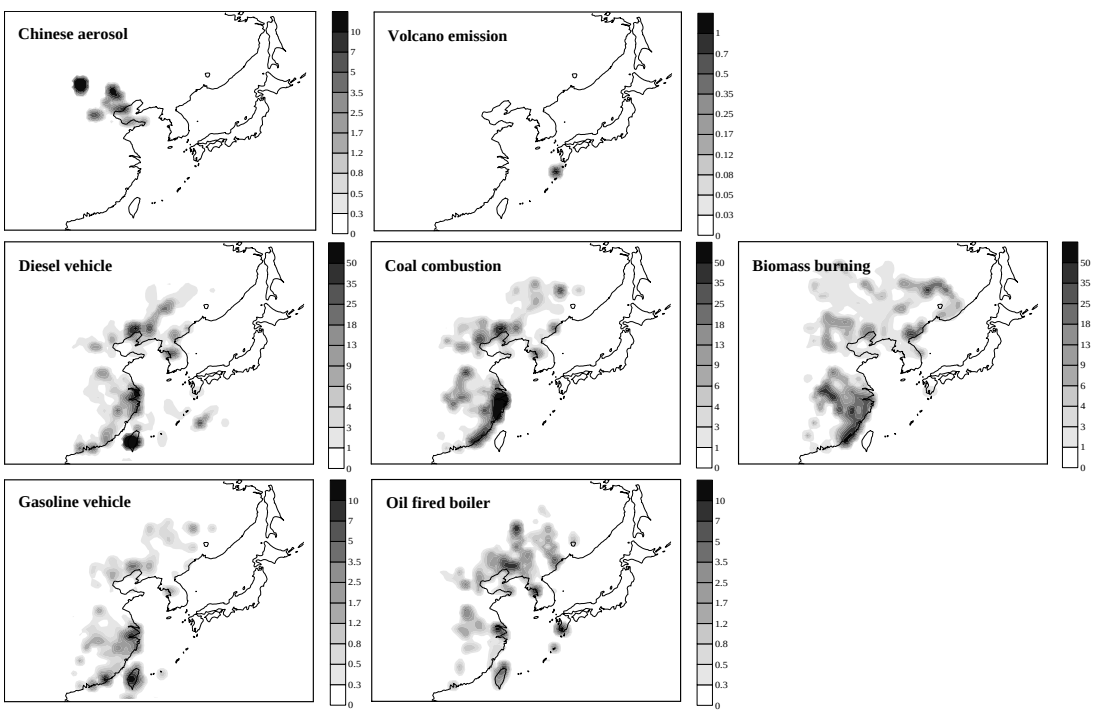

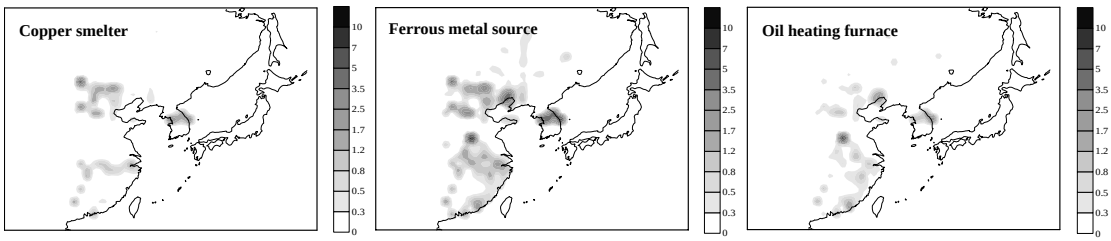

Figure 4. Potential source areas of twelve possible aerosol sources impacting the chemical composition of ambient aerosol at Gosan, Korea over the study period.

REFERENCES

Cahill T. A., Goodart, C., Nelson, J. W., Eldred, R. A., Nasstrom, J. S., Feeny, P. J., 1985. Design and evaluation of the DRUM impactor. Proceedings of the International Symposium on Particulate and Multi-Phase Processes (vol. 2). Ariman, T. and Nejat, T. (Eds.), Taylor and Francis, Philadelphia, Pa., pp. 319-325.

Cahill, T. A., and P. Wakabayashi, 1993. Compositional analysis of size-segregated aerosol samples, in Measurement Challenges in Atmospheric Chemistry, edited by L. Newman, Adv. Chem. Ser., 232, 211-228.

Carmichael, G., 2001a, Datasets (Year 2000) – SO_2 ($1^o \times 1^o$, Volcanos), URL: http://www.cgrer.uiowa.edu/ people/carmichael/ACESS/so2_volcano.txt (assessed in February, 2005).

Carmichael, G., 2001b, Datasets (Year 2000) – NOx ($1^o \times 1^o$, Area), URL: http://www.cgrer.uiowa.edu/people/ carmichael/ACESS/nox_area_1deg.txt (assessed in February, 2005).

Cheng, M. D., Hopke, P. K., Zeng, Y., 1993, A receptor methodology for determining source regions of particle sulfate composition observed at Dorset, Ontario. Journal of Geophysical Research-Atmosphere 98, 16839-16849.

Dasgupta, S., Wang, H., Wheeler, D., 1997, Surviving Success: Policy Reform And The Future Of Industrial Pollution In China**,** Working paper, URL: http://www.worldbank.org/nipr/work_paper/survive/china-new.pdf (assessed in February, 2005).

Draxler, R., Hess, G. D., 1998. An overview of the HYSPLIT_4 modeling system for trajectories, dispersion and deposition. Australian Meteorological Magazine 47, 295-308.

Global land cover facility (GLCF), 2001, Gloval land cover data sets – one degree, URL: http://glcf.umiacs.umd.edu/data/landcover/data.shtml (assessed in February 2005).

Han, J. S., Moon, K. J., Lee, S. J., Kim, Y. J., Ryu, S. Y., Cliff, S. S., Yi, S. M., 2005. Size-resolved source apportionment of ambient particles by positive matrix factorization. Atmospheric Chemistry and Physics Discussions 5, 1-30, SRef-ID: 1680-7375.

Han, Y. J., Holsen, T. M., Hopke, P. K., Cheong, J. P., Kim, H., Yi, S. M., 2004. Identification of source locations for atmospheric dry composition of heavy metals during yellow-sand events in Seoul, Korea in 1998 using hybrid receptor models. Atmospheric Environment 38, 5353-5361.

Hien, P. D., V. T. Bac, N. T. H., Thinh, 2004. PMF receptor modeling of fine and coarse PM10 in air masses governing monsoon conditions in Hanoi, northern Vietnam. Atmos. Environ. 38, 189-201.
Hopke, P. K., Gao, N., Cheng, M. D., 1993. Combining chemical and meteorological data to infer source areas of airborne pollutants. Chemometrics and Intelligent Laboratory Systems 19, 187-199.
Hsu, Y. K., Holsen, T. M., Hopke, P. K., 2003. Comparison of hybrid receptor models to locate PCB sources in Chicago. Atmospheric Environment 37, 545-562.
Kim, E., T. V. Larson, P. K. Hopke, C. Slaughter, L. E. Sheppard, C. Claiborn, 2003. Source identification of PM2.5 in an arid Northwest U.S. City by positive matrix factorization. Atmos. Res. 66, 291-305.
Lee, E., C. K. Chan, P. Paatero, 1999. Application of positive matrix factorization in source apportionment of particulate pollutants in Hong Kong. Atmos. Environ. 33, 3201-3212.
Lin, C. J., Cheng, M. D., Schroeder, W. H., 2001. Transport patterns and potential sources of totla gaseous mercury measured in Canadian high Arctic in 1995. Atmospheric Envirnment 35, 1141-1154.
Lupu, A. and Maenhaut, W., 2002. Application and comparison of two statistical trajectory techniques for identification of source regions of atmospheric aerosol species. Atmospheric Environment 36, 5607-5618.
New Ideals in Pollution Regulation (NIPR), Industrial Pollution Modeling and Data - China pollution intensities, URL: http://www.worldbank.org/nipr/data/china/index.html (assessed in February 2005).
Paatero, P., 1996. User's Guide for Positive Matrix Factorization Programs PMF2.EXE and PMF3.EXE, University of Helsinki, Helsinki.
Paatero, P., 1997. Least squares formulation of robust non-negative factor analysis. Atmos. Environ. 37, 23-35.
Perry, K. D., S. S. Cliff, and M. P. Jimenez-Cruz, 2004. Evidence for hygroscopic mineral dust particles from the Intercontinental Transport and Chemical Transformation Experiment, J. Geophys. Res., 109, D23S28.
Seibert, P., Kromp-Kolb, H., Baltensperger, U., Jost, D. T., Schwikowski, M., Kasper, A., Puxbaum, H., 1994. Trajectory analysis of aerosol measurements at high Alpine sites. In: Borrell, P.M., Borrell, P., Cvitas, T., Seiler, W. (Eds.), Transport and Transformation of Pollutants in the Troposphere. Academic Publishing, Den Haag, pp. 689-693.
Stohl, A., 1996. Trajectory statistics-a new method to establish source-receptor relationships of air pollutants and its application to the transport of particulate sulfate
Stohl, A., 1998, Computation, accuracy and applications of trajectories – A review and bibliography, Atmospheric Environment, 32(6), 947-966.

Proceedings of the Third International Symposium on Air Quality Management at Urban, Regional and Global Scales. 26-30 September 2005, Istanbul – Turkey

ATMOSPHERIC AEROSOLS DURING POLLUTION EPISODES IN HONG KONG

S. C. Lee[a,*], Y. Cheng[a], K. F. Ho[a], J. J. Cao[b], P. KK Louie[c] and J. C. Chow[d]

[a] Department of Civil and Structural Engineering, Research Center for Environmental Technology and Management,
The Hong Kong Polytechnic University, Hung Hum, Kowloon, Hong Kong, China
[b] State Key Laboratory of Loess & Quaternary Geology, Institute of Earth Environment, Chinese Academy of Sciences, Xi'an, China
[c] Hong Kong Environmental Protection Department
[d] a Division of Atmospheric Sciences, Desert Research Institute, 2215 Raggio Parkway, Reno, NV 89512, USA, *ceslee@polyu.edu.hk (S.C. Lee).

ABSTRACT

The highest frequency of pollution episodes occurred in winter and spring in Hong Kong. Time series for $PM_{1.0}$, $PM_{2.5}$ and the concentrations of carbonaceous aerosols were determined for samples collected from a heavily-traffic road in Hong Kong from January 21 to May 31, 2004. Seven episode days for $PM_{1.0}$ and $PM_{2.5}$ were observed during the whole measuring period with much higher fine particle loadings ($PM_{1.0}$ and $PM_{2.5}$) exceeding the observed average concentration by a factor of two. Of the six episode days (one susceptive sample was exclusive), four days were in winter with heavy northeasterly wind, the other two days were in spring with a low wind speed from south. During the six episode days, elevated OC and EC concentrations were also observed, while the total carbonaceous aerosols only accounted for ~33% for $PM_{1.0}$ and ~37% for $PM_{2.5}$, respectively. In contrast, it was founded that carbonaceous aerosols accounted for ~88% and ~78% for $PM_{1.0}$ and $PM_{2.5}$ when local street-level pollution was dominated source in spring. The correspondence of $PM_{1.0}$ to regional episodes seemed much sensitive than that of $PM_{2.5}$. The effect of wet removal mechanism was found to be more effective for fine particle and OC in winter possibly due to the presence of soluble secondary aerosols (e. g. polar organic materials and sulfates) in aged air mass transported to Hong Kong.

Key Words: Organic Carbon (OC); Elemental Carbon (EC); $PM_{1.0}$; $PM_{2.5}$

1. INTRODUCTION

In recent years, the problem of fine particles in urban area has attracted increased concerns since the evidence from epidemiology and toxicology (Dockery et al. 1993; Schwartz et al. 1996; Katsouyanni et al. 2001) has suggested statistical significant association between morbidity and ambient fine particle concentrations. Aerosol samples taken in urban areas show that motor vehicular emissions, especially for diesel exhausts, usually constitute the most significant source of ultrafine and fine particles in an urban environment (Zhu et al. 2002; Shi et al. 2001; Charron and

Harrison, 2003). Therefore it is important to understand the levels of fine particles and regular variation near roadways especially regarding the public health of those traveling on and living in close proximity to roads.

Hong Kong (22.12N, 114.08E) is located on the southeastern coast of the Asiatic mainland with quite mountainous and some terrain changes rapidly from sea level to an elevation of several hundred meters or higher. The population spreads unevenly over this region. The sampling site in this study located in the most residential and commercial areas, around Victoria Harbor. Thus high concentrations of air pollutions in side the street canyons were expected in the region. The climate in Hong Kong is sub-tropical with four seasons, under influence of the Asian monsoon. In winter, northeasterly wind becomes the most prevailing wind. Continental emissions from the interior Asia intrude into Hong Kong and the South China Sea with northeasterly wind. Pollution episodes observed by EPD (http://www.epd.gov.hk/) were thought to associate with stagnating high-pressure systems that brought subsiding polluted airstreams over Hong Kong, transported from north or northeast (South China). Therefore the levels of air quality in Hong Kong are universally high in winter and transit period of spring due to the influence not only from local sources but also from polluted air mass transported from South China.

At present, Hong Kong Environment Protection Department (HKEPD) has recognized the two air pollution issues faced (http://www.epd.gov.hk/). One is local street-level pollution. The other is the regional smog problem. Diesel vehicles are the main source of street-level pollution. Smog, however, is caused by a combination of pollutants from motor vehicles, industry and power plants both in Hong Kong and in the Pearl River Delta region. Although several studies on PM_{10} (Yu et al. 2004; Qin et al. 1997) and $PM_{2.5}$ (Louie et al. 2004; Ho et al. 2003; Cao et al. 2003) in Hong Kong have been conducted in the past, the studies that focus on the roadside pollution and regional pollution are quite limited and few studies has been given to investigation on $PM_{1.0}$, which is quite significant because of it is dominated proportion in vehicle exhausts and in air masses transported from remote area. Therefore continuous 24-hour measurements on $PM_{1.0}$ and $PM_{2.5}$ were launched near a major road from January 21 to May 31, 2004. For the purpose of comparison, $PM_{2.5}$ mass data from four monitoring stations operated by EPD was also reported. One of them is ground-level roadside monitoring station (Central) and the other three are general ambient monitoring stations (Tap Mun, Tsuan Wan, and Tung Chung). In this study, winter was classified as those days before March 1st, and spring was the days after March 1st. The objectives of this study are: to determine the levels of fine particles ($PM_{1.0}$ and $PM_{2.5}$) and carbonaceous aerosols in roadside environment; to explore the relationship of mass, OC, and EC between $PM_{1.0}$ and $PM_{2.5}$ in roadside environment; to characterize the meteorological parameter and chemical properties of fine particles during the highest PM days (episode days) and the lowest PM days (days that local vehicle emissions were dominated source); to identify the factors that induce the significant fluctuations of fine particles and carbonaceous aerosols.

2. METHODOLOGY

Sampling Site

The measurements of $PM_{1.0}$ (fine particle with diameter less than 1 μm) and $PM_{2.5}$ (fine particle with diameter less than 2.5 μm) were took place at the roadside air quality monitoring site in the campus of the Hong Kong Polytechnic University (PU) (Figure 1) that locates near Victoria Harbor. It is the most residential and commercial areas in Hong Kong around Victoria Harbor. The sampling was conducted from January 21, 2004 to May 31, 2004, yielding a total of 132 days of data. The sampling location, PU roadside station, is about one meter away from the curb of Hong Chong Road, which leads to the Cross Harbor Tunnel (one of the two busiest cross-harbor tunnels in Hong Kong, having four lanes to each direction), with the objective to investigate air quality experienced by the pedestrians in an environment close to vehicular traffic. The traffic flow on Hong Chong Road is extremely high, with about 119,759 per day (the 2003 annual traffic census). No industries or other anthropogenic sources were found in the vicinity. Thus the PU roadside was considered to be a typical roadside environment in Hong Kong, with significant influence from primary vehicular emissions. The presented traffic data were obtained in terms of the number of cars running in both directions per day.

Sample Collection

Daily $PM_{1.0}$ and $PM_{2.5}$ samples were collected with two-paralleled Plus Model 2025 Sequential Air Sampler (Rupprecht and Patashnick Co. Inc., Albany, NY) operated at 16.7 l min^{-1}. The particles were collected on quartz filters with 47 mm in diameter, which were weighted twice before and after sampling using a Microbalance (Sartorius Microbalance, Sartorius AG, Goettingen, Germany) with the sensitivity of 1 μg in the 0-250 mg range.

Before sampling, quartz filters were preheated in an electric furnace at 800 for at least 3 hours in order to remove carbonaceous contaminants. The samples were balanced in a desiccator with temperature of 20 -30 and relative humidity of 30%-40% for 24 hours before and after sampling. The filters are handled only with tweezers cleaned by dry KimWipes (Kimberly-Clark Corporation, USA) to reduce the possible of contamination. After weighting, sampled filters were stored in a refrigerator at about 4 before chemical analysis to prevent the evaporation of volatile components.

Analysis of Organic and Elemental Carbon

The samples were analyzed for OC and EC using Desert Research Institute (DRI) Thermal/Optical Carbon Analyzer Model 2001 with the IMPROVE thermal/optical reflectance (TOR) protocol (Chow et al. 1993). The DRI thermal/optical carbon analyzer is based on the preferential oxidation of organic carbon (OC) and elemental carbon (EC) compounds at different temperatures. It relies on the fact that organic compounds can be volatilized from the sample deposit in a helium (He) atmosphere at low temperatures, while elemental carbon is not oxidized and removed. The TOR protocol heats the sample on quartz filter with a punched area of 0.526 cm^2 stepwise at temperatures of 120□ (OC1), 250□ (OC2), 450□ (OC3) and 550□ (OC4) in a

non-oxidizing helium atmosphere, and 550□ (EC1), 700□ (EC2) and 800□ (EC3) in an oxidizing atmosphere with 2% oxygen in helium. The carbon evolved is oxidized to carbon oxide (CO_2) and then reduced to methane (CH_4) for quantification with a flame ionization detector (FID). The pyrolysis of OC is continuously monitored by a He-Ne laser at a wavelength of 632.8 nm. OC is defined as the portion of carbon evolved before the temperature at which the filter reflectance resumes the initial level, whereas the carbon evolved beyond this temperature is defined as EC. The minimum detection limit (MDL) of carbon combustion methods is 0.82 μg cm^{-2} for total organic carbon, 0.19 μg cm^{-2} for total elemental carbon, and 0.93 μg cm^{-2} for total carbon. All of samples in this study have concentrations higher than MDL. Replicated analyses were performed for ~10% of all samples.

$PM_{2.5}$ Monitoring Sites and Data Collection

The air quality monitoring network in Hong Kong operated by the HKEPD comprises fourteen fixed monitoring stations. At the three general stations (Tung Chung, Tsuan Wan, and Tap Mun) and one roadside station (Central), $PM_{2.5}$ mass were routinely monitored with the Tapered Element Oscillating Microbalance (TEOM). Figure 1 shows the geographical distribution of stations. The ambient stations located on rooftops of four- to six-storey buildings, with unobstructed air flows from most directions. The selection of these three monitoring stations was to evaluate the air quality in ambient atmosphere. Besides, the three monitoring stations cross through the whole Hong Kong territory from northeast to southwest, thus providing a good spatial representation of air quality in Hong Kong. The data of roadside station (Central) was used to make comparison with the results of PU roadside station in this study.

3. DISCUSSION

Concentrations of Mass, OC and EC

Table 1 summarized the average mass concentrations of $PM_{1.0}$ and $PM_{2.5}$ measured at PU roadside station. On average, the mass concentrations of $PM_{1.0}$ and $PM_{2.5}$ were 35.9±12.4 μg m^{-3} and 52.3±18.3 μg m^{-3}, respectively, throughout the total 132 sampling days. The ranges of particle concentrations varied significantly, varying from 17.5 μg m^{-3} to 85.0 μg m^{-3} for $PM_{1.0}$ and from 24.3 μg m^{-3} to 111.4 μg m^{-3} for $PM_{2.5}$, respectively. Observed $PM_{2.5}$ loading at PU roadside were comparable with Central (the average concentration in Central is 53.3±21.7 μg m^{-3}), another roadside station operated by HKEPD. This gives confidence that the measurements at PU station represent a typical roadside level. The $PM_{2.5}$ mass showed a clear spatial pattern in Hong Kong (Table 1). The average mass concentrations of $PM_{2.5}$ collected from PU roadside and Central roadside were higher than the other three ambient monitoring stations (Tung Chung, Tsuan Wan, and Tap Mun). Among the ambient stations, high $PM_{2.5}$ levels were observed in urban atmosphere (43.2±24.1 μg m^{-3} in Tung Chung and 43.4±21.6 μg m^{-3} in Tsuan Wan), while in background atmosphere, the lowest particle loading were obtained (35.9±16.2 μg m^{-3} in Tap Mun). Tap Mun had the lowest average mass concentration because it located on a small island, surrounding by marine. No local pollution sources exist in the vicinity. All of mass data measured at ambient stations showed a clear seasonality with high concentrations

in winter and low concentrations in summer (Table 1). While this trend was ambiguous in roadside environment (Table 1).

A statistical summary of the daily average concentration of OC and EC in $PM_{1.0}$ at PU roadside are given in Table 1. The overall average concentrations of OC and EC were 7.0±2.6 μg m^{-3} and 9.5±3.5 μg m^{-3}, respectively. OC showed a higher level in winter (8.3±3.3 μg m^{-3}) than in spring (6.4±1.9 μg m^{-3}), while EC was slightly higher in spring (9.7±3.3 μg m^{-3}) than in winter (9.0±3.8 μg m^{-3}). Up to now, the data of carbonaceous content in $PM_{1.0}$ was scarce throughout the world. Li and Lin (2002) measured the TC and EC concentrations of $PM_{1.0}$ via a combustion technique (Table 2), which was conducted in Taipei during October of 1999. The concentrations of OC (11.5±2.8 μg m^{-3}) and EC (11.3±1.7 μg m^{-3}) observed at the traffic station were slightly higher than that in this study. While the levels of carbonaceous aerosols collected in this study were much higher than that obtained in urban ambient atmosphere of Taipei (3.4±0.9 μg m^{-3} and1.3±0.7 μg m^{-3} for $PM_{1.0}$ and $PM_{2.5}$, respectively).

The daily average concentration of OC in $PM_{2.5}$ was 11.0±4.7 μg m^{-3} with a higher concentration in winter (54.1±21.1 μg m^{-3}) and lower concentration in spring (51.1±17.0 μg m^{-3}). While the average concentration of EC was 12.2±4.4 μg m^{-3} with a higher value (12.7±4.2 μg m^{-3}) in spring than in winter (11.0±4.7 μg m^{-3}). The levels of carbonaceous aerosols were compared with previous studies listed in table 2. Since there is no standard analysis method till now, different thermal methods were used in those studies, which might result in large difference in OC and EC measurements. The OC and EC measured in this study were a little higher than those observed in previous studies (Cao et al. 2003; Ho et al. 2003) (Table 2). This is due to the different distance between this study (1 meter away) and previous studies (more than 30 meters away). Zhu et al. (2002) observed dramatic decrease of number concentrations of ultrafine particles near the 710 freeway when measurement moved from 4 meters away from the road curb to 17 meters away. This suggested that the increased carbonaceous levels in this study mainly attribute to much closer distant from road. The OC concentration in $PM_{2.5}$ was comparable to the results from other roadside studies in Hong Kong (Yu et al. 2004) and in Macao (Wu et al. 2003). However, the EC concentration observed at the roadsides of Hong Kong (this study; Yu et al. 2004) was higher than Macao. This perhaps due to the higher diesel vehicle fractions in Hong Kong since the EC abundance in diesel-fueled vehicles could be twice that of gasoline-fueled vehicles (Watson et al. 1994). Generally speaking, both of OC and EC concentrations in $PM_{2.5}$ measured at a roadside in Hong Kong were much higher than those in urban atmosphere (Cao et al. 2003; Wu et al. 2003; Lin and Tai 2001; Lee and Kang 2001; Ohta et al.1998).

On average, $PM_{1.0}$ consisted 19.4% of OC and 26.4% of EC, respectively, and $PM_{2.5}$ consisted 21.1% of OC and 23.4% of EC. The concentrations of mass, OC, and EC in $PM_{1.0}$ and $PM_{2.5}$ were quite similar between weekdays and Saturday, while slightly reduced concentrations were observed on Sunday due to the decreased of vehicular traffic.

The Relationships between $PM_{1.0}$ and $PM_{2.5}$

Particles with different size ranges possibly differ not only in size and morphology but also in formation mechanisms; sources; and chemical, physical, and biological properties. Several studies have been conducted to explore the relationship between $PM_{1.0}$ and $PM_{2.5}$ mass. Cabada et al. (2004) found that there were good correlations existed between $PM_{2.5}$ and PM_x particles with diameter less than x μm , when PM_x is close to $PM_{2.5}$, through investigating the relationship among different particle fractions in Pittsburgh Supersite with MOUDI sampler. Vallius et al. (2000) and Keywood et al. (1999) reported the same findings and suggested that there were similar sources between $PM_{1.0}$ and $PM_{2.5}$. In contrast, Lundgren et al. (1996) evaluated the $PM_{1.0}/PM_{2.5}/PM_{10}$ characteristics in Phoenix, Arizona with a trichotomous sampler. It was concluded that $PM_{1.0-2.5}$ was caused by dispersion aerosol, while $PM_{1.0}$ minimized interference from natural sources compared with $PM_{2.5}$ and PM_{10}. Therefore $PM_{1.0}$ was considered to be a better indicator of primary particles in a roadside microenvironment than $PM_{2.5}$.

The relationship between $PM_{1.0}$ and $PM_{2.5}$ is still controversial up to now. Regression analysis was conducted in two seasons in this study, as illustrated in Figure 2. In winter, very good correlations (r=0.97) exist between $PM_{1.0}$ and $PM_{2.5}$ mass. On average, around 70% of the $PM_{2.5}$ mass was in particles smaller than 1 μm. While the correlation is moderate (r=0.80) in spring and $PM_{1.0}$ contributed to only about 50% of $PM_{2.5}$. The regression analyses for OC in $PM_{1.0}$ and $PM_{2.5}$ reported the similar relationship for winter and spring, while the correlation coefficient in spring (r=0.78) is much lower than that in winter (r=0.91). OC in $PM_{1.0}$ accounted for 50-60% of OC in $PM_{2.5}$. This result demonstrated that the relationship between $PM_{1.0}$ and $PM_{2.5}$ varied in terms of different seasons. Factors related meteorological conditions perhaps contributed to the changes of relationship between $PM_{1.0}$ and $PM_{2.5}$. However, good correlation between $PM_{1.0}$ and $PM_{2.5}$ was measured for EC concentrations in both winter (r=0.96) and spring (r=0.88). $PM_{1.0}$ EC accounted for 70-80% of $PM_{2.5}$ EC. Generally, EC originates from incomplete combustion of carbon-containing material and does not formed in atmosphere due to its nearly inert property (Ogren and Charlson, 1983). The main source of EC in urban atmosphere is relative simple, mostly from vehicular emissions in this study. This perhaps explained the reason of good correlation of EC between $PM_{1.0}$ and $PM_{2.5}$ regardless of seasonal difference.

Time Series of Fine Particles

Figure 3 shows the daily variability of $PM_{1.0}$ and $PM_{2.5}$ at PU roadside station from January 2004 to May 2004. The trend was quite similar between $PM_{1.0}$ and $PM_{2.5}$ with a high correlation coefficient (R^2) of 0.86. Time series of fine particles exhibited seven episode days in January 30, February 14-15, February 23, February 26, April 19-20, respectively, with higher $PM_{1.0}$ and $PM_{2.5}$ levels than the observed average concentration (35.9±12.4μg m^{-3} and 52.3±18.3 μg m^{-3} for $PM_{1.0}$ and $PM_{2.5}$, respectively) by a factor of two (Table 3). These days had the highest 5% PM during the whole measuring days. Central also showed the same peaks in the same episode days and the average loading of $PM_{2.5}$ was two times higher than the average concentration (53.3±21.7 μg m^{-3}). The same phenomena were also observed at ambient monitoring stations (Tung Chung, Tsuan Wan, Tap Mun) during the same episode days. For instance, the average $PM_{2.5}$ loading exceeded the average level

(43.4±21.6 μg m^{-3}) during the same high aerosol days by a factor of 2.4 at Tsuan Wan (Figure 3). This suggested that the observed episode days with about two times higher PM loading at PU roadside reasonably represent fine particle episodes in a regional scale.

Of the seven episode days, five days in winter were dominated by northeasterly winds (wind direction 0°–90°) and all of daily wind speed exceeded 15 km h^{-1} with maximum of 42.7 km h^{-1}, except for February 14 (8.7 km h^{-1}). This suggested air mass originated from northeast region might be a major factor to observed high level of fine particles in most episode days. While in the other two days of April there were a high-pressure ridge observed over southeast China. Therefore although the prevailing wind was from the south (wind direction 90°–270°), namely from marine, fine particles still accumulated due to the subsiding airstreams and relative low mixing height.

Carbonaceous aerosols showed quite similar fluctuations with fine particles observed at PU roadside (Figure 4), especially for OC. Figure 4 only displays the time series of mass, carbonaceous aerosols in $PM_{1.0}$. The OC concentrations in $PM_{1.0}$ and $PM_{2.5}$ were about two times higher than observed average concentrations (7.0 μg m^{-3} and 11.0 μg m^{-3} for $PM_{1.0}$ and $PM_{2.5}$, respectively) during episode days, and EC increased by a factor of 1.3 for both $PM_{1.0}$ and $PM_{2.5}$, reflecting carbonaceous aerosols were affected in a certain degree by regional pollution episodes although vehicular emissions were believed to be the main source at PU roadside. While, during episode days, TC only accounted for 33.4% and 37.3% of $PM_{1.0}$ and $PM_{2.5}$ (Table 3), which are much lower than average contributions (about 47.5% and 46.4% for $PM_{1.0}$ and $PM_{2.5}$, respectively). This suggested that although elevated concentrations existed for carbonaceous aerosols during episode days, non-carbonaceous aerosols occupied a large number of proportions of $PM_{1.0}$ and $PM_{2.5}$. The above calculation about carbonaceous aerosols excluded February 14, in which wind speed is the third lowest (8.7 Km h^{-1}, Table 3) during measuring days of winter (average wind speed in winter was 23.5 Km h^{-1}). The concentrations of OC and EC in $PM_{1.0}$ (23.3 μg m^{-3} and 22.9 μg m^{-3}, respectively) and $PM_{2.5}$ (35.8 μg m^{-3} and 28.6 μg m^{-3}, respectively) were much higher than other episode days (Table 3) and TC accounted for 54.4% of $PM_{1.0}$ and 62.5% of $PM_{2.5}$, respectively.

For the purpose of comparison, the lowest 5% $PM_{1.0}$ and $PM_{2.5}$ days, which were the same days for $PM_{1.0}$ and $PM_{2.5}$, was selected. As showed in Table 3, they were April 25, May 3, May 12-14, and May 30-31, with the average mass of 20.8 μg m^{-3} for $PM_{1.0}$ and 27.5 μg m^{-3} for $PM_{2.5}$, respectively. The wind in these days exclusively was from marine. The airstream originating from marine brought relative clean air to Hong Kong. Thus local street-level source was expected to be main contributor to air pollution. $PM_{2.5}$ on May 12-14 and May 30-31 were also within the lowest 5% $PM_{2.5}$ days in ambient (Tap Mun, Tsuan Wan, and Tung Chung). Carbonaceous aerosols were dominated species in the lowest 5% PM days at PU roadside station, with averaged 88.9% and 78.5% of TC in $PM_{1.0}$ and $PM_{2.5}$, respectively. The average proportion of EC exceeded 50% for both $PM_{1.0}$ and $PM_{2.5}$. Average OC/EC ratios in $PM_{1.0}$ and $PM_{2.5}$ were 0.6 and 0.5, respectively, which were much lower than those observed in episode days (1.0 and 1.5 for $PM_{1.0}$ and $PM_{2.5}$, respectively).

In winter, wet scavenging effect was very clear for particle mass and OC through the comparison between rainy days (including drizzle) and non-rainy days (Table 4). The average concentrations of $PM_{1.0}$ and $PM_{2.5}$ in rainy days at PU roadside station were 32.1±2.5 μg m^{-3} and 40.8±4.7 μg m^{-3}, respectively, which is much lower than particle loading in non-rainy days, about 42.5±16.3 μg m^{-3} for $PM_{1.0}$ and 56.5±22.0 μg m^{-3} for $PM_{2.5}$. OC concentration also showed low levels in rainy days (6.9±1.1 μg m^{-3} and 9.8±3.9 μg m^{-3} in $PM_{1.0}$ and $PM_{2.5}$, respectively) and high levels in non-rainy days (8.5±3.9 μg m^{-3} and 8.9±3.9 μg m^{-3} in $PM_{1.0}$ and $PM_{2.5}$, respectively) in winter. The same phenomena were observed in ambient atmosphere (Table 4). Although rainfall is much heavier in spring than in winter, it seemed that the relationship between particles and precipitation was not very clear (Table 4). As mentioned above, Hong Kong was influenced by not only local source but also regional source in winter. Elevated OC concentrations observed in winter maybe were due to the contribution of secondary organic matter in transported aged air mass (Yu et al. 2004). Rainout was thought to be the principal removal mechanism (Pandis et al.1993) for aged aerosol since the presence of more soluble secondary aerosols (e. g. organic materials and sulfates). However, in spring less secondary aerosols present in atmosphere, which leads to the low wet removal rate.

Although wet scavenging is likely to be the dominant removal mechanism for EC (Ogren and Charlson, 1983), the effect is believed to depend on the extent to which the EC is coated with hygroscopic substance (Ogren et al. 1984). In other words, it depends on whether EC is internal mixture or external mixture. An internal mixture is one where EC is physically in contact with other, perhaps more abundant, hygroscopic aerosol constituents (e.g., sulfates), with the other compounds dominating the physical and chemical properties of the EC-containing particles (Ogren and Charlson, 1983). External mixture defines EC physically isolated from other constituents, such that the properties of the EC-containing particles with respect to water are determined by EC alone (Ogren and Charlson, 1983). Since urban aerosol samples taken near a source region were reported to exhibit a large degree of external mixing state (Covert and Heintzenberg, 1984). Therefore it is not surprised the poor wet scavenging effect of EC observed (Table 4).

Human behavior is another factor affecting the PM mass concentration and it's carbonaceous proportion. It was public holiday for Chinese Lunar New Year from January 22 to 25 in Hong Kong, in which most of commercial activities and production activities stopped. PM mass concentrations decreased gradually due to less passing traffic on the road, especially for diesel-fueled vehicles. On January 25, the lowest mass concentration in winter observed for both $PM_{1.0}$ and $PM_{2.5}$. The average OC in $PM_{1.0}$ during Chinese Lunar New Year accounted for 23.4% of $PM_{1.0}$ mass, which was higher than observed average value (19.7%) throughout the whole measuring period. While EC only accounted for 19.4% of $PM_{1.0}$, which was lower than observed average value (27.8%).

4. CONCLUSION

Aerosol fine particle samples collected continuously at the heavily-traffic road in

Hong Kong, PU roadside station, provided a near-five-month data set in winter and spring. An integrated data set, including aerosol mass, the concentration of carbonaceous aerosols associated episode and non-episode days, has been obtained, which is especially important because it can virtually help us enhance the understand of two important air pollution problems faced by Hong Kong: the local-street pollution and regional smog pollution.

Continuous measurements of $PM_{1.0}$ and $PM_{2.5}$ over nearly 5 months in PU roadside showed that carbonaceous aerosols were major components in fine particles, constituting 45.7% of $PM_{1.0}$ (35.9±12.4 μg m^{-3}) and 44.4% of $PM_{2.5}$ (52.3±18.3 μg m^{-3}). The average organic carbons in $PM_{1.0}$ and $PM_{2.5}$ were 7.0±2.6 μg m^{-3} and 11.0±4.7 μg m^{-3}, respectively and the average EC concentrations were 9.5±3.5 μg m^{-3} and 12.2±4.4 μg m^{-3}, respectively. Particle mass and OC showed a slightly higher concentrates in winter than that in spring. The $PM_{2.5}$ mass showed a clear spatial variability. In terms of mass concentration levels and assigning the sites in descending order with site characteristics, it is observed that roadside>urban>background.

The occurrences of episodes were observed to be commonly associated with high northeasterly wind in winter, while low wind speed from south in spring. The mean concentrations of fine particles during episode days were two times higher than the average value throughout the whole measuring days. Although elevated concentrations of OC and EC were observed during episode days, the contributions of carbonaceous aerosols were extremely lower than that in the lowest PM days. For example, the fraction of $PM_{1.0}$ accounted for by OC and EC was ~16% and ~17%. While PM1.0 was composed of ~22% for OC and ~49% for EC, respectively, when a local-street pollution was dominate source for particle aerosols.

In winter, rainout might be the principal removal mechanism for mass and OC since the presence of soluble secondary aerosols (e. g. organic materials and sulfates) in transported aged air mass. While no removal effect was found for EC. In addition, less commercial activities and human activities also lead to lower particle levels.

5. ACKNOWLEDGEMENTS

This project is supported by the Research Grants Council of Hong Kong (PolyU5145/03E) and Area of Strategic Development on Atmospheric and Urban Air Pollution (A516) funded by The Hong Kong Polytechnic University.

The authors are grateful to Hong Kong Environmental Protection Department (HKEPD) for provision of the data sets and permission for publication. The content of this paper does not necessarily reflect the views and policies of the HKSAR Government, nor does mention of the trade names or commercial products constitute endorsement or recommendation of use.

REFERENCES

Cabada, J. C., Rees, S., Takahama, S., Khlystov, A., Pandis, S. N., Davidson, C. I., and Robinson, A. L. (2004). Mass size distributions and size resolved chemical

composition of fine particulate matter at the Pittsburgh supersite. Atmos. Env.38:3127–3141.
Cao, J. J., Lee, S. C., Ho, K. F., Zhang, X. Y., Zou, S. C., Fung, K., Chow, J. C., and Watson, J. G. (2003). Characteristics of carbonaceous aerosol in Pearl River Delta Region, China during 2001 winter period. Atmos. Env.37:1451–1460.
Charron, A., and Harrison, R. M. (2003). Primary particle formation from vehicle emissions during exhaust dilution in the roadside atmosphere. Atmos. Env.37 (29):4109-4119.
Chow, J. C., Watson, J. G., Pritchett, L. C., Pierson, W. R., Frazier, C. A., and Purcell, R. G. (1993). The DRI thermal/optical reflectance carbon analysis system: description, evaluation and applications in US air quality studies. Atmos. Env.27A (8):1185–1201.
Covert, D. S. and Heintzenberg, J. (1984). Measurement of the degree of internal/external mixing of hygroscopic compounds and soot in atmospheric aerosols. Sci. Total Environ. 36:347-352.
Dockery, D. W., Arden, P. C., Xu, X. P., Spengler, J. D., Ware, J. H., Fay, M. E., Ferris, B. G., and Speizer, F. E. 1993. An association between air pollution and mortality in six U.S. cities. N. Engl. J. Med. 329(24):1753-1759.
Ho, K. F., Lee, S. C., Chan, C. K., Yu, J. C., Chow, J. C., and Yao, X. H. (2003). Characterization of chemical species in $PM_{2.5}$ and PM_{10} aerosols in Hong Kong. Atmos. Env.37:31-39.
Katsouyanni, K., Touloumi, G., Samoli, E., Gryparis, A., Le Tertre, A., Monopolis, Y., Rossi, G., Zmirou, D., Ballester, F., Boumghar, A., Anderson, H. R., Wojtyniak, B., Paldy, A., Braunstein, R., Pekkanen, J., Schindler, C., and Schwartz, J. (2001). Confounding and effect modification in the short-term effects of ambient particles on total mortality: results from 29 European cities within APHEA2 project. Epidemiology. 12 (5):521-531.
Keywood, M. D., Ayers, G. P., Gras, J. L. Gillett, R. W., and Cohen, D. D. (1999). Relationships between size segregated mass concentration data and ultrafine particle number concentrations in urban areas. Atmos. Env.33:2907-2913.
Lee, H. S., and Kang, B. W. (2001). Chemical characteristics of principal $PM_{2.5}$ species in Chongju, South Korea. Atmos. Env.35:739–746.
Li, C. S., and Lin, C. H. (2002). $PM_1/PM_{2.5}/PM_{10}$ characteristics in the urban atmosphere of Taipei. Aerosol Sci. Technol. 36 (4):469-473.
Lin, J. J., and Tai, H. S. (2001). Concentrations and distributions of carbonaceous species in ambient particles in Kaohsiung City, Taiwan. Atmos. Env.35:2627–2636.
Louie, P. K.K., Chow, J. C., Chen L.-W. A., Watson, J. G., Leung, G., and Sin, D. W.M. (2004). $PM_{2.5}$ chemical composition in Hong Kong: urban and regional variations. Sci. Total Environ. (in press).
Lundgren, D. A., Hlaing, D. N., Rich, T. A. and Marple, V. A. (1996). $PM_{10}/PM_{2.5}/PM_1$ Data from a Trichotomous sampler. Aerosol Sci. Technol. 25:353-357.
Ohta, S., Hori, M., Yamagata, S., and Murao, N. (1998). Chemical characterization of atmospheric fine particles in Sapporo with determination of water content. Atmos. Env.32 (6):1021–1025.
Qin,Y., Chan, C. K., and Chan, L. Y. (1997). Characteristics of chemical compositions of atmospheric aerosols in Hong Kong: spatial and seasonal distributions. Sci. Total Environ. 206:25-37.

Ogren, J. A., and Charlson, R. J. (1983). Elemental carbon in the atmosphere: cycle and lifetime. Tellus. 35B:241-254.
Ogren, J. A., Groblicki, P. J., and Charlson, R. J. (1984). Measurement of the removal rate of elemental carbon from the atmosphere. Sci. Total Environ. 36:329-338.
Pandis, S. N., Wexler, A. S., and Seinfeld, J. H. (1993). Secondary organic aerosol formation and transport-II. Predcting the ambient secondary organic aerosol size distribution. Atmos. Env., 27A(15):2403-2416.
Schwartz, J., Dockery, D. W., and Neas, L. M. (1996). Is daily mortality associated specifically with fine particles? J. Air & Waste Manage. Assoc. 46:927-939.
Shi, J. P., Evans, D. E., Khan, A. A., and Harrison, R. M. (2001). Source and concentration of nanoparticles (<10 nm diameter) in the urban atmosphere. Atmos. Env.35:1193–1202.
Vallius, M. J., Ruuskanen, J., Mirme, A., and Pekkanen, J. (2000). Concentrations and estimated soot content of PM_1, $PM_{2.5}$, and PM_{10} in a subarctic urban atmosphere. Environ. Sci. and Technol. 34:1919-1925.
Watson, J., Chow, J. C., Lowenthal, D. H., Pritchett, L. C., and Frazier, C. A. (1994). Differences in the carbon composition of source profiles for diesel- and gasoline-powered vehicles. Atmos. Env. 28:2493-2505.
Wu, Y., Hao, J. M., Fu, L. X., Hu, J. N, Wang, Z. S., and Tang U. W. (2003). Chemical characteristics of airborne particulate matter near major roads and at background locations in Macao, China. Sci. Total Environ. 317(1-3):159-172.
Yu, J. Z., Tung, J. WT., Wu A. WM., Lau A. KH., Louie, P. KK., and Fung, J. CH. (2004). Abundance and seasonal characteristics of elemental and organic carbon in Hong Kong PM_{10}. Atmos. Env. 38(10):1511-1521.
Zhu, Y. F., Hinds, W. C., Kim, S., Shen, S., and Sioutas, C. (2002). Study of ultrafine particles near a major highway with heavy-duty diesel traffic. Atmos. Env. 36:4323–4335.

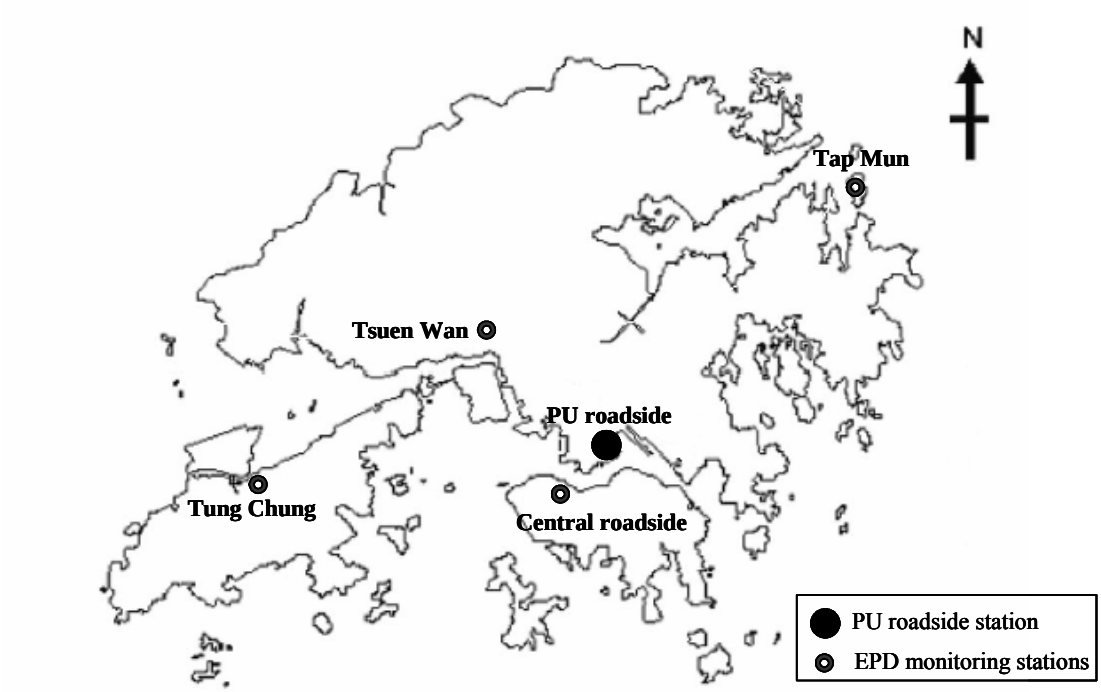

Figure 1. Sampling locations

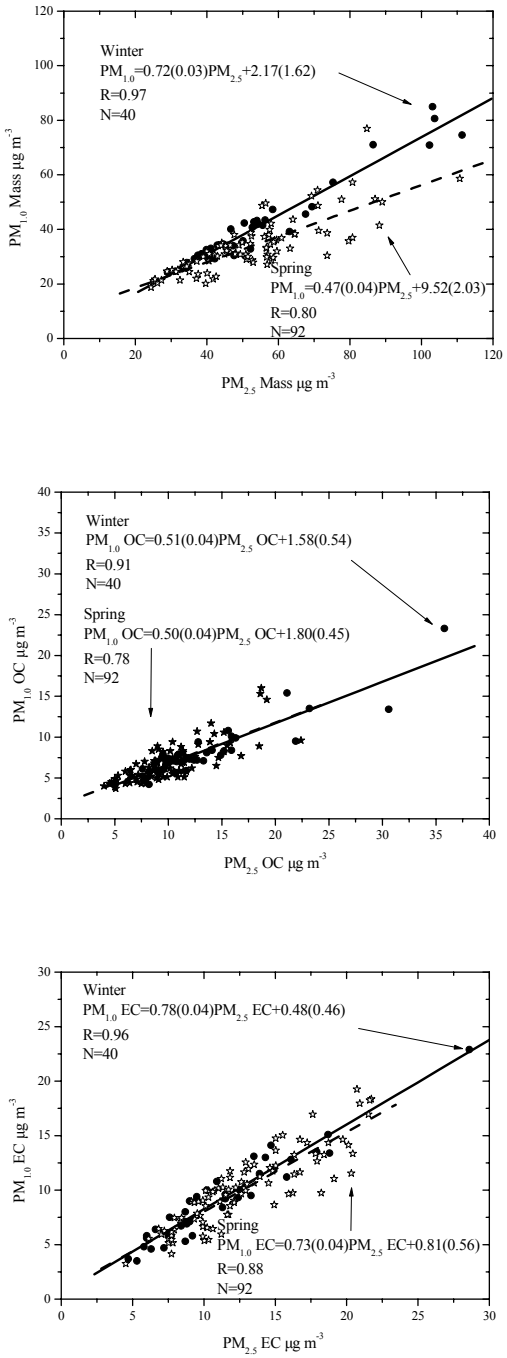

Figure 2. Correlations of Mass, OC, and EC between $PM_{1.0}$ and $PM_{2.5}$. Standard error is in bracket.

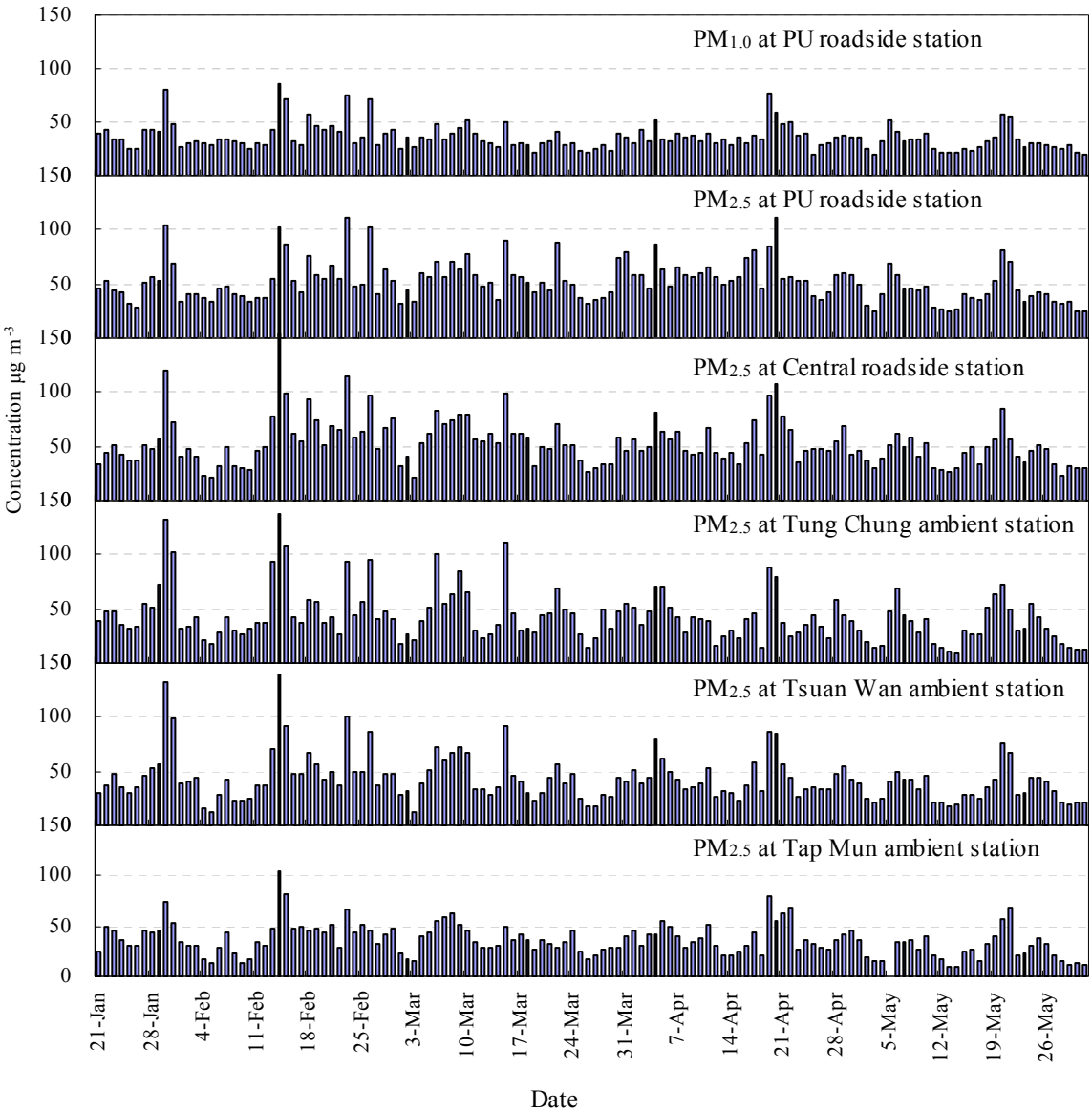

Figure 3. Daily 24-h average $PM_{1.0}$ and $PM_{2.5}$ concentrations at PU roadside and monitoring stations operated by EPD during January to May 2004.

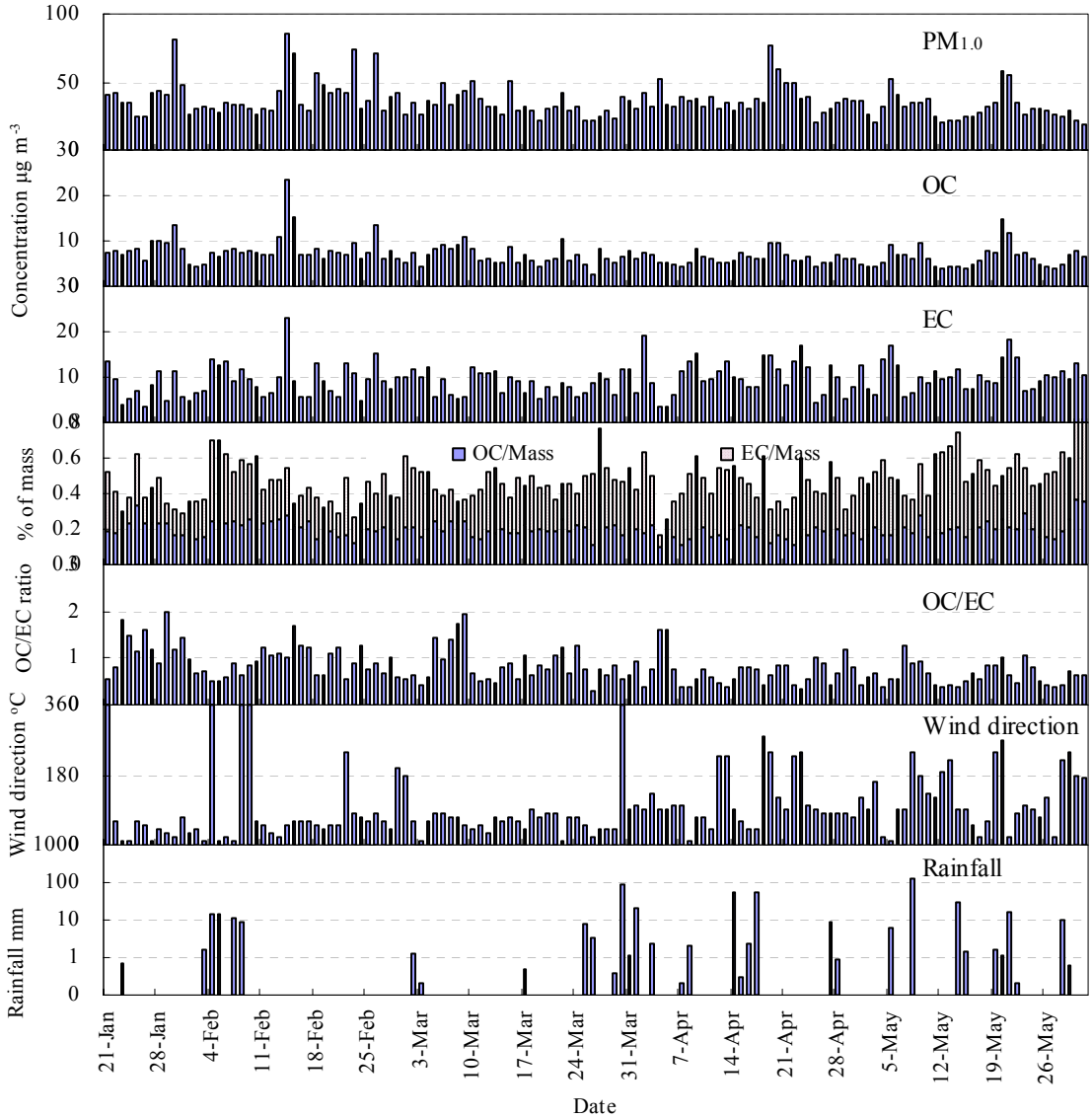

Figure 4. Daily 24-h average $PM_{1.0}$, OC, EC concentrations, and OC/mass, EC/mass, OC/EC ratios at PU roadside during January to May 2004, with corresponding meteorological data.

Table 1. Seasonal average of particle mass and carbonaceous aerosols in PU roadside station and four monitoring stations

		PU roadside						Central[a]	Tung Chung[b]	Tsuan Wan[b]	Tap Mun[b]
		$PM_{1.0}$ ($\mu g\ m^{-3}$)			$PM_{2.5}$ ($\mu g\ m^{-3}$)			$PM_{2.5}$ ($\mu g\ m^{-3}$)			
		Mass	OC	EC	Mass	OC	EC	Mass	Mass	Mass	Mass
Winter	Jan	41.4± 15.1	8.6± 2.1	7.7± 3.4	52.7± 20.3	13.9± 3.9	10.3± 4.4	54.1± 24.3	58.8± 31.7	55.0± 32.1	43.7± 13.6
	Feb	40.8± 15.9	8.2± 3.7	9.6± 3.9	54.6± 21.7	13.0± 6.6	11.3± 4.9	61.1± 30.4	49.4± 28.5	49.6± 27.3	41.3± 19.4
	Average	40.9± 15.5	8.3± 3.3	9.0± 3.8	54.1± 21.1	13.2± 6.0	11.0± 4.7	59.2± 28.7	52.0± 29.3	51.1± 28.4	42.0± 17.9
Spring	Mar	33.1± 8.1	6.7± 1.9	8.6± 2.4	54.2± 16.3	11.0± 3.2	11.3± 3.1	53.8± 18.6	44.8± 23.3	41.5± 18.6	35.1± 12.1
	Apr	37.2± 11.4	6.1± 1.3	10.0± 4.1	59.6± 15.4	11.0± 3.6	14.7± 4.8	56.0± 17.5	41.5± 17.8	44.9± 16.7	39.5± 14.4
	May	31.0± 9.7	6.4± 2.4	10.4± 3.1	40.9± 14.0	8.2± 3.6	12.3± 3.9	42.6± 13.3	31.8± 17.9	33.8± 14.0	25.6± 14.3
	Average	33.8± 10.1	6.4± 1.9	9.7± 3.3	51.5± 17.0	10.0± 3.7	12.7± 4.2	50.8± 17.4	39.4± 20.4	40.0± 17.0	33.3± 14.7
Total		35.9± 12.4	7.0± 2.6	9.5± 3.5	52.3± 18.3	11.0± 4.7	12.2± 4.4	53.3± 21.7	43.2± 24.1	43.4± 21.6	35.9± 16.2

[a] Roadside monitoring station; b Ambient monitoring station

Table 2. Levels of carbonaceous aerosols in urban atmosphere in Asia.

Location	Sampling Period	Size	TC ($\mu g\ m^{-3}$)	OC ($\mu g\ m^{-3}$)	EC ($\mu g\ m^{-3}$)	OC/EC	Location	Method	Reference
Hong Kong, PU	2004.1-2	$PM_{1.0}$	17.3	8.3 ± 3.3	9.0 ± 3.8	1	Roadside	IMPROVE-TOR	This study
Tai Wan, Taipei	1999.1	$PM_{1.0}$	22.9	11.5 ± 2.8	11.3 ± 1.7		Roadside	Combustion	Li C.S. 2002
Tai Wan, Taipei	1999.12	$PM_{1.0}$	4.7	3.4 ± 0.9	1.3 ± 0.7		Urban	Combustion	Li C.S. 2002
Hong Kong, PU	2004.1-2	$PM_{2.5}$	24.2	13.2 ± 6.0	11.0 ± 4.7	1.3	Roadside	IMPROVE-TOR	This study
Hong Kong, PU	2000.11-2001.2	$PM_{2.5}$	15.3	9.5 ± 2.0	5.8 ± 1.1	1.6	Roadside	TMO[a]-EA[b]	Ho K.F. 2003
Hong Kong, PU	2002.1-2	$PM_{2.5}$	16.7	10.6 ± 3.7	6.1 ± 1.8	1.7	Roadside	IMPROVE-TOR	Cao J.J. 2003
Hong Kong, MK	2000.11-2001.10	$PM_{2.5}$	36.8	16.7 ± 7.6	20.2 ± 4.2	0.8	Roadside	IMPROVE-TOR	Louie P. 2004
Hong Kong, TW	2000.11-2001.10	$PM_{2.5}$	14.1	8.7 ± 5.3	5.4 ± 1.4	1.6	Urban	IMPROVE-TOR	Louie P. 2004
Hong Kong, HT	2000.11-2001.10	$PM_{2.5}$	5.9	4.2 ± 3.7	1.7 ± 0.9	2.5	Rural	IMPROVE-TOR	Louie P. 2004
Tai Wan, Taipei	1999.1	$PM_{2.5}$	23.6	12.2 ± 3.0	11.4 ± 2.5		Roadside	Combustion	Li C.S. 2002
Tai Wan, Taipei	1999.12	$PM_{2.5}$	6.2	3.4 ± 0.5	2.9 ± 0.3		Urban	Combustion	Li C.S. 2002
China, Guang Zhou	2002.1-2	$PM_{2.5}$	23.8	17.8 ± 10.2	6.0 ± 3.2	2.9	Urban	IMPROVE-TOR	Cao J.J. 2003
China, Shen Zhen	2002.1-2	$PM_{2.5}$	19.2	13.2 ± 4.1	6.1 ± 1.8	2.2	Urban	IMPROVE-TOR	Cao J.J. 2003
China, Zhu Hai	2002.1-2	$PM_{2.5}$	17.3	12.2 ± 4.4	5.0 ± 1.6	2.4	Urban	IMPROVE-TOR	Cao J.J. 2003
China, Macao	2001.11-12	$PM_{2.5}$	16.6	12.2	4.4	2.8	Roadside	TOT-EA[b]	Wu Y. 2003
Tai Wan	1998.11 - 1999.4	$PM_{2.5}$	14.5	10.4	4	2.6	Urban	EA[b]	Lin J. J. 2001
Korea, Chongju	1995, Fall	$PM_{2.5}$	12.4	6	6.4	0.9	Urban	IMPROVE-TOR	Lee H. S. 2001
	1995, Winter	$PM_{2.5}$	9.3	5	4.3	1.2	Urban	IMPROVE-TOR	Lee H. S. 2001
Japan, Sapporo	1992.9-10	$PM_{2.0}$	9.1	4.1	5	0.8	Urban	EA[b]	Ohta S. 1998
	1992.1-2	$PM_{2.0}$	9	3.9	5.1	0.8	Urban	EA[b]	Ohta S. 1998
Hong Kong, MK	2001.1-12	PM_{10}	26.8	16.3 ± 6.2	10.5 ± 2.9	1.6	Roadside	NOISH-TOR	Yu J.Z. 2004
Japan,Uji	1998.9-10	PM_{10}	6.4	1.8	4.6	0.4	Urban	R&P 5400	Holler R. 2002
	1998.11-12	PM_{10}	10.2	2.5	7.7	0.3	Urban	R&P 5400	Holler R. 2002

[a] Thermal manganese dioxide oxidation

[b] Elemental analysis

Table 3. Summary statistics for the concentrations of PM, carbonaceous aerosols; and ratios during the highest and lowest 5% PM days in 2004 with corresponding meteorological data.

			The highest 5% PM days (episode days)							The lowest 5% PM days						
Date			30 Jan	14 Feb	15 Feb	23 Feb	26 Feb	19 Apr	20 Apr	25 Apr	3 May	12 May	13 May	14 May	30 May	31 May
$PM_{1.0}$	Mass	$\mu g\ m^{-3}$	80.6	85.0	71.0	74.6	70.9	77.3	59.0	20.5	20.1	20.7	21.5	21.8	22.1	19.1
	OC	$\mu g\ m^{-3}$	13.5	23.3	15.4	9.5	13.4	9.4	9.6	4.3	4.3	3.7	4.3	4.5	8.0	6.7
	EC	$\mu g\ m^{-3}$	11.5	22.9	9.2	10.8	15.1	14.8	11.6	4.2	6.3	9.4	10.0	11.7	13.0	10.3
	OC/EC		1.2	1.0	1.7	0.9	0.9	0.6	0.8	1.0	0.7	0.4	0.4	0.4	0.6	0.6
	$OC/PM_{1.0}$	%	16.7	27.4	21.7	12.7	18.9	12.2	16.3	21.0	21.4	17.9	20.0	20.6	36.2	35.0
	$EC/PM_{1.0}$	%	14.3	26.9	13.0	14.5	21.3	19.1	19.7	20.5	31.3	45.4	46.5	53.7	59.0	53.9
$PM_{2.5}$	Mass	$\mu g\ m^{-3}$	103.7	103.1	86.5	111.4	102.3	84.8	110.8	39.7	24.3	26.2	25.1	27.3	25.5	24.4
	OC	$\mu g\ m^{-3}$	23.2	35.8	21.1	21.9	30.6	13.9	22.4	6.0	4.5	5.1	4.5	5.0	8.1	7.0
	EC	$\mu g\ m^{-3}$	13.9	28.6	11.5	10.9	18.7	15.0	20.3	7.7	7.2	10.3	10.1	12.8	15.5	12.2
	OC/EC		1.7	1.3	1.8	2.0	1.6	0.9	1.1	0.8	0.6	0.5	0.4	0.4	0.5	0.6
	$OC/PM_{2.5}$	%	22.4	34.7	24.4	19.7	30.0	16.3	20.2	15.2	18.5	19.2	17.9	18.3	31.7	28.5
	$EC/PM_{2.5}$	%	13.4	27.8	13.3	9.7	18.3	17.6	18.3	19.5	29.6	39.4	40.2	46.7	60.8	50.0
	RH	%	83	59	66	72	80	69	79	88	80	81	80	90	81	76
	Rainfall	mm												31.6		
	WD[a]	^oC	20	50	60	80	80	240	120	90	160	190	220	90	180	170
	WS[b]	$Km\ h^{-1}$	15.1	8.7	28.9	42.7	18.2	7.5	6.1	31.5	10.8	10.7	12.8	22.8	14.4	7.5

[a] Wind direction, [b] Wind speed

Table 4. Comparison of fine particles and carbonaceous aerosols between rainy days and non-rainy days.

	Season		Winter		Spring	
			Rainny days	Non-rainny days	Rainny days	Non-rainny days
	N[a]		6	34	31	61
PU roadside station	$PM_{1.0}$	μg m^{-3}	32.1± 2.5	42.5± 16.3	32.4± 9.3	34.4± 10.4
	$PM_{2.5}$	μg m^{-3}	40.8± 4.7	56.5± 22.0	52.0± 16.0	51.2± 17.6
	OC in $PM_{1.0}$	μg m^{-3}	6.9± 1.1	8.5± 3.5	6.4± 2.3	6.4± 1.7
	EC in $PM_{1.0}$	μg m^{-3}	9.8± 3.9	8.9± 3.9	10.0± 3.3	9.5± 3.4
	OC in $PM_{2.5}$	μg m^{-3}	10.4± 2.3	13.7± 6.3	10.5± 3.6	9.8± 3.7
	EC in $PM_{2.5}$	μg m^{-3}	11.9± 4.4	10.9± 4.8	13.7± 4.3	12.3± 4.1
EPD monitoring station	Central	μg m^{-3}	36.6± 13.2	63.2± 29.0	46.4± 14.8	53.0± 18.4
($PM_{2.5}$)	Tung Chung	μg m^{-3}	33.2± 12.3	55.3± 30.3	36.5± 15.7	40.8± 22.4
	Tsuan Wan	μg m^{-3}	30.8± 15.8	54.6± 28.8	36.2± 14.7	41.9± 17.9
	Tap Mun	μg m^{-3}	28.9± 13.5	44.3± 17.7	29.9± 14.3	35.1± 14.7

[a] number of days